2010

Skin Hardness and Elasticity Measurement Device

ME 450 Fall 2010
Professor Grant Kruger

Team Derma - 17

Brandon Kerins
Joseph Kirby
Divyarajsinh Raol
Matthew Valvano

December 15, 2010

Sponsors:
Professor Gordon Krauss
Professor Gary Fisher

University of Michigan

Abstract

Skin provides many functions critical to the human body, including regulation of body temperature and protection from water loss. The properties of skin related to these functions, primarily elasticity and hardness, are directly affected by chronological aging and photo-aging and vary among locations on the body. The ability to quantify these properties is important so the aged status of skin can be characterized for patients and skin healing therapies can be evaluated. Therefore, the intention of this project is to develop a tool to measure the stretching and indentation resistance of skin at various rates and size scales.

EXECUTIVE SUMMARY

As skin ages the mechanical properties that influence skin's resistance to tensile and compressive forces are known to degrade. This can result in a negative impact on the ability of skin to perform critical functions such as prevention of water-loss, regulation of body temperature, and protecting the rest of the body from the outside environment. It would be exceedingly beneficial for research in the dermatology field to have the ability to properly characterize this change in properties. Therefore, our sponsors, Professor Gary Fisher and Professor Gordon Krauss, tasked us with designing and developing a tool to measure the elasticity and hardness of skin.

The feedback gained from our sponsors was used to create a ranked order of customer requirements. The main focus of the design is to be able to accurately measure the hardness and elasticity of skin. During the concept generation we were able to refine the mobility requirement to be a handheld device, one that can reach anywhere on the patient's body. The tests should also take less than one hour to complete. Other requirements are to minimize costs by limiting the complexity of any design, integration of computer control to collect data from any sensors, and the ability to test on ranges starting from the micron level.

The engineering specifications were developed as a way of achieving our customer requirements. A literature research of current test devices aided us in forming specific values that are to be used as benchmark targets for our design. For either test a force of 1 N maximum is to be applied on the patient. To be able to reach anywhere on the body, the device should orient 360º in the plane parallel to skin surface, and a mass limit of 9 kg to be easily held by the operator. The range of testing area should be 0.1-20 mm to satisfy the customer requirement. Number of sensors and power consumption should be kept to a minimum.

By means of a functional decomposition, and brainstorming, we developed numerous sub concepts and concepts based on multiple sub functions to meet the customer requirements and specifications. Researching many measurement methods was important in influencing our concepts. Pugh charts are concept evaluation tool we employed to compare each of our designs subsystems. Each component was rated on how well it meets customer requirements and engineering specifications. The best concepts for each sub function were determined and used to create numerous complete designs, which were compared in a final Pugh chart, creating an alpha design.

From the alpha design a final design/prototype was produced. This included a full analysis of both mechanical and electrical parameters. It has been determined that the total prototype cost is $1,489.

With the completion of the prototype, this device has the capability of meeting all customer requirements and engineering specifications. Calibration and validation has been performed on both mechanical and electrical components. It has been observed that the mechanical portion of the device is fully functional, allowing for micron level movement resolution using the driver and controller implemented. However, calibration data of the load cells show that these curves are noise dominant, limiting data repeatability. With these results, design critiques and considerations were created to aid in future development of the device.

TABLE OF CONTENTS

1. PROJECT INTRODUCTION

Determining the age of skin is important to the world of dermatology, it can be used to evaluate skin healing therapies. Currently, the most effective method is by taking a biopsy of the skin directly from the patient, which is obtrusive and discomforting to the patient, however provides no quantitative analysis of the skin's condition. The objective of this project is to characterize the age of skin by designing a device to measure its hardness and elasticity. The sponsors for our project are Professor Gordon Krauss, of the College of Engineering at the University of Michigan and Professor Gary Fisher, of the Department of Dermatology at the University of Michigan.

This project was created due to the interest in developing a more accurate device that allows a researcher, or persons using the device to determine the age of skin without the need of a biopsy. There are currently multiple devices on the market that measure skin elasticity or hardness, however, these devices are not accurate in determining the mechanical properties because they fail to isolate the dermis and epidermis layers of the skin, information about these layers are discussed in Section 2.1. This has lead to the design problem to develop a cost effective mobile device that can measure skin elasticity and hardness to an adequate degree.

The outcome of this project will be a device that meets the above expectations, and if possible, have the ability to be defined and developed further for use outside the research lab.

2. INFORMATION SOURCES

2.1 Background Information

To fully comprehend the design problem it is important to understand background information on skin and its aging. Skin has three major layers; the epidermis, dermis, and the fatty tissue (Fig.1). The majority of aging occurs in the dermis region of the skin. Various factors of skin aging are, but not limited to; chronological aging (due to the patient's age), skin pigmentation (the coloring of the patient's skin), and sun exposure (the amount of time a person spends tanning or other activities with long sun exposure). These effects can be seen in the collagen fibrils. These fibrils are located in, and are a major component of, the dermis. They aid in keeping the cell matrix of the dermis intact which affects the overall strength of the skin.

Figure 1: Layers of skin

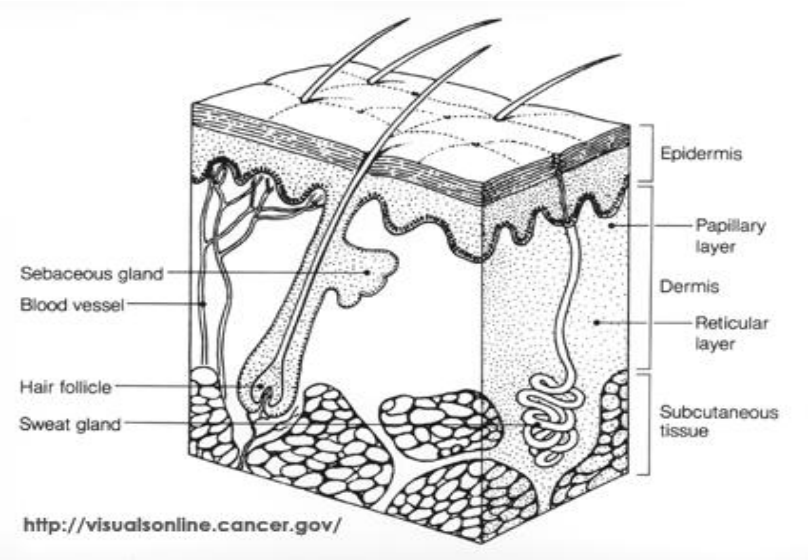

The effect of aging can be seen in comparing young skin collagen fibrils to old skin. In young skin, collagen fibrils are high in volume and be random in placement. They also have the tendency to appear as continuous strands. They also have strong cross-linking between the strands. This leads to added rigidity and increases the strength in the skin (Fig. 2a). Collagen fibrils of older skin share different properties. These fibrils have a lower volume and our more densely packed than before. This is also caused by degradation by enzymes, leaving open space in the dermis to be filled with proteins (Fig. 2b). This change in collagen fibrils over time leads to a change in skin properties overtime as well. This fact helped create the problem that this project is looking to solve.

Figure 2a: Young aged collagen fibrils

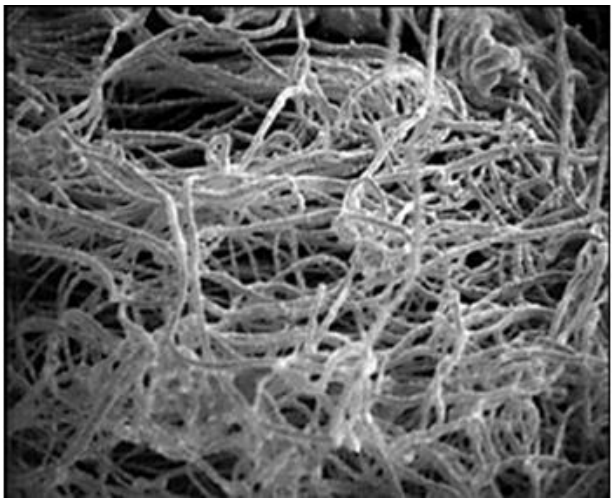

Figure 2b: Old aged collagen fibrils

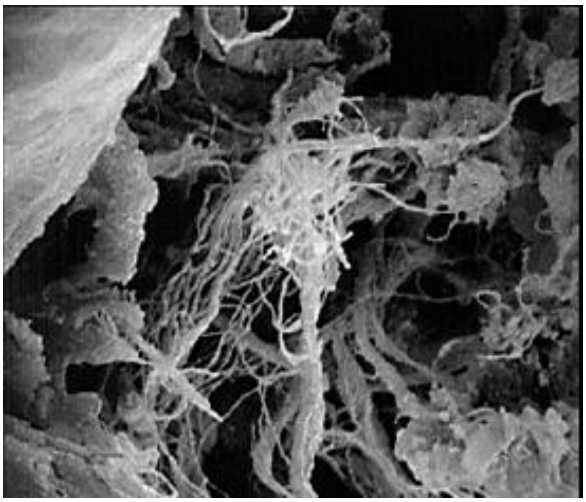

Pictures provided by Dr Fisher at sponsor meeting, 2010

Viscoelastic Effects [3, 10, 11]
Human skin functions as a viscoelastic material where it exhibits non-linear strain behavior, dependent upon time, during constant stress application. This behavior is governed by the material creep, which is where a material deforms under constant stress in a slow, continual manner. When measuring total strain of a viscoelastic material, the creep strain must be included with the elastic strain at the instant of measurement. After stress is removed from a specimen, the material will instantly recover from elastic strain, but recovery from creep strain is time dependent and based upon material properties. In addition, the rate at which a stress is applied to a material such as skin directly affects the resulting total strain. If stress is incremented to a certain value at a fast rate, the final total strain will be considerably lower compared to that of a slow rate. In cases of constant strain application, viscoelastic materials will experience a stress relaxation effect where stress in the specimen decreases with application time. Due to these non-linear behaviors associated with this type of material, it is important to have a high sampling rate when capturing stress-strain data. This will allow for data sets with clearly defined initial linear elastic strain, creep strain, elastic strain recovery, and creep strain recovery.

2.2 Engineering Parameters

Elasticity: Skins tendency to resume to its original shape and dimension after releasing the stretching force [6].

Viscoelasticity: Viscoelasticity is the property of materials that exhibit both viscous and elastic characteristics when undergoing deformation. Since skin is not a homogeneous and isotropic medium, the modulus of elasticity can change over time and under different experimental conditions [10].

Stiffness: It is the resistance of the body to deformation when a set of loading points and boundary conditions are prescribes on the elastic body [6].

Young's Modulus: It is a measure of the stiffness of an isotropic elastic material. It is defined as the ration of the uniaxial stress over the uniaxial strain in the elastic region of the material [6].

2.3 Measurement Techniques

Several techniques have been used in the past to study *in vivo* mechanical properties of human skin. These are described as below:

1. Tonometric measurements that measure the ability of the skin to withstand vertical forces of indentations. It provides a simple noninvasive means of measuring hardness [13]. A durometer uses this technique. In an experiment a Rex Durometer Max-hand meter 1700 without a foot attachment (Rex Gauge Company, Inc., Glenview, IL) was used to measure hardness of the skin. This device is the international standard for the hardness measurement of plastic, rubber, and

other non metallic material. The durometer was provided with a calibrated gauge that registers linearly the relative degree of hardness.

Figure 3: Contact between durometer and skin [13]

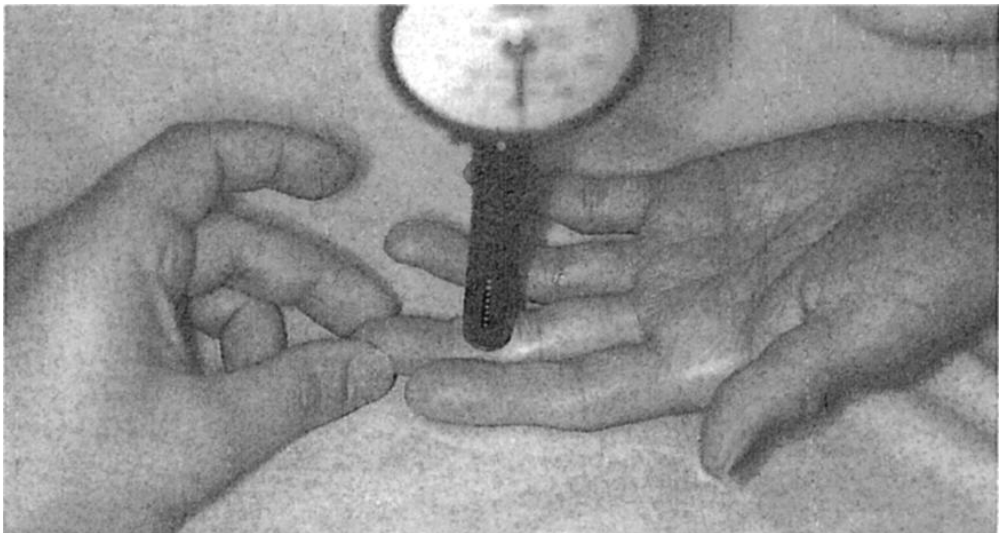

Figure 3 shows the durometer being held on the ventral surface of the index figure. The measurements were measured as a result of a spring-loaded interior that senses hardness by applying an indentation load on the specimen. For measurements, the durometer was used at 25ºC and rested by gravity against the skin: four consecutive readings were taken at the same site. Initial hardness was defined as the reading recorded in 1 second of firm contact and the final reading was taken in 15 seconds of the durometer with the skin. In between readings the durometer was reset to 0. The durometer is not appropriate for measurement of skin hardness at all anatomic sites. It insensitive when used in areas of skin, such as forehead, that do not have much subcutaneous tissue.

2. Traction in which a linear displacement is applied in the horizontal plane of the skin. There are two devices that have been commercialized which are the bioskin tension meter [17] and the extensometer sold by Stiefel laboratories, UK [14]. The quasi static extensometer [2] was designed by J, Evans in 1967 [5]. This device applies a known rate of extension to the skin via double sided adhesive tape on two metal tabs. The resulting load was transmitted by a chain which encircled two frictionless pulley wheels at the end of the strain gauged cantilever arms (Fig. 4).

Figure 4: The quasi extensometer [2]

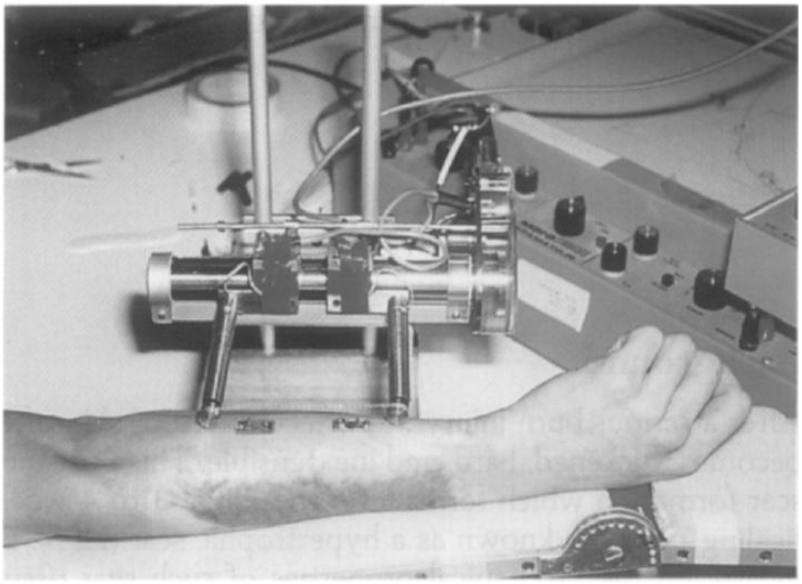

A constant speed dc motor was used to drive the arms apart and apply a surface extension rate to the skin of 0.35 mm/s to maximum load of 100 g (about 1 N). Values for the load force and extension are plotted against each other (Fig. 5).

Figure 5: Load-extension plot used to determine elasticity [3]

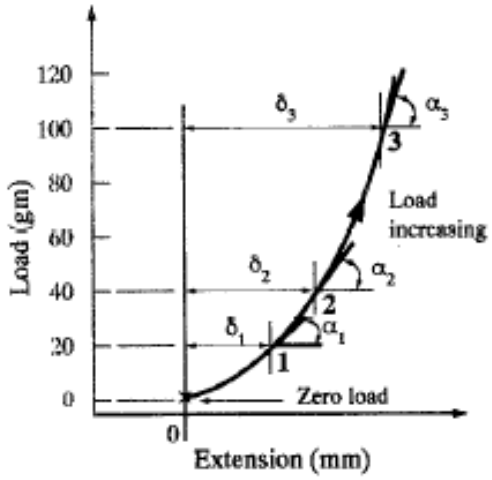

Figure 5 shows a typical non-linear behavior of tissue but its shape is influenced by rate of extension. The elasticity is therefore the load per unit tissue width divided by the strain. The strain can be found by measuring the extension (δ) at each load and dividing it by the original unstretched skin length. The maximum force applied by the test is 1 N. The elasticity is given in units of N/m as opposed to GPa (N/m^2), and can be found from the gradients on the graph.

3. One technique used in documented experiments for exploring the viscoelastic behavior and measuring extensibility of skin implemented a device to apply a torque to the skin sometimes

referred to as a twistometer [12]. In a method found to minimize the effects of the hypodermis (subcutaneous fat) and muscle, the torque was applied parallel to the surface of a section of skin. The amount of torque applied was calculated to remain within the linear zone of the stress-strain curve and to result in an approximate twist angle of 2 - 6°. The device consisted of a stationary outer ring and a rotating inner disk, both adhered to the skin. An area of free skin between the ring and the disk is the skin from which the results will be derived. With this, a constant, instantaneous torque was applied for sixty seconds and the resulting twist angle of the disk is recorded. This data lead to the determination of parameters of immediate extensibility (U_E), the viscoelastic deformation (U_V), and immediate recovery (U_R) all in units of radians (Fig. 6). The derived formula (Eq. 1) was used to calculate the Young's Modulus, where M is the torque (Nm), R_1 and R_2 are radii (m) of skin area analyzed, and $E\rho$ is the skin thickness (m) [4].

$$E = \frac{M}{0.8\pi R_1 R_2 E_p U_E} \tag{1}$$

In addition, the resulting ratio U_R/U_E was used as a measure of skin elasticity which describes the skin's ability to recover after being strained.

Figure 6: Theoretical results of extensibility parameters of torsion testing [12]

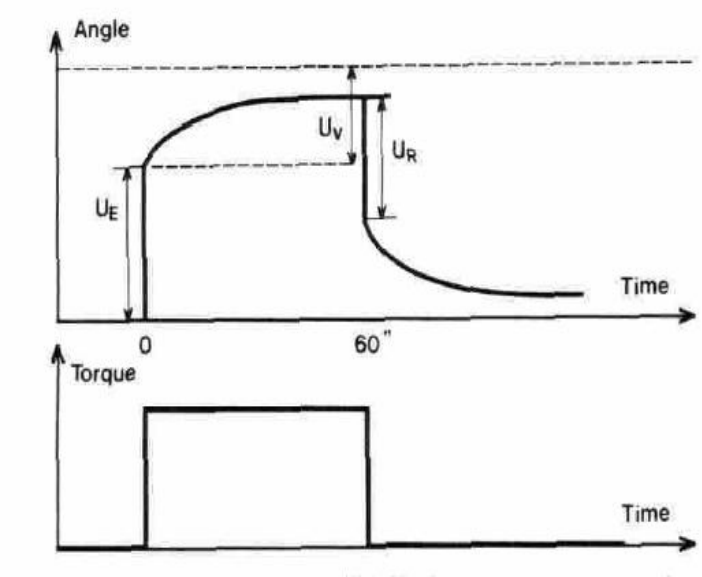

4. Indentation uses the application of thrust through a disc glued to the skin [2]. The dynamic indentation test method proposes that although skin is comprised of three layers, it acts like a monolayer material. As a result, the behavior of skin can be treated as if it were a homogeneous material. Using constant amplitude of motion ranging from 1-10 μm the effects of the underlying layers can be minimized. A sinusoidal displacement is applied to the skin using a cylindrical indenter (2 mm radius), and the resulting force is then measured. An impedance head,

comprising of a force sensor and accelerometer, is used to measure the force and displacement. The frequency of the displacement ranges from 10-60 Hz and incremented by 5 Hz. Contact with the skin is determined by measuring the phase angle of the signal at a low frequency (15 Hz). Before contact is made the phase will be constant at 180º and upon contact it decreases due to damping effects. The stiffness and damping as functions of frequency can then be determined for the elastic and viscous effects, respectively. The Young's modulus can then be determined from these two quantities. The result will be a complex number, where the real part is due to elastic behavior and the imaginary part is due to viscous behavior [18, 19].

5. Suction in which a negative pressure is applied to the skin. There are two devices have been commercialized, Cutometer (Courage + Khazaka electronic GmbH) [7] and the Dermaflex A (Cortex Technology, Denmark) [16]. In one of the study, a new device called Echorheometer [3], comprising of a suction system with an ultrasound scanner (A mode, TM- mode and B-mode) [15] was developed. This enabled them to perform simultaneous visualization and measurement of the deformation of skin structures. Using this device the behavior of dermis and subcutaneous fat was investigated on the volar forearm of 10 volunteers. This technique was based on a partial vacuum created in a small cylinder partly filled with water which causes deformation by suction of the skin. The end of the cylinder was held firmly on the surface of the skin (Fig. 7). The cylinder is detachable with centre aperture of diameter L_0 =2, 4, 6, 8 or 10mm.

Figure 7: View of the cylinder placed on skin [3]

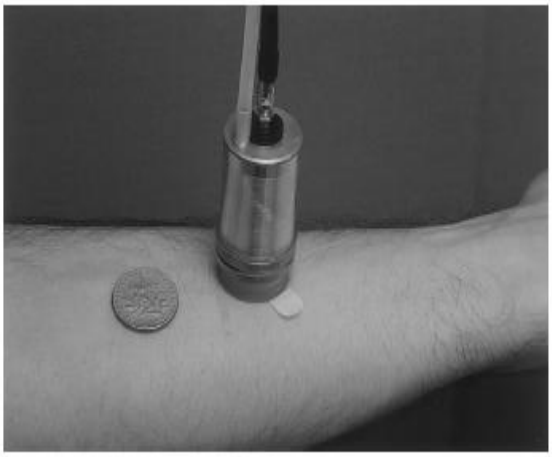

A pump evacuates air from the chamber and a pressure sensor (electro-vacuum regulator) controls the pressure between -10 to -500 mbar. The partial vacuum was applied in two ways, either static (fixed pressure followed by return to atmospheric pressure) or dynamic (gradient of increasing then decreasing negative pressure) (Fig.8) with stress loading and unloading times (1s to 5 min) and number of cycles (1-10).

Figure 8: Controlled suction on the skin as a function of time(s)

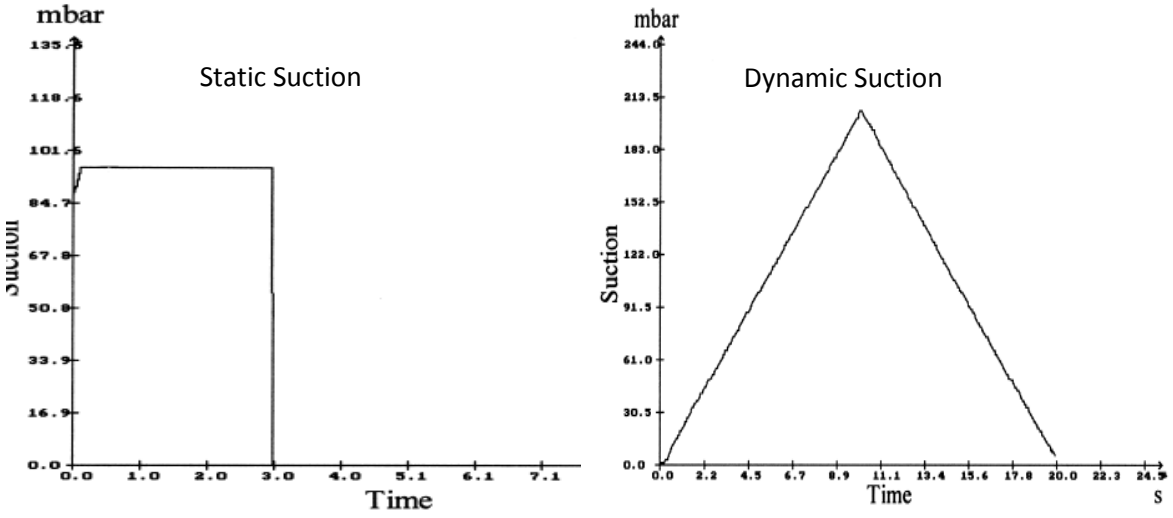

The resistance to the suction stress is due to the dermis rather than subcutaneous fat but the relative effects cannot be evaluated as subcutaneous fat undergoes greater strain than the dermis. The skin at rest has its own natural tension and response to stress is linear. With greater deformation, the intrinsic dermal elasticity contributes more to dermal stress resistance and hence the relation is nonlinear.

Another device using similar technique of suction pressure is the Cutometer MPA 580 [7] sold by Courage + Khazaka electronic GmbH (Fig. 9). It consists of a probe that is pressed on to skin and partial vacuum is created. Negative pressure is created in the device and skin is sucked into the probe. The probe consists of optical measuring system that consists of a light source, a light receptor and two prisms facing each other that projects the light from transmitter to receptor. The Cutometer is controlled by windows based software which then plots the resistance of the skin sucked by negative pressure and its ability to return to original position (elasticity).

Figure 9: Cutometer MPA 580 configuration [7]

It was used for measuring skin elasticity by H.P.Dobrev [1]. The time/strain mode was used with a 5 second application of a vacuum of 400 mbar, followed by a 5 seconds relaxation. A typical skin deformation curve was composed of U_e immediate distention; U_v delayed distention; U_f final distention; U_r immediate retraction and U_a final retraction (Fig. 10). U_e and U_r are linked with stretching of collagen and elastic fibers and hence reflect the skin rigidity. U_v and U_v/U_e represent the viscoelastic part of the deformation and are result of the displacement of the interstitial fluid. U_f, U_a/U_f and U_r/U_f measure the ability of skin to return to its initial position after deformation.

Figure 10: Skin deformation curve obtained with cutometer [1]

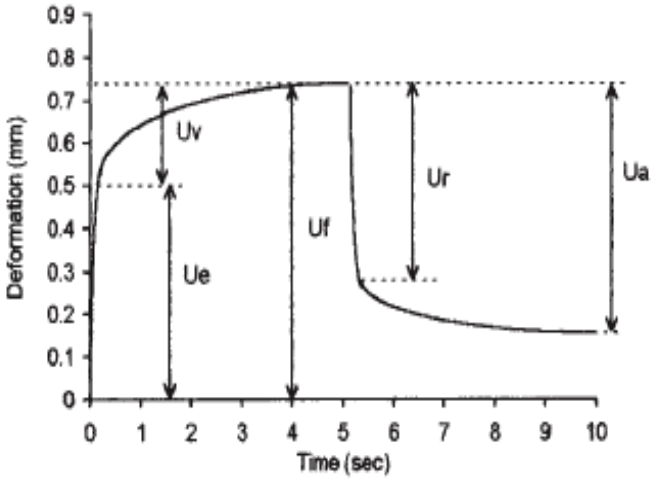

3. PROJECT REQUIREMENTS AND SPECIFICATIONS

3.1 Customer Requirements

Communicating with our sponsors we asked them to define what they wanted out of this project and the device, with this knowledge we set up a list of requirements. We used these requirements to form a survey that we then handed out to the sponsors to gauge which ones they viewed as most important (Table 1).

Table 1: Ranked and weighted customer requirements

Customer Requirement	Relative Importance
Properly Measure Elasticity/Hardness of Skin	10
Accuracy of Properties Measured	10
Ability to Test Any Location on the Body	8
Selectable Testing Rates	7
Product Life	6
Minimize Costs	5
Ergonomics	5
Mobility	4
Computer Integration	3
Testing Time (1 Hour)	3

The highest ranking customer requirements were to measure the skin's hardness, measure the modulus of elasticity, and to obtain accurate results. The measurements of the mechanical properties are essentially the goal of this device; however, what will set us apart is the ability to obtain accurate results. Current testing procedures are inaccurate in that they fail to negate any possible effects from the fatty tissue, muscle or bone. The accuracy of this device and the measurements we obtain will be determined by the range the forces, torques or pressures are run at; the sensors used to obtain the data; and the sampling rate of our data acquisition software. Also there is no one device currently in production that measures both the hardness and elasticity.

In decreasing order of importance, another customer requirement is to have selectable testing rates. For example, when stretching the skin to measure the elasticity of the skin, one can increase or decrease the time it takes to reach the final stretch length. The third requirement is that the device should have the ability to test at any location on the body. The ability to measure material properties of the skin at different locations is crucial since properties can change depending upon this location. The next requirement is the product life, which depends on the robustness of our design. The design must be able to withstand repeated use and configuration. The customer also wants a minimized cost, and we will explore every opportunity to minimize them throughout the design, by carefully selecting what components we will use. Next, the device should also be easy to use; the operator should be able to use the device without any strain and discomfort. Aiding in the ease of use will be the products mobility. The product should be

able to be handled by one person and to fit into a standard 100 square foot examination room. Testing time is also an important requirement from the customer. Testing time on an individual on a patient should not exceed one hour, this will be determined by how easy this is to operate, as well as its mobility, and sampling rate of software. We also need this device to have computer integration allowing for the data being collected to be processed, and for device inputs to be selected, such as testing rates as stated above.

When designing our device we want to make sure that it meets every requirement the customer has asked. However, the most important requirements such as measuring the elasticity and hardness of the skin accurately, easily and cost effectively.

3.2 Engineering Specifications

By determining what we needed to take into account to achieve each of our project requirements, we came up with a list of the engineering specifications. These were discussed while introducing the product requirements, and target values are listed in Table 2. Each of these values was determined through our literature review of current devices in use, and will be used as our benchmark depending on which test method we employ.

Table 2: Engineering specifications and targets

Engineering Specification	Target / Range
Variable Pressure	(-)1 - (-)50 kPa (Target)
Variable Torque	1 - 30 mNm (Target)
Force Applied	Up to 1 N (Target)
Oscillation Rate	10 - 60 Hz (Target)
Adjustable Orientation	360° (In plane parallel to surface) (Target)
Minimize Number of Sensors	6
Data Sampling Rate	100 Hz (Minimum)
Mass Limit	9 Kg (Maximum)
Skin Sample Size	0.1 - 20 mm (Target)
Power Consumption Limit	75 Watts (Maximum)
Medical Grade Materials	N/A

Variable Test Settings

Depending upon which methods of testing are used for the measurement of elastic and hardness properties of skin, it is important to have variable test device settings. Due to the viscoelastic nature of skin, we will need our final device to have the ability to maintain the level of stress applied to the skin analyzed. These stresses must not be excessive enough to cause any damage to the skin or discomfort to the patient while being significant enough to lie within the recordable range of sensors. Therefore, we have researched and produced ranges that lie within the linear portion of existing skin stress-strain data curves for multiple possible methods. The application of a pressurized device should produce a pressure range from 1-50 kPa [1], a torsion device should apply torques between 1 and 30 mNm [5], an extensometer device should apply forces ranging up to 1 N [3], and a dynamic indenter should achieve an oscillation rate (frequency range) of 10-60 Hz [18].

Adjustable Orientation

When measuring skin samples at varying locations, a project requirement, it will be necessary to have the ability to configure the device to both properly contact with the surface and measure at any angle. We have determined that the device will have an engineering specification to achieve full 360 degree rotation in the plane parallel to the skin surface. In addition, we plan to develop a mechanical structure to assist in positioning of the test instruments.

Number of Sensors

Implementation of sensors will be important to the functionality of our device and will improve data acquisition. The specific sensors or gauges to be included will directly depend on which testing methods are adopted for the finalized design. We have developed a target of installing a minimum six sensing components to aid another engineering specification to minimize both costs and complexity. Even though this was set as a target value, we will continue to explore the possibility of further reducing this number by developing common methods of testing for elasticity and hardness.

Data Sampling Rate

Viscoelastic materials, when stressed, will have a total strain including linear elastic strain and creep strain. Because we wish to isolate each of these, a stress will need to be applied at a rapid rate; minimizing the effect of creep rate on linear elastic data. To properly capture results corresponding with the rate of stress apply, a high sampling rate must be used for data acquisition. We have determined that a minimum sampling rate of 100 Hz would be adequate for most testing procedures. Once testing methods are finalized, it will be our goal to maximize this value without producing an excessive amount of data.

Mass Limit

The measurement device and all associated components must be easily operational within a standard observation room (approximately 100 sq. ft.) and, in addition, is required to be mobile. Therefore, we have deemed that the full final design mass should not exceed 9 kg. Through our engineering process, we will consider the minimization of mass for all subsystems we develop.

Skin Sample Size

When comparing analysis for different samples of skin, it may also be important to explore the effect of varied sample size on resulting properties. As per request, we have developed an engineering specification stating that our device will allow for a variable skin sample test length of 0.1 - 20 mm in a direction perpendicular or tangential to applied stress. This will be accomplished by designing the components that interface with the skin sample to be modular, thus, allowing the user to select a specific size by interchanging a single part.

Power Consumption Limit

Our final design will require an adequate power source to power possible components such as DC motors, sensors and mechatronic control modules, and data acquisition systems. Thus, it is important to understand and optimize the power consumption so operation costs can be minimized. In consideration of this, we have set an engineering specification for the upper limit on power rating to be 75 Watts. We intend to minimize this power consumption by selecting highly energy efficient components. This power rating is comparable to small electronics such as various household devices.

Medical Grade Materials

When developing any tool that directly interacts with any part of the human body, it is important to ensure that the materials used pose no threat to the patient. We have formed an engineering specification so that only medical grade materials will be used for components designed for contact with skin. For certain methods of measurement we will also need to consider the use of an adhesive between the test device and skin surface. This must have the ability to maintain a secure bond during testing without causing any damage or excessive irritation.

3.3 Quality Function Deployment (QFD)

By filling out a QFD, we were able to easily determine the relationship between our project requirements and the engineering specifications. The relationship was either strong, weak or none. The QFD automatically calculated the importance of each specification depending on these relationships. The most is important is to select the proper sensors to be incorporated within the design. In decreasing order of importance, the next two are the variable pressure range and skin sample test range. The variable torque range, medical grade materials, applied force to skin, sampling rate, device mass limit, power wattage, followed by orientation to skin surface, still have relatively high importance.

Comparing to the benchmark designs that are currently used, we anticipate our design will win out by achieving our main requirements to accurately measure the modulus of elasticity and hardness of skin. It should also be the easiest to use for an operator. Other products have been around a longer time and have refined designs that are cheaper and lower testing times. A more complete assessment is given in the QFD (Appendix E).

4. CONCEPT GENERATION

The major function of the device that our team focused on is the ability to measure the skin properties. We created a functional decomposition diagram to break the function into many subsystems (Fig. 11). Two of the major sub functions are measure elasticity and measure hardness. Both subsystems were than broken down into smaller sub functions. For our device these two breakdowns are almost identical. However, they were treated different when designing concepts due to the fact that elasticity is mainly measured across the skin surface, whereas hardness is measured into the skin surface.

Both sub functions break into three further sub functions, skin contact, measuring, and actuation. Skin contact is important due to the fact that we cannot apply a large force to the skin when the device is touching. This leads to the sub function of skin detection, for the device and or the operator to know that the device is touching the skin and whether or not there is a significant force applied. For the elasticity it is important that the test maintains skin contact the entire duration, therefore a sub function to adhere to the skin is present.

The sub function of measuring the skin there are two sub functions describing what this device has to measure. These sub functions are force and displacement. These two sub functions supply the data to the operator that is crucial to calculating the elasticity and hardness of the skin. This leads to the sub function of the actuator. In order to measure force and displacement and ultimately elastic/hardness an actuator is required. This actuator has to then translate the power it produces through a guide to perform the desired function. This is regulated by a sub function of limits, which consist of information supplied by the user and possible feedback controls.

From this functional decomposition we have created many different concepts. The methodology we used to create concepts was to make sub system concepts for the elasticity measurement test, the hardness measurement test, Actuation methods, and skin adhesion and detection. These concepts were created to match the customer requirements, along side of taking considerations from methods researched that are currently in use. Pugh charts were made for each sub function. From this, all the concepts of each sub section were ranked from best to worst. Using these rankings, we created five fully developed concepts to further analyze to select the alpha design. All other sub concepts and concepts can be seen in Appendix D.

Figure 11: Functional decomposition of measurement devices

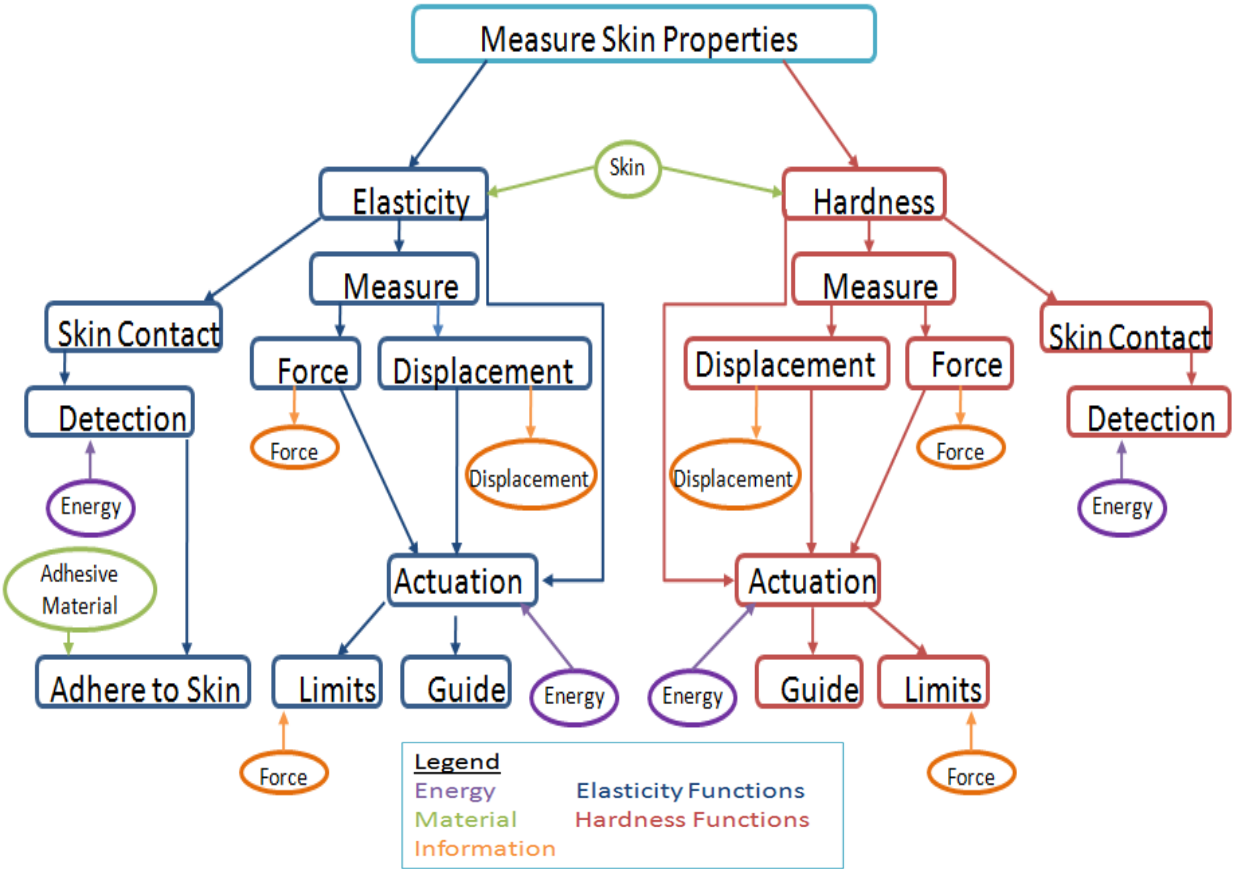

5. CONCEPT SELECTION PROCESS

5.1 Pugh Chart Method

We employed the use of a Pugh charts as a method of evaluating and selecting each of our concept designs. This method of analysis was applied to each subsystem, as defined by the functional decomposition, of our device to determine which concept would be most practical and properly functional. Weighting criteria were derived from both the customer requirements and engineering specifications that directly affected the particular subsystem. These criteria were then individually weighted based on relative importance to the final device. Each concept was analyzed for each criterion and given a rating for each from 1 to 5, 5 representing that the concept best satisfies the condition. By multiplying the rating and weighting for each criteria and concept we were able to determine which concepts best met our customer requirements and engineering specifications. Combination of the best subsystems allowed us to come up with numerous concepts, with the five best described below and the rest shown in Appendix D. The highest overall ranked design was chosen as our alpha design.

5.2 Concept Designs

Concept 1

This concept is powered by a DC motor and has two attachments to measure the properties of the skin. To measure elasticity, the attachment consists of horizontal rack and pinion which converts the rotational motion of DC motor to linear motion used to drive a pin which stretches the skin while the other pin is stationary They are adhered to the skin by cyanoacrylate cement. The displacement and force are measured by displacement and force sensors. The second attachment is an indenter which measures the hardness of the skin. The indenter tip is pressed on to the surface of skin by a screw and the displacement is measured by a LVDT displacement sensor. The sensors are then connected to computer using a DAQ. The attachments are adhered to skin by Hollister medical spray.

Figure 12: DC powered horizontal rack & pinion and screw driven indentation design

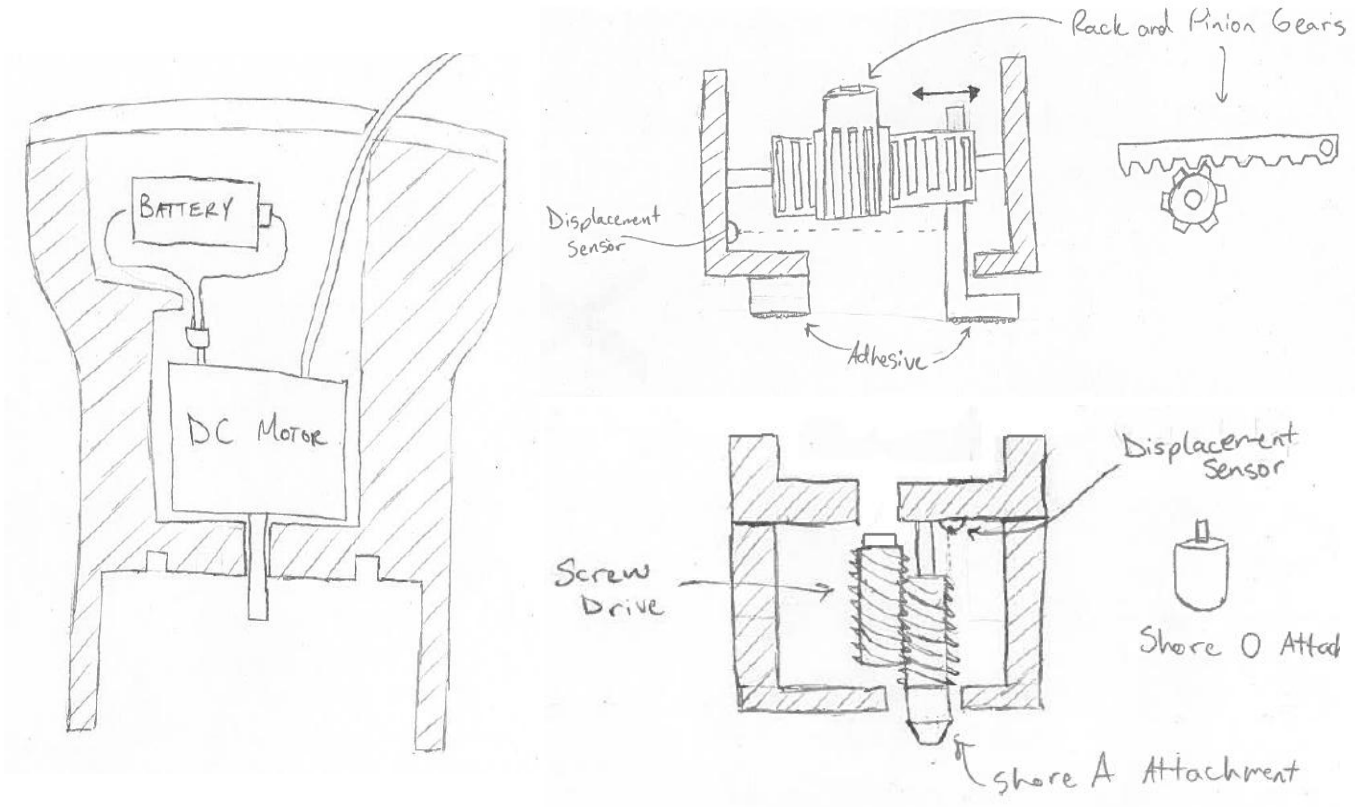

Advantages to this design are that it is a modular device, using the same DC motor for both tests. Also this device has adjustable supports so that the device itself does not negatively impact the results recorded by the test. This device is also highly mobile, allowing for handheld configuration and for testing on any skin location. This also leads to the disadvantage that the stability of the device depends on the user. Due to the modularity of this device material wear and increase in testing time could be an issue that arises.

Concept 2

Two devices powered by DC motor and linear actuator are used to measure the elasticity and hardness respectfully. The elasticity measuring device consists of a pin attached to the rack and pinion. The pin is linearly displaced by the rotational motion provided by the DC motor. Strain gauges are used to measure the displacement and an accelerometer is used measure the force applied. The hardness measuring device has a linear actuator that linearly displaces the indenter and causing deformation on the surface of the skin. Load strain gauges are used to measure the force and displacement and the data is sent to DAQ. They are adhered to skin by medical adhesive.

Figure 13: DC powered horizontal rack & pinion and linear actuated indentation design

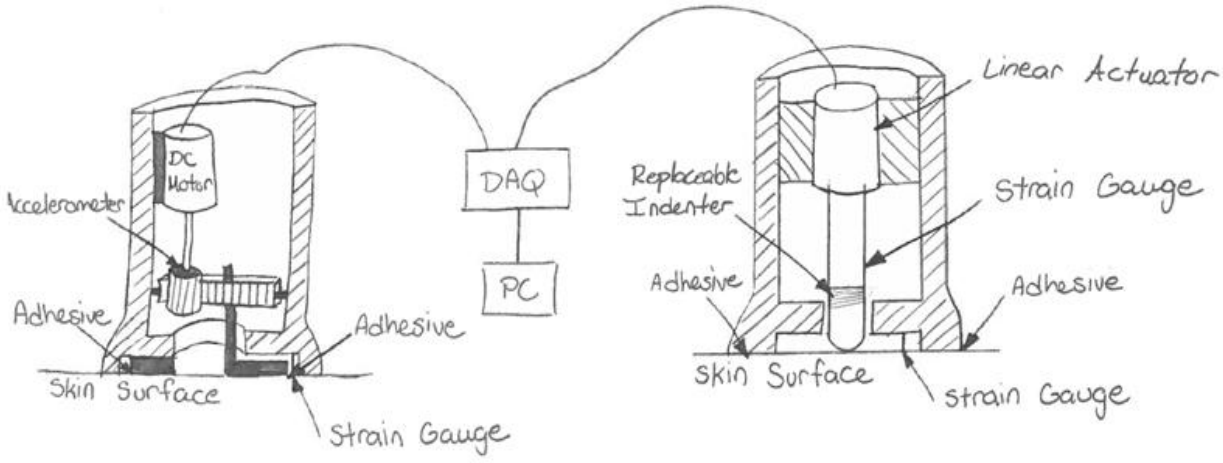

Advantages to this design are that it is a highly mobile device. Due to this it can measure any skin location on the body it also allows for variable testing rates. However, this device is very high in cost due to the device being two separate devices. High cost is also due to the fact that one uses a DC motor, while the other uses a linear actuator. Not using the same actuation method for both measurement tools is not desired.

Concept 3

This device has two attachments. One uses the principle of suction pressure to create deformations in the skin and the second attachment applies pressure to induce indentation. It is placed vertically on the surface of the skin and is strapped down using a double sided adhesive tape. It consists of pressure pump and creates a partial vacuum inside the chamber. A pressure sensor is placed in the chamber and an optical sensor measures the deformation caused by pressure. The initial pressure reading is recorded when there is no deformation in skin. The second attachment the pressure pump applies pressure on a plunger that pushes the indenter downward. The displacement is measured by an optical sensor and the force is measured by a load cell.

Figure 14: Pneumatic suction and indentation design

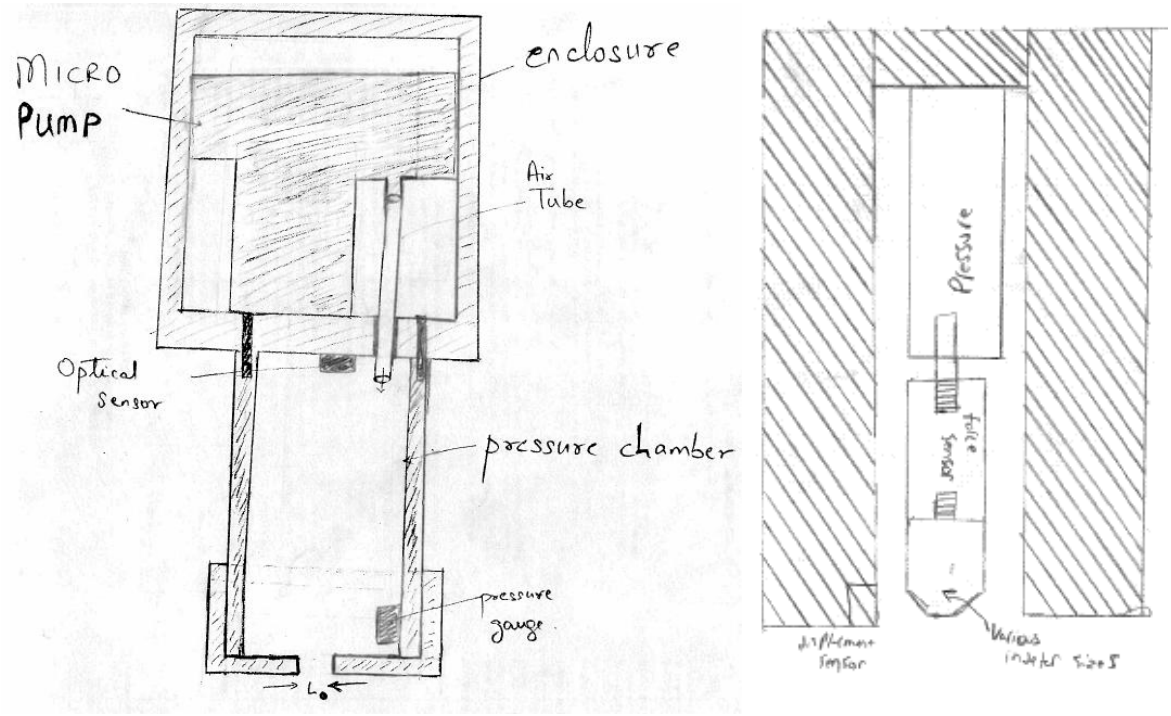

Advantages of this design are that it is modular and could used to measure properties at any skin location on the body. However, maintaining constant pressure will be challenging and hence will make the design complex.

Concept 4

This concept was designed to be a modular device with common attachments to a base. Two separate modules would exist; one for measurement of elastic properties (Young's Modulus) and another for measurement of hardness. The first module would consist of a DC motor driven cylinder used to apply a torque to the skin. Both this cylinder and a stationary outer ring would be adhered to the skin, and the free area of skin between these would be that which is analyzed. Cylinders of various diameters could be interchangeable to gain the ability to analyze different size ranges of skin. The motor would be controlled to ensure a constant torque application during viscoelastic strain of the skin. Angular rotation of cylinder would be recorded via sensors and relayed to the DAQ system in place. The second module would consist of a screw indenter powered by DC motor to measure the hardness of skin. Various indenter tips of different sizes (Shore) can be attached and the displacement caused by them is measured by displacement sensor.

Figure 15: DC powered torsion and screw driven indentation design

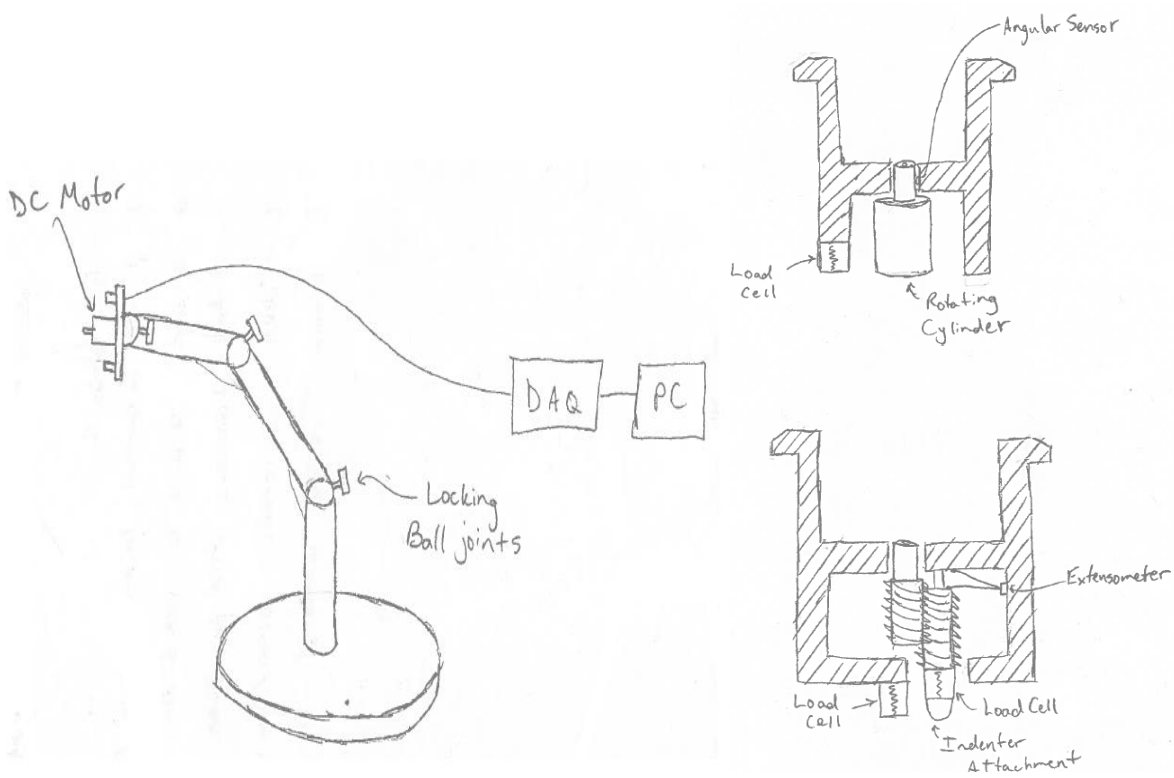

Advantages to this device are that it is modular; sharing a DC motor would reduce cost and design complexity. Secondly, it is attached to a frame allowing for stable placement on the skin taking the operators movement out of the equation. However, this comes with some disadvantages such as this device has to remain attached to its fixture, preventing it from measuring any location of the body without re-orientating the patient. Also, as a torsion device this limits the sample sizes this device can measure due to the method in which the torsion test operates.

Concept 5

A method for measuring the elasticity of skin is by dynamic indentation. This process works by applying a sinusoidal displacement signal onto the skin with a cylindrical indenter. This result in a sinusoidal force being applied as well, only 180º out of phase. Using constant amplitude of motion ranging from 1-10 μm the effects of the underlying layers can be minimized. An impedance head, comprising of a force sensor and accelerometer, is used to measure the magnitudes of force and displacement. The impedance head has coaxial outputs for collecting the data. The impedance head attaches to a linear translation stage that controls the indenter motion. The frequency of the displacement ranges from 10-60 Hz using a fast Fourier transform (FFT). Contact with the skin is determined by measuring the phase angle of the signal at a low frequency (15 Hz). Before contact is made the phase will be constant at 180º and upon contact it

decreases due to damping effects. The stiffness and damping as functions of frequency can then be determined for the elastic and viscous effects, respectively. The Young's Modulus can then be determined from these two quantities. The result will be a complex number, where the real part is due to elastic behavior and the imaginary part is due to viscous behavior [18, 19].

To measure the hardness, the source signal will apply a linear displacement at a constant force. The indenter has to be replaced to a standard shape depending on Shore A and Shore O scales. The impedance head can be used to measure the magnitudes of force and displacement as the indenter presses into the skin. Skin contact will be made once the force sensor in the impedance head reads a non-zero force.

Figure 16: Dynamic and constant force indentation design

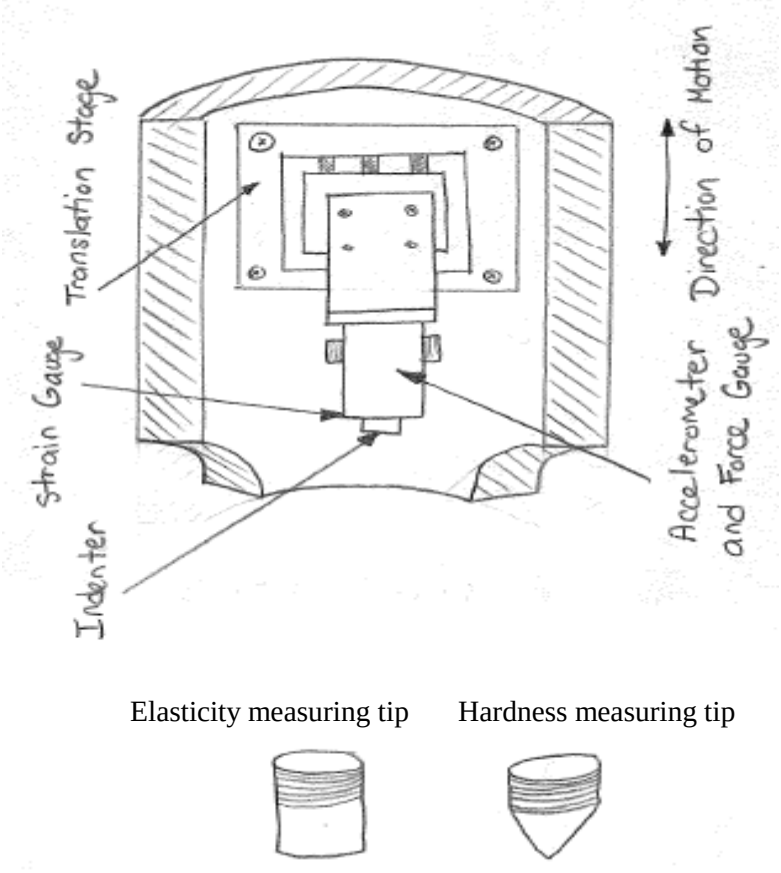

Feedback control is critical for both operations to ensure the desired force is maintained. Feedback is also useful when determining skin contact has been made, and calibrating the device to set that as zero displacement.

Advantages of this design are that it is one handheld device, and there are no modules to interchanges other than the indenter tips. It is good at maintaining the required force, and at variable testing rates. Although it is one device, the design is moderately complex due to the high

accuracy sensors involved. It is not good for measuring skin down the micron level as required. The incorporation of these high accuracy sensors also results in increased costs; translation stages, impedance heads, and load cells are expensive. The design must also consider the cost of a signal amplifier and DAQ.

5.3 Final Concept Pugh Chart

The five concept designs described above were then rated against customer requirement using Pugh chart method shown below in Table.3. This Pugh chart is based off of all the customer requirements, and weighted accordingly to their specification. This table shows that concept 1 was our best design, and will be selected as our alpha design.

Table 3: Pugh chart comparing design concepts to customer requirements

Customer Requirements	Weight	Concept 1	Concept 2	Concept 3	Concept 4	Concept 5
Minimize Costs	5	4	1	3	3	3
Mobility	4	5	3	2	2	3
Product Life	6	3	3	3	3	3
Ergonomics	5	4	4	3	3	4
Test Any Location on Body	8	4	4	4	3	3
Computer Integration	3	5	4	3	4	4
Testing Time	3	4	4	3	4	3
Accuracy of Measured Properties	10	4	4	3	3	3
Measure Elasticity/Hardness	10	5	5	4	4	3
Selectable Test Rates	7	4	5	3	4	4
Total Rating		255	236	197	202	198

6. ALPHA DESIGN

6.1 Common Housing

Through the processes of Pugh chart analysis as previously described, we were able to identify one concept that best satisfies all customer requirements. This resulting design is a modular device with separate modules for both elasticity and hardness testing which attach to a common housing. This housing contains a single DC motor which provides the method of actuation for all testing. The device itself is meant to be handheld, and therefore, configuration is determined by the user. However, this results in reduced stability during testing, dependent upon user ability to constrain motion. To add a method of counteracting this issue, we developed a method of employing moving support arms on either side of the housing. The adjustable nature of these supports allows the capability to determine a reasonable distance from the test area without affecting the results by adding unwanted forces or displacements. Another option is to explore a suspension system within the housing to isolate the testing components from any outside forces by either the operator or patient. One downfall associated with the use of a modular design is the

concern associated with repeated attachment and removal. This could result in both an increase rate of material wear and a longer test time per patient.

Figure 17: Alpha design housing with attached testing module

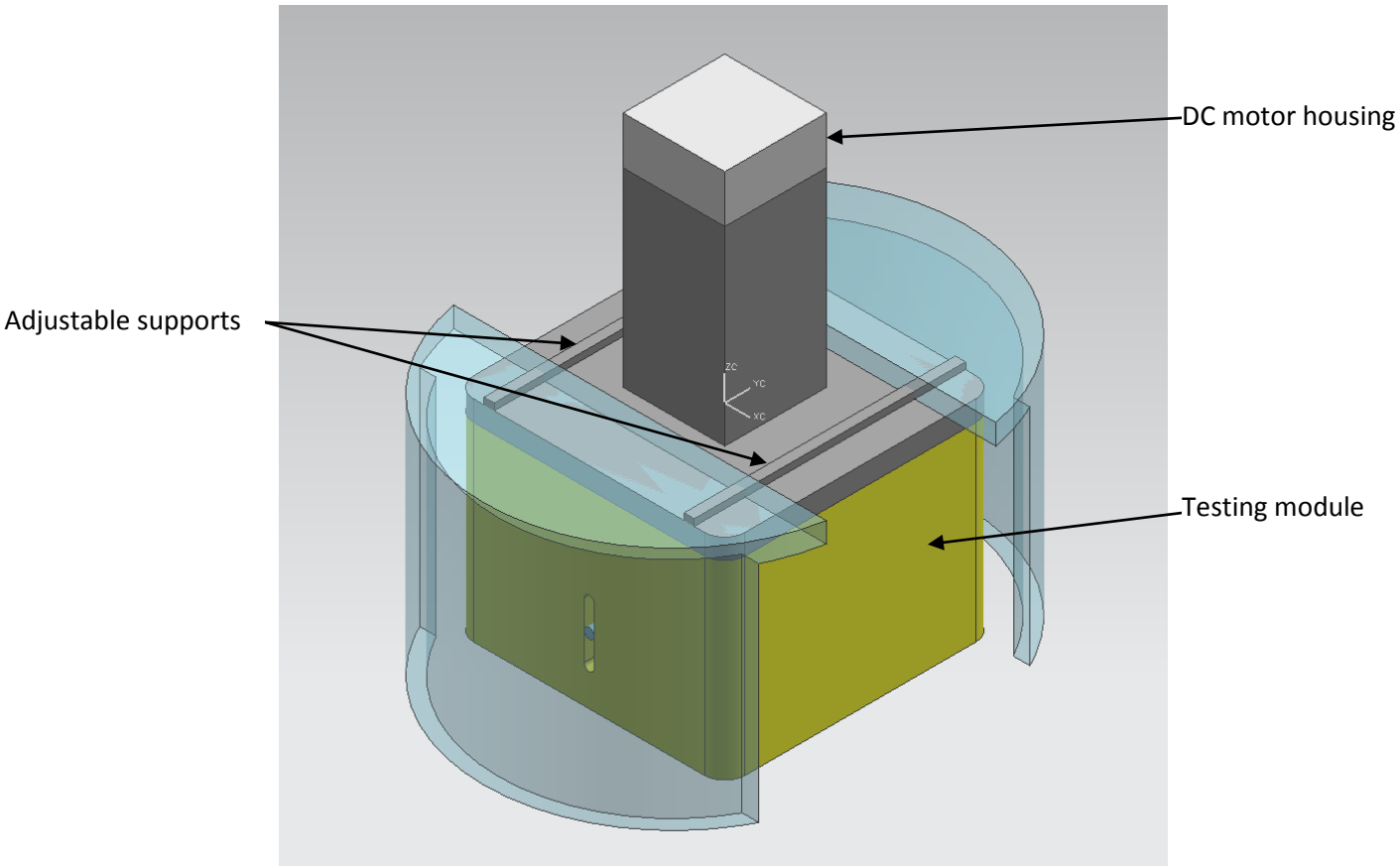

6.2 Elasticity Measurement Module

The measurement module for skin elasticity is driven by a rack and pinion system, which converts the rotational motion produced by the DC motor to a linear motion. Two paddles are adhered to the skin to apply a stress to the test sample. One of the paddles is fixed to the exterior of the module, while the other is fixed to the moving rack. Our proposed method of displacement measurement would include the application of two accelerometers, attached to both the module and the rack. This decision was made to accommodate for slight movements made by the user which could affect a displacement reading made by another gauge such as an extensometer. With these two displacement readings, it would be possible to isolate the actual movement of the rack from that of the entire module. Measurements of applied force would be acquired using the application of strain gauges oriented about the pin attaching the moving paddle to the rack. Additionally, skin contact force sensing would be achieved through the use of a load cell attached to the base of the module, in-line with the paddles. This would provide feedback directly to the user and notify them whether or not proper contact is maintained throughout test procedures.

Figure 18: Cross-section view of elasticity measurement module

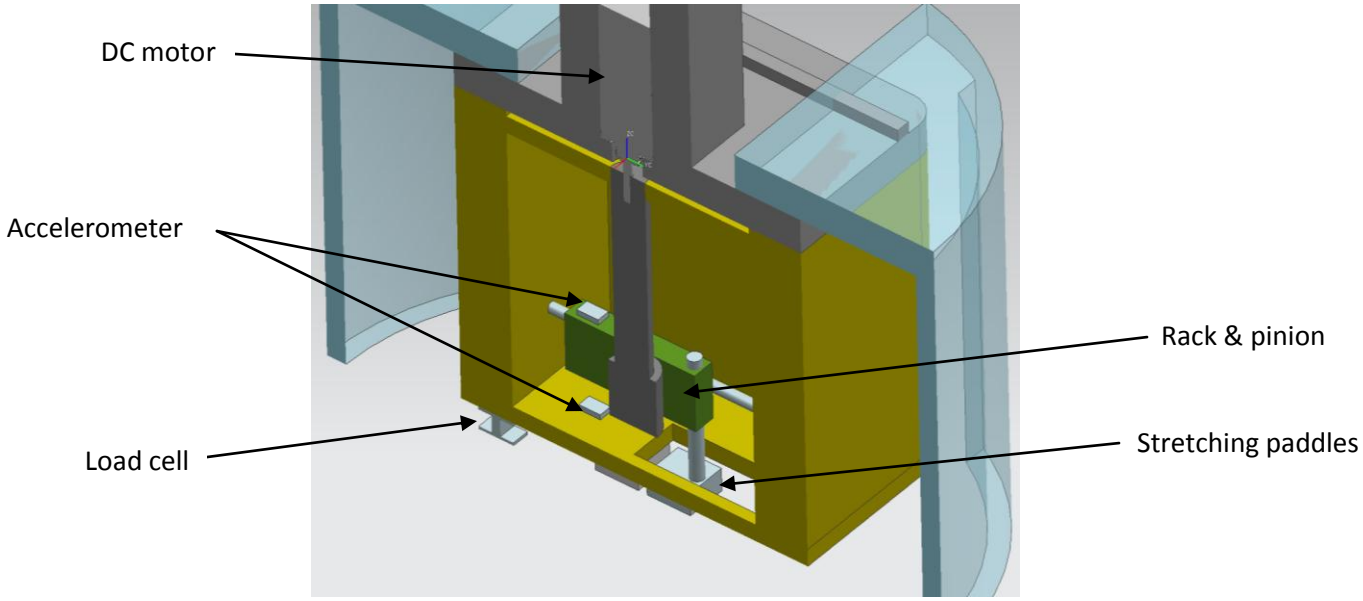

6.3 Hardness Measurement Module

The measurement module for skin hardness employs the use of a screw driver sheath component for actuation. This component converts the rotational motion of the DC motor to a vertical indentation motion. The indenter component of the design would be developed to accept tips of varying size and shape. Displacement, as similar to the elasticity module, is proposed to be measure using two accelerometers to isolate the vertical indentation motion from that of the module. A load cell would be installed between the indenter tip and the moving sheath to obtain measurement of force applied to the skin. Again, as with the elasticity module, a contact sensing load cell would be positioned on the bottom of the housing.

Figure 19: Cross-section view of hardness measurement module

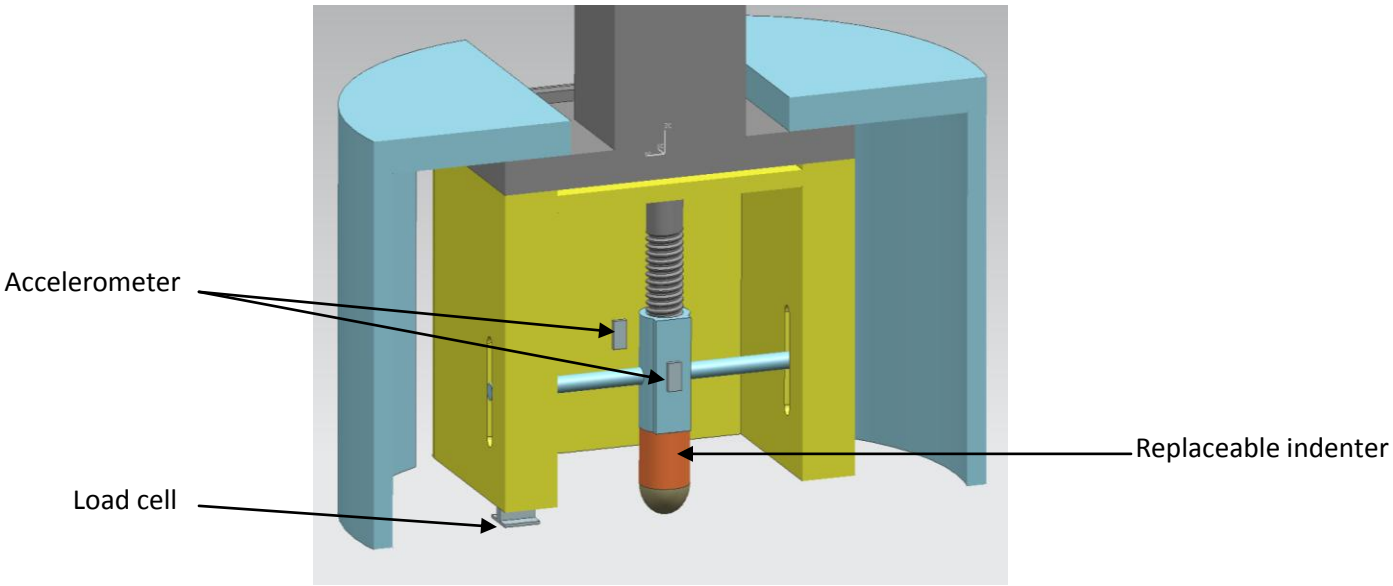

6.4 Data Capture Method

Using software, such as LabVIEW, on a PC we can control the functioning of the device using the feedback provided by the sensors. An example would be the load cell which detects skin contact, and can be calibrated to zero the displacement when this occurs. Other sensors will provide information on the force and displacement for each test and allow us to calculate the required properties. A DAQ converts the analog data provided by the sensors to digital values that can be manipulated by the PC. A signal amplifier is simply used to increase the amplitude of the signal.

7. ENGINEERING ANALYSIS

7.1 Applied Fundamentals

Continuous research in the field of material science will be exceedingly beneficial to further development and understanding of our project. We are currently using information from this field pertaining to the modeling of viscoelastic materials, which we intend to apply to skin analysis. One common viscoelastic model (Fig. 20) describes such materials as a spring and damper system. Under a constant stress (σ), the material will exhibit an instantaneous elastic strain (ε_e) (Eq. 3) and a time (t) dependent transient creep strain (ε_{tc}) (Eq. 4) [20]. It is our goal to use our resulting data to isolate the elastic strain from the total strain (ε), and determine the Young's Modulus (E_1).

Figure 20: Strain versus time behavior for viscoelastic model [20]

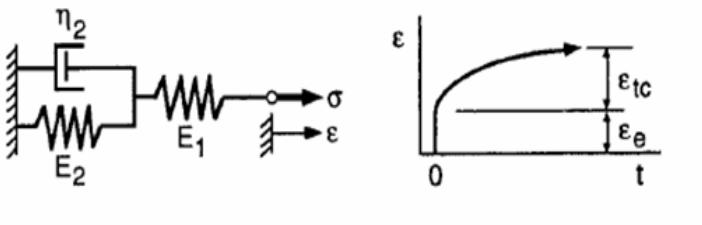

$$\varepsilon = \varepsilon_e + \varepsilon_{tc} \tag{2}$$

$$\varepsilon_e = \frac{\sigma}{E_1} \tag{3}$$

$$\varepsilon_{tc} = \frac{\sigma}{E_2}\left(1 - e^{-E_2 t/\eta_2}\right) \tag{4}$$

Where η_2 is the viscosity and E_2 is the Young's Modulus of the viscous portion.

7.2 Calibration

When developing measurement devices, it is important to calibrate all gauges and sensors to maintain result accuracy and repeatability among tests. It may also be necessary to include an option of on demand calibration to assure the user that correct data is recorded. Before any testing, we plan to perform a calibration for all measurement components. For measurements of displacement, zero points and upper bounds on total movement must be established. With our plan to implement gear and screw systems, the voltage input to the DC motor must be timed with the corresponding pitches. In addition, adjustments will need to be made to the control system we develop to ensure that over-stressing and control instability will not occur.

7.3 Testing Method

Once the device is calibrated, we will perform both elasticity and hardness testing. It will be important to carry out these initial tests on known materials, to confirm that properties are measured properly. Various size ranges and test rates will be analyzed for these materials to further verify the full capabilities desired. As different size ranges are examined the forces applied must be scaled to maintain a constant stress applied between tests. We have determined that the stress applied during an extension test should be approximately 65 kPa [3] and an indention test should be 900 kPa [22]. Further testing and analysis will need to be done to develop a correlation between various sized indenter tips. This will allow us to confirm that consistent hardness ratings are recorded by each.

8. ENGINEERING DESIGN PARAMETER ANALYSIS

After design review many items regarding the alpha design needed to be addressed, and a plan to correct them had to be made. This involved many aspects of the concept itself. One big factor that changed our alpha design was complexity. We needed to minimize complexity as much as possible. One way we achieved this was by splitting the elastic device and hardness device into two separate units. Instead of being modular by a single motor they are now modular by motor control system and data acquisition. However, doing this increased the cost of the device, now needing two motors and two sets of device housings. We believe this cost increase was a necessary sacrifice in order to maintain device robustness. In separating these two devices from each other we left the actual function of the mechanical system close to unchanged. However, this is not the case with the housing. This separation gave our team the ability to minimize housing size according to the internal components of the device (rack and pinion system of the elastic device, and screw indentation of the hardness device). Alongside of this major change were functioning changes of the devices them self. This information and full analysis is broken down in detail in Sections 9 and 10.

Design of the control and electrical system (Section 11) has changed greatly since design review 2. First off, in our alpha design it was proposed to use a single DC motor for position control.

However, to be able to move precisely to micro level movement it was decided that using two stepper motors (one for each device) was appropriate, since the stepper motor can be told to move a certain amount of steps which translates to a specific rotational distance. To control this stepper motor we also had to research and determine a control system.

We originally presented different types of sensors that would be utilized in our system to capture the required data needed for our project. It became apparent after design review 2 that accelerometers were not an appropriate choice of force measurement. Through research it has been determined that load cells would be a more appropriate choice. However, purchase of a load cell is expensive, and it was decided that strain gauges would be utilized to build our own load cells. The strain data can then be converted to stress or force.

We also had to design a complete circuit system to connect the strain gauge system to a data acquisition system. This circuit required a lot of research and analysis to make sure the data being read by the data acquisition. First, a data acquisition device had to be chosen to meet engineering specifications. Secondly, appropriate circuit decisions had to be made such as wire gage, how the signal from the gauges will get amplified, and how they will make it to the data acquisition device without receiving noise making rendering the data useless.

Also analyzed was the computer integration into the entire device, along with safety measures taken. These two items are dependent on the type of software the motor control uses and what the strain gauges use. A full description and analysis of this can be read in Section 11.

9. FINAL DESIGN DESCRIPTION

Through engineering analysis and a detailed design process, our original alpha concept has been further developed to best meet both functional and technical requirements. Throughout our process of improvement, we considered the optimization of many features of the design including device stability during testing, precision adjustments, ease of manufacturing and assembly, and component packaging. These features greatly impacted and are apparent in the final versions of both measurement devices.

9.1 Elasticity Measuring Device

Figure 21: Elasticity measuring device cut section

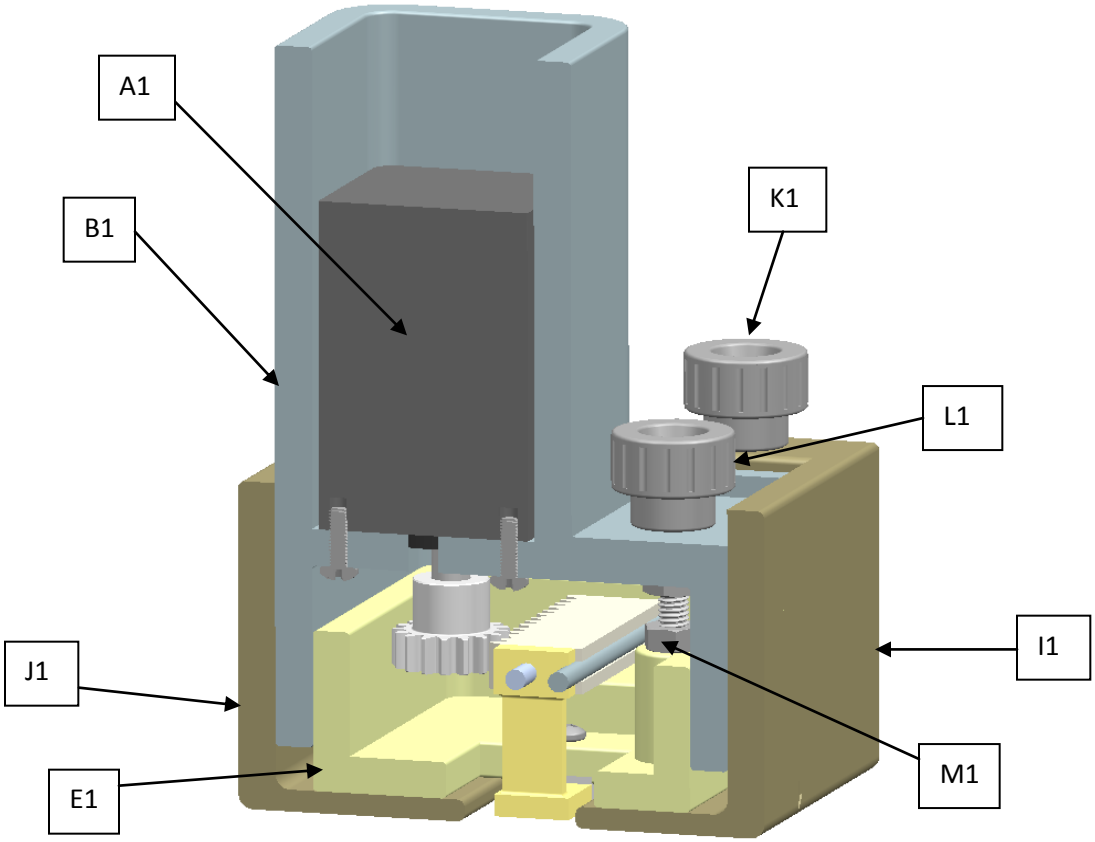

Figure 22: Elasticity measuring device internal components

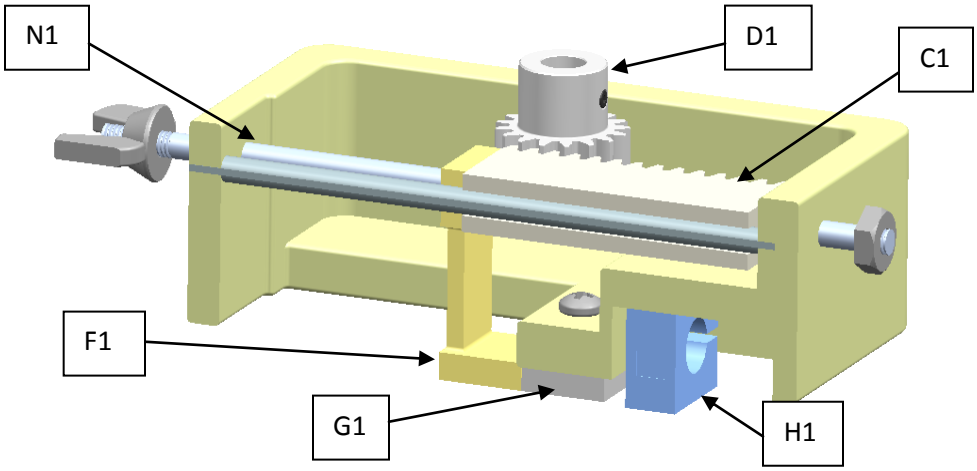

The intention of the elasticity testing device is the proper measurement of the elastic modulus of various skin samples at selectable sizes and force applications. Our device will accomplish this by applying a constant force to the sample and measure the resulting change in length and corresponding axial strain. Thus, we have developed a rack and pinion system capable of producing the desired load cases and motion. This type of system is implemented to convert an input of rotational motion, provided by a stepper motor (A1) in our design, to that of a linear horizontal motion. The stepper motor is fixed to the upper housing (B1) of the model by four machine screws and is contained within the hollow section that is meant for gripping by the user.

The rotation is directly applied to the rack (C1) through the use of a stainless steel spur gear (D1). This gear is connected to the shaft of the stepper motor and maintained in position with a set screw included by the manufacturer of the gear. The rack, which is made of carbon steel, is suspended by two separate stainless steel shafts which run along the entire length of the lower housing (E1). One of these shafts runs through a hole machined into the middle area of the rack constraining the motion to one axis. The second shaft, running through a slot machined along the edge of the rack, provides stability by preventing any rotation of the rack about the first shaft. These design considerations aid in the assurance that the gear and rack will not bind during actuation. However, with these shafts, it will also be important to machine the holes in accordance with a close-running fit [27] to allow for accurate positioning while eliminating the possibility of sticking at low speed motion. A silicon based lubricant can also be used to further reduce the coefficient of friction between the surfaces.

As the rack moves along these shafts, it also propels an L-shaped paddle (F1) made of ABS plastic. This paddle is fixed to the rack using a dissimilar-material epoxy and has similarly machined holes for motion along the two shafts. The stretching motion is ultimately created by adhering both this moving paddle and an aluminum stationary paddle (G1), fixed to the lower housing with a machine screw, to the test surface and actuating the system. Resulting strains in the moving paddle are recorded by the configured strain gauges as this occurs and are converted to force values by the data acquisition system. This force recorded will be representative of that which is being applied to the test surface. Rather than using various displacement sensors, it was decided to use the recorded number of steps moved by the stepper motor as the method of measuring linear motion. Not only does this design option considerably reduce the project cost, but also the complexity of the system by limiting the number of components needing to be mounted in a constrained volume.

When applying the device to a test surface, it will be important to know that an unwanted level of force is not being applied normal to the surface. Therefore, a “C” style load cell (H1), made of ABS plastic and using a single strain gauge configuration, was implemented in the design of the final device. The bottom surface of the load cell aligns with the bases of the two paddles such that it will properly measure the force of any contact surface in the same plane. A single strain

gauge model was selected due to size constraints on the design of the load cell and the lack space available between other components.

To maintain even and stable contact with the test surface during experimentation, our design incorporates the use of two separate support structures (I1, J1). In an optimal setting, these supports are designed to be in plane with the surfaces of the moving and stationary paddles. When analyzing various locations on the body or different size scales, it will be important to the user to have the ability to change the distance of these supports from the test area. Thus, we have designed this component to have an adjustable range of 12.5 mm. Control knobs (K1) will be used for tightening and loosening the upper arms of the supports allowing for locking configurations. The upper arms are guided by a slot track formed into the upper housing surface.

The final main feature of the elasticity device is the ability of the user to adjust the height of the paddles and load cell relative to the supports. This aspect of the design allows the user to respond to the feedback provided by the load cell and reduce the load applied to the test surface. Our design accomplishes this through the use of an additional control knob (L) which is threaded through a nut (M1) which is fixed to the surface of the lower housing section with epoxy. The shaft which runs through the assembly (N1) and the slot in the side wall of the upper housing are designed to limit the vertical adjustment to 3.2 mm. This motion is limited to prevent interference between components and wiring from the strain gauges and the loss of gear tooth engagement between the rack and spur gear.

9.2 Hardness Measuring Device

Figure 23: Hardness measuring device cut sections

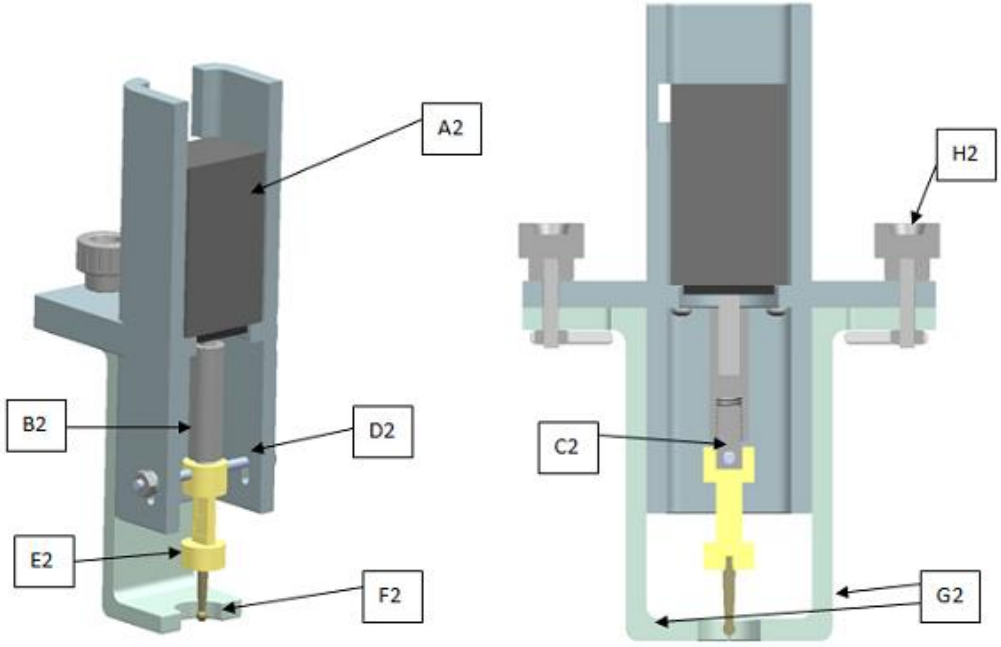

The intention of this device is to measure the relative hardness of the dermis layer of skin at varying locations on the body, load applications, and with differing indenter tips. Our device will accomplish this by applying a specified normal force to the test surface and measuring resulting indentation into the material. Therefore, we have developed a system of threaded shafts which will allow for this prescribed motion. With this, an input of rotational motion, again provided by a stepper motor (A2), is converted to a linear vertical motion. The stepper motor is fixed to the main housing component through the use of four machine screws and sets within the area designed for handling of the device.

This rotation is directly transferred to the zinc coated steel upper shaft (B2) of the system which is fixed around the motor shaft through the use of a set screw. This upper shaft has female threads on its bottom end to allow mating with the second shaft (C2), a partially threaded carbon steel rod. A pin (D2) running through this second shaft prevents it from freely rotating, therefore resulting in a vertical screw motion. This motion is ultimately limited by the guide slots through which the pin slides. A range of indentation up to 5 mm was selected to be greater than that of the average thickness of the skin (2 – 3 mm) while remaining low enough to avoid levels of indentation which could be harmful to the patient. The load cell for measurement of applied force (E2), made of ABS plastic, is attached to the second shaft and held fixed by the same pin. This mates with the indenter tip (F2) through a drilled and tapped hole. The user then has the ability to easily interchange indenter tips with varying tip diameters.

During testing, measurements of strain due to indentation are recorded by the strain gauges configured on the flat area on the load cell and translated into force values by our data acquisition system. These values directly correspond to the force applied to the test surface by the indenter tip. Values of displacement are again determined by tracking the steps taken by the stepper motor and converted into linear motion values based upon the threading of the two shafts.

Similar to that of the elasticity measurement device, the hardness device also contains a system of adjustable supports (G2) to improve stability during testing. These again are positioned along a track formed into the main housing and so as to guide the sliding motion of both components. Control knobs (H2) were added into the system to allow the user to loosen or tighten the supports to ease the method of positioning. The motion of each of the supports is limited by a slot giving a total motion range of 12.5 mm. In addition, the user can choose to invert the support orientation to result in a considerably greater distance from the test area for applications of larger body locations.

10. FINAL DESIGN ANALYSIS: MECHANICAL SYSTEM

10.1 Material Analysis

10.1.1 Material Selection and Manufacturing Process Using CES

We implemented the use of CES software to aid selection of the housing material and load cells. Most of the mechanical components for our design are purchased and require small amounts of machining to thread or cut to length.

We began by constraining certain elements of our housing design, and created a resulting plot of material elasticity against density. The first criteria were to limit the density of the material to be no more than 1720 kg/m^3. This value was determined by summing the mass of all the components in our design and determining what mass for the housing will allow the device to remain easily held by one hand, the result was 250 g. The volume of the housing was found to be 1.32×10^5 mm^3. A customer requirement was to minimize cost, so we selected an appropriate price range was \$0-\$5/kg. A toughness rating of 100 kJ/m^2 or more will prevent fracture of the device if it were to accidentally be dropped. A higher material index is also desirable, meaning for low densities we want a large elastic modulus. The final criteria is an observation, as opposed to quantification, can the available material be formed with the resources we have available.

Figure 24: CES plot of materials that meet defined criteria for housing

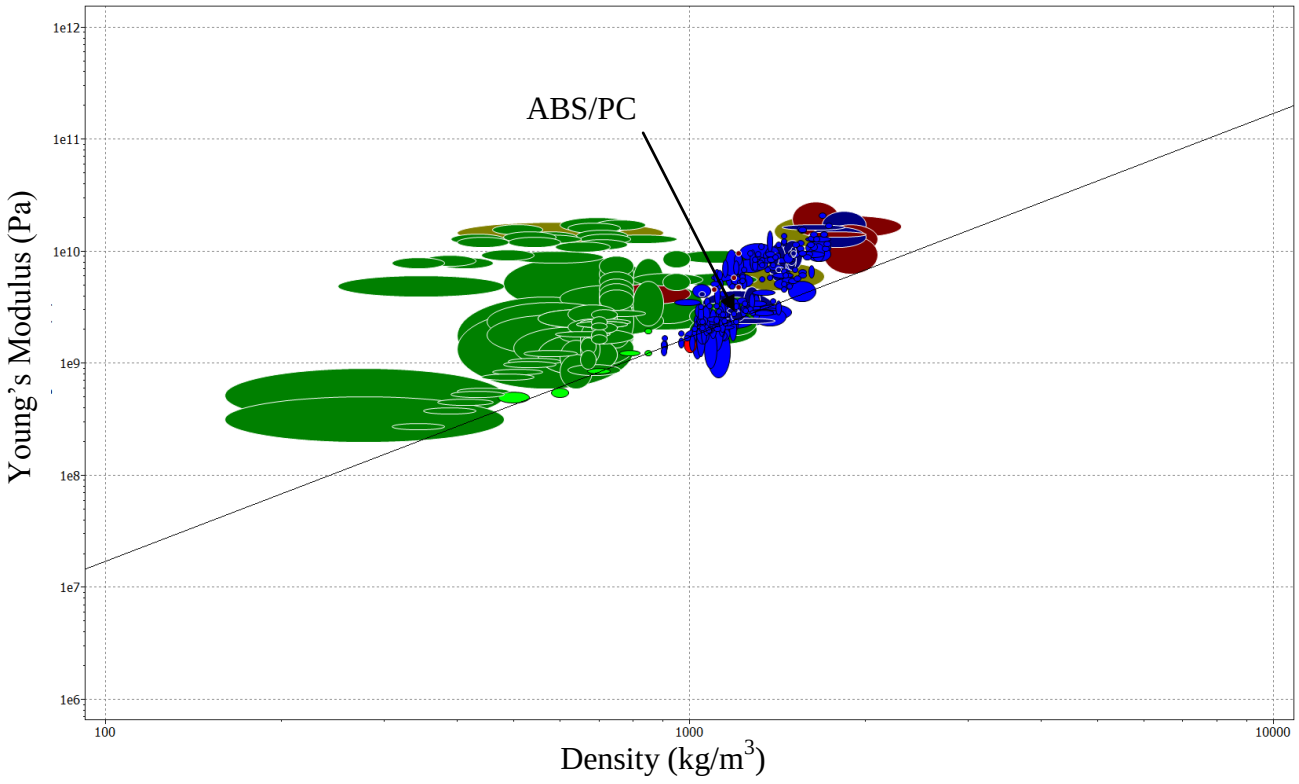

In Figure 24, the green materials are wood products, the reds are glass composites, and the blues are plastic materials. The green and red can be discarded after reviewing our fifth criteria of manufacturability. We are left with a multitude of plastic materials to choose from: PEM, PVC, and ABS to name a few. We selected ABS/PC for our design primarily because of its availability of on campus at the UM3D Lab for rapid prototyping. The design would take a total of 55 hours to complete and can be run overnight; however, it displaces the manufacturing time from our group to the laboratory technicians. The focus of our team could then be shifted to fabrication of other mechanical and electrical components. The rapid prototyping offers excellent precision with tolerances of 150 µm over a 200 mm range, can make the complex shapes, and there is no material waste.

CES was also used for material selection of the load cells, with a more complete analysis given in Appendix C. Each load cell was limited to a maximum material cost of $5. The bending load cell was also designed to withstand 0.1 mm deflections and 1 N loads. The indentation load cell was designed to withstand compressive failure and buckling from loads of 8 N. The results were similar as the test for the housing, with a majority of the materials being plastics. ABS/PC was chosen again because of its availability, resulting in saved time and costs from not having to send work out.

An analysis of mass production was then undertaken on the load cells, assuming 1 million units will be sold. According to CES, the ABS plastic can be either extruded or injection molded. Injection molding was chosen as the best route because of its low labor cost, repeatable high tolerances, minimal material waste, ability to make complex shapes, and no finishing after molding.

Other options we looked into were purchasing premade housings from an online seller, but we were unable to find anything suitable with our design dimensions. The use of large blocks and machining through CNC would cost $400 for ABS, $230 for PVC, and $300 for aluminum. The quote for rapid prototyping is $160, significantly cheaper than any of the other options.

10.1.2 Environmental Impact Using SimaPro

The two load cells that were used in the previous section's CES analysis were then input into SimaPro to determine the life cycle impact each would have on the environment. Since each load cell is made from the same material, the results will just be scaled depending on the mass of each component. In this case, the bending load cell has a weight of 0.80 g and the indentation load cell has a weight of 2.01 g. Raw material usage is 1.234 g and 3.085 g for the bending load cell and indentation load cell, respectively. Air emissions were by far the highest value at 2.977 g and 7.442 g. Water emissions are much lower at 0.105 g and 0.262 g. Soil pollution has the smallest emissions and is a factor 1000 less at 0.142 mg and 0.356 mg.

In comparing to several different categories of environmental damage, the bending load cell has 40% of the impact as the indentation load cell. The cause for this number is that it is 40% of the mass. The damage can be classified into the following three areas: human health, eco-toxicity, and resources. The load cells can be compared against each other for each category, and in both cases human health was the biggest factor, followed by resources, and then eco-toxicity. Summing up the values for each category allows each load cell to be compared to each other, resulting in the indentation load cell having over twice the impact.

Due to the small masses required, the environmental impact is not that severe, but is not negligible. If a larger amount were needed there may be adverse effects we would have to consider. The design strictly limited in the number of available materials because of the Young's modulus that was necessary.

10.2 Hardness device

10.2.1 Adjustable Supports Analysis

When analyzing the structural integrity of the indentation device, we believed it to be necessary to determine the expected deflections in the support system. This component was expected to be the weakest section of the design and would need to support the weight of the other parts during testing without any major deflections. Therefore, we performed a static FEM (Finite Element Model) analysis to determine both deflections and stresses in the supports. The model was generated in Hypermesh v10.0 using 6778 second order tetrahedral elements. Material properties for ABS plastic were defined with an Elastic Modulus of 2.9 GPa and a Poisson's Ratio of 0.387. The model was held constrained at both the areas of loading and contact with the test surface. A distributed load of 3.1 N was applied to simulate the gravitational effect of the weight of the remaining components. The built-in solver Optistruct was used to produce simulation results for this static load case.

Figure 25a: Contour plot of displacement in supports under distributed 3.1 N loading

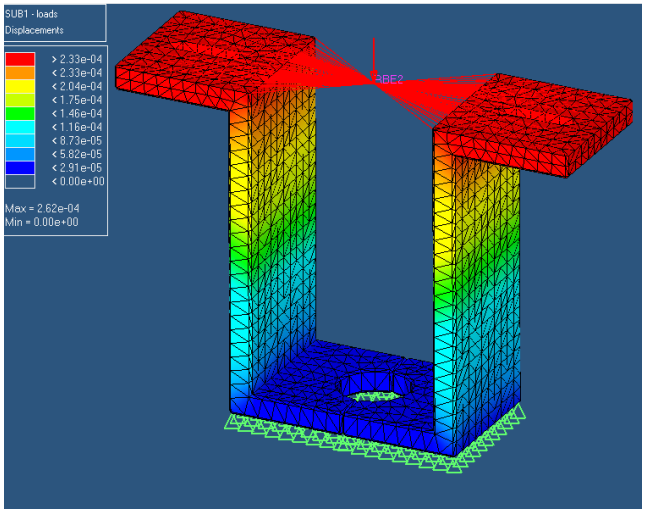

Figure 25b: Contour plot of von Mises stress in supports under distributed 3.1 N loading

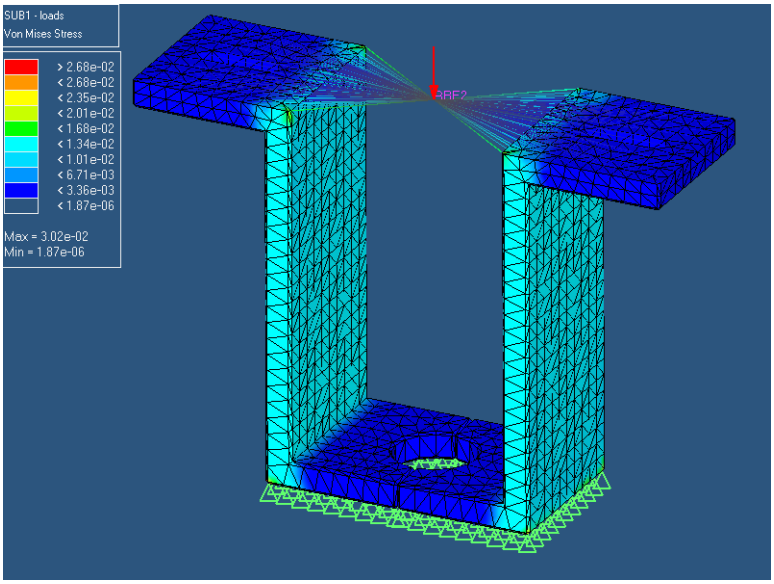

Thus, we have found that under these conditions, we should expect a maximum displacement of .26 microns and maximum stresses at 17.1 kPa. Both of these results show that the designed components will not only have an insignificant effect upon the displacement of the indenter but also fall considerably below the 65 MPa yield stress of ABS plastic with a safety factor of 3800.

10.2.2 Indentation Load Cell Analysis

The load cell for the hardness measurement device was also determined to be another component necessary to analyze using finite elements to determine resulting stresses and displacements. This will not only assure us that the design will not fail during use, but also give an estimation of the strain encountered by the mounted gauges. A model was created in Hypermesh v10.0 using 7144 second order tetrahedral elements. Material properties for ABS plastic were again defined with an Elastic Modulus of 2.9 GPa and a Poisson's Ratio of 0.387. The model was held fully constrained at the location of interaction between the load cell and male threaded shaft. An 8 N load was applied at the location of the indenter tip to simulate our max loading condition. Optistruct was used to produce static loading results.

Figure 26a: Contour plot of displacement in supports under 8 N loading

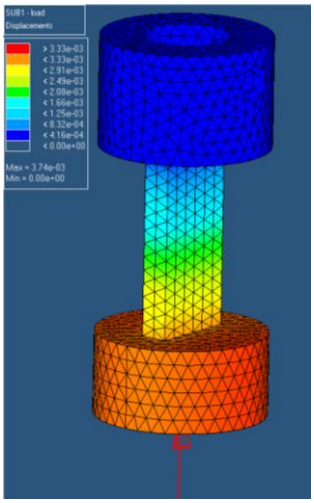

Figure 26b: Contour plot of von Mises stress in load cell under 8 N loading (cross sect.)

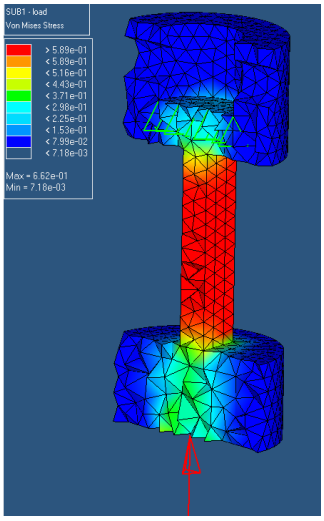

Under this loading condition, it was found that a maximum displacement of 3.74 microns and maximum stresses of 662 kPa will result. Therefore, this component will survive our estimated max loading with a safety factor of 98 before plastic deformations occur.

10.3 Elasticity Measuring Device

To determine if a paddle, made of ABS plastic, with a thickness of 2mm is sufficient, utilization of the beam deflection formula was needed. This calculation is as follows:

$$\delta = \frac{4FL^3}{Ebh^3} \tag{5}$$

Where F is the maximum force applied to the paddle, this is assumed to be 1N, L is the total length of the paddle (16mm), E is the elastic modulus of ABS plastic (2.3 GPa), b is the width

(10mm), and h is the thickness (2mm). It was then determined that the maximum deflection of this beam would be 89 micron. This value insures that the bean will not deflect too much too affect the strain data, and will not permanently deform the paddle. An analysis of this paddle in respect to the stain gauge system is located in Section 11.

The friction force between the rack and the rods passing through will play an important role in the elastic device. As the actuation is provided the gear will turn and the rack will slide on it. In order to calculate friction force the following equation was used.

$$F = \mu mg \tag{6}$$

The friction was calculated for both with and without lubrication applied. It was found using the lubrication will significantly decrease the friction force created due to sliding (Appendix G).

A finite element analysis of the moving paddle component of the elasticity measurement device was determined to be important so possible stress issues under loading could be addressed. The model was generated in Hypermesh v10.0 using 6964 second order tetrahedral elements. ABS plastic material properties were defined with an Elastic Modulus of 2.9 GPa and a Poisson's Ratio of 0.387. The model was fully constrained at the interaction between the paddle and the gear rack and constrained in the vertical direction at the interaction between the paddle and skin surface, simulating perfect adhesion. A max estimated 1 N load was applied to the base of the load cell to simulate a stretching force applied to the skin. Optistruct was used as a solver to produce von Mises stress results.

Figure 27: Contour plot of von Mises stress in paddle under 1 N loading

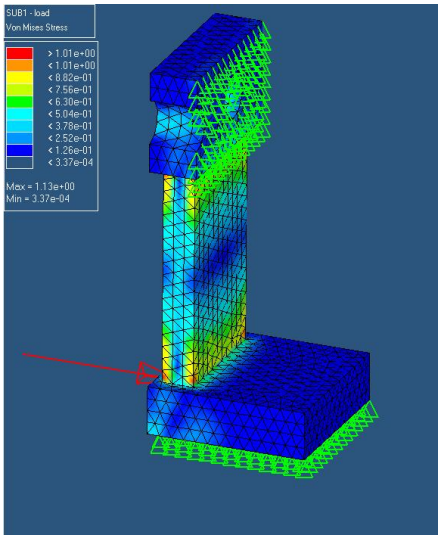

It was therefore found that maximum stresses under this loading condition are expected to be 1.13 MPa. This results in a safety factor of 57 on force application before the onset of plastic deformation and component failure.

11. FINAL DESIGN ANALYSIS: CONTROL AND ELECTRICAL SYSTEM

11.1 Actuation System

Utilizing an appropriate actuation system for each device is critical to having a functional prototype and final product. Unlike in our alpha design (Section 6), our devices will be using a stepper motor. To make sure we selected the most appropriate stepper motor and driver/control system for it, we analyzed multiple solutions. This section will analyze the selected stepper motor and driver/control system and state why they were selected.

11.1.1 Stepper Motor

For our prototype it has been determined that we will be using two stepper motors, one for each device. The motor we selected is a Pololu Bipolar 28 x45 mm Stepper Motor (Fig. 28) [28]. This motor has a rating of 1.8° per step. It also has a draw of 670 mA at 4.5V. Having a step size at 1.8° is useful, allowing us to have smaller stepping range when micro stepping, explained in the next section. This small stepping size is the smallest found in the motor size price range we are designing for, which makes it suitable for our prototype. The stepper motor is rated of maximum torque capability of 91.8 mNm. From this we did an analysis by calculating the maximum toque that would be applied by our system if a 1N load was subjected. To perform this calculation we simply broke down our analysis until the formula was:

$$T_{max} = F \; x \; R_{Gear} \tag{7}$$

Where, R_{Gear} is equal to the radius of the gear which is 8 mm. Thus the maximum applied load to the system is 9 mNm. This creates a safety factor of 10, allowing us to assume that with this safety factor the stepper motor will never skip a step. However, there are other elements of torque in the system, but these values are minor, and with a safety factor of 10 will not affect the performance of the motor. Since this motor will not miss a step we decided that we can then measure the actual displacement from each device by recording how many steps the stepper motor moves. Doing this eliminates the need for expensive displacement sensors which can be $100+ each, and maintains a satisfactory amount of accuracy. It can then be said that this motor satisfies requirements and specifications that have been set.

Figure 28: Pololu bipolar stepper motor & dimensions

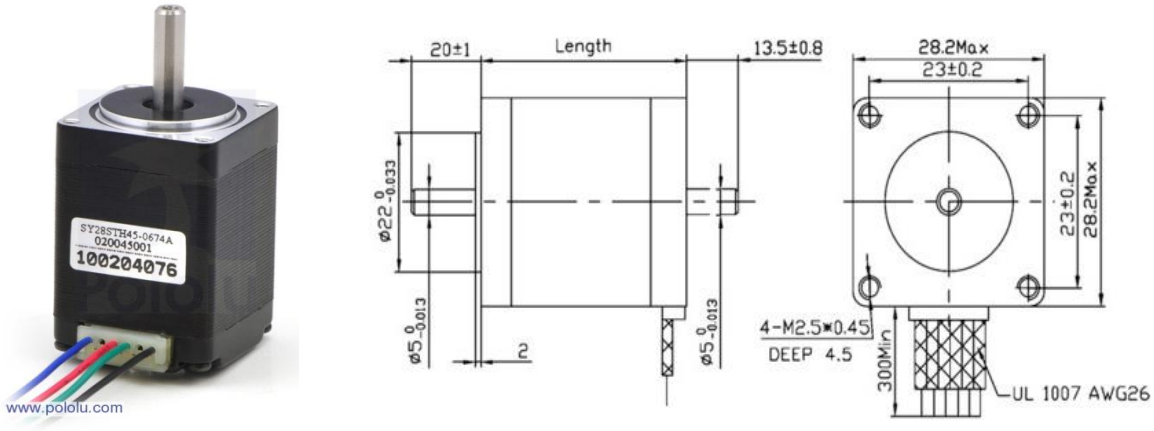

11.1.2 Driver / Controller System

After reviewing various types of driver/ control system we decided to use the Advanced Micro Systems (AMS) driver / control system, DCB-261 (Figure 29) [29]. This driver control system is fully compatible with the stepper motor described above. Allowing for a maximum 1A adjustable phase current, this is above the motors required phase current. It also has the voltage capability to supply 4.5 volts to power the motor. This system also has over 30 motion commands allowing us to move the motor precisely how we need it to move. A full block diagram of this driver/control system can be found in Figure 30.

The DCB-261 also allows for micro stepping down to 1/8 of a normal step. To make sure this small of a step fits our specifications, we had to calculate the minimum linear movement available in both the elastic and hardness device.

For the elastic device, we have rotational movement of the motor that translates into linear movement of the paddle. According to specifications the smallest sample size we need to acquire data for is roughly 100 microns. It is then seen that to test this small of a sample size we need a linear movement down to the micron level. With this being stated we calculated the smallest movement the paddle could move utilizing 1/8 of the motors step (Eq. 8).

$$\theta \; x \; \frac{\pi}{180} \; x \; R_{Gear} = L_d \tag{8}$$

This equation takes θ which is the motor step angle multiplied by 1/8 (.225°), converts it to radians, and multiplies it by R_{Gear}, which is the radius of the gear (8 mm). This gives us the minimum distance per micro step (L_d). We assume that the linear displacement is equal to the arc length traveled by the gear. Backlash of the gear is compensated and described further in the report. From this calculation we see that the minimum distance is equal to 31.4 microns. This

distance is rather large but will satisfy the tests we need to complete. This distance could be made smaller if a lower fraction micro step was used. However, as discussed earlier this comes at a hefty price increase.

We also have to compute similar analysis to the hardness test. This is to determine the minimum amount the indenter will move. This was done utilizing one full step of the motor (Eq. 9).

$$\frac{\theta}{360}\ x\ P = I_d \tag{9}$$

In this formula θ equals the angle of a full step (1.8°), which is then divided by 360 degrees per revolution. This number is then multiplied by P which is the pitch of the thread used in the indenter in metric. Thread of this rod is ¼-28 converting to metric this pitch is then .907 mm. Multiplying pitch by the amount of revolutions per step gives us the indenter displacement (I_d). At a full step this value is approximately 4.5 microns. This indenter movement is acceptable when performing this test since layers of skin are very thin and our ideal distance moved is on the micron level. If a smaller distance is required then micro stepping could be used. From these two calculations above it shows that this driver/controller system selected will appropriately assist in controlling the motor at a desirable accuracy and step distance.

To fully power this device a 50 W power supply is needed. AMS makes a power supply model that is 50 W which is fully compatible with this driver/controller. To connect this device to the computer a SIN-11 RS-422 to RS-232 adapter is needed. This intelligent adapter enables the device to be controlled entirely through LabVIEW. There is also the benefit of that when using this driver /control system there is no need for 3rd party hardware to make the system work. This eliminates the chance of different components conflicting with each other. There are other options available from this vender such as smaller micro stepping, but for the application of our prototype and cost to upgrade the driver controller system (+$150), the DCB-261 meets the requirements our prototype needs to meet.

Figure 29: (DCB-261) Motor driver and controller

Figure 30: DCB-261 Block diagram

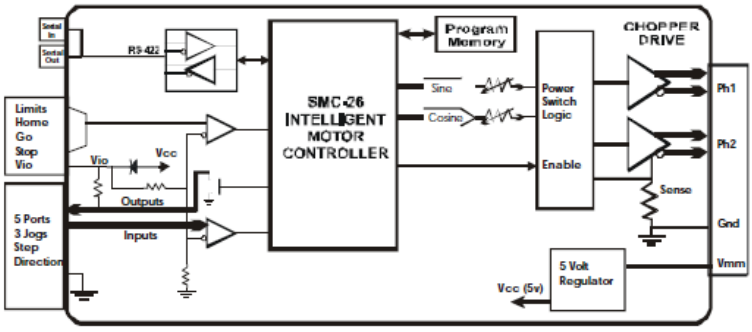

11.2 Load Cells

11.2.1 Strain Gauges

Strain Gauges are devices whose electrical resistance varies proportional to the strain applied. It is used for measuring both strain and force on the body. One of the most commonly used strain gauges are bonded metal strain gauge. It consists of a very fine metallic wire in a grid pattern arranged in parallel direction to maximize the strain sensitivity. The grid is bonded to a thin backing which is known as a carrier as shown in Fig. 31 [30].

Figure 31: Strain Gauge

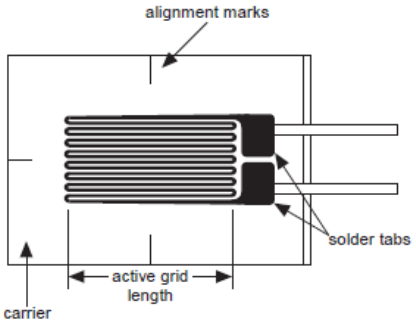

The strain gauge works on the principle that the electrical resistance of a wire changes when the wires are compressed or stretched as the resistance of the wire is directly proportional to the length of wire [30].

$$R = \frac{\rho L}{A} \tag{10}$$

Where R is the resistance, ρ is the resistivity, L is the length and A is the cross section area of the wire. The change in resistance could be then measured by the measuring the change in voltage when a known amount of voltage (excitation voltage, V_{ex}) is applied to the strain gauge. Two important parameters of strain gauge are resistance of the strain gauge that is the measure of the electrical resistance between two metal ribbons known as nominal resistance (R_g) and gauge

factor (GF) that is sensitivity of strain gauge to strain. It is defined as the ratio of the change in electrical resistance to the fractional change in the length (strain) [31].

$$GF = \frac{\frac{\Delta R}{R}}{\frac{\Delta L}{L}} = \frac{\frac{\Delta R}{R}}{strain} \tag{11}$$

In an ideal condition the resistance of the strain gauge should change to the applied stress. However, it will also change due to temperature effects. In order to measure a small change in resistance and compensate for temperature sensitivity the strain gauges are always used in Wheatstone bridge configuration as shown in Fig. 32 [31].

Figure 32: Wheatstone Configuration

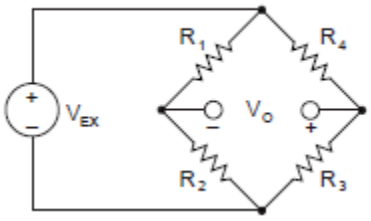

The output voltage of the bridge (V_o) is measure by the bridge current equation.

$$V_o = V_{ex}\left[\frac{R_3}{R_3+R_4} - \frac{R_2}{R_1+R_2}\right] \tag{12}$$

The strain gauge can be used to measure in three different configurations, Quarter bridge, half bridge and Full bridge. In a Quarter bridge configuration (Fig. 33) one strain gauge is used with three known resistors. The output of this configuration is very sensitive to the change in temperature and is also non linear, thus decreasing the accuracy of the device.

Figure 33: Quarter Bridge Configuration

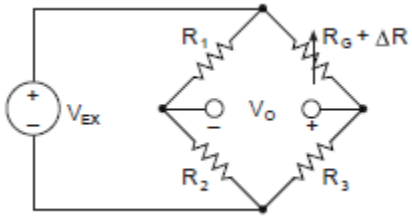

The strain gauges could also be used in a Half bridge configuration (Fig. 34), where the bridge has two strain gauges. This results in linear output and also doubles the sensitivity to the applied

stress as compared to the quarter bridge configuration. It also helps compensating temperature effects, thus increasing the accuracy.

Figure 34: Half Bridge Configuration

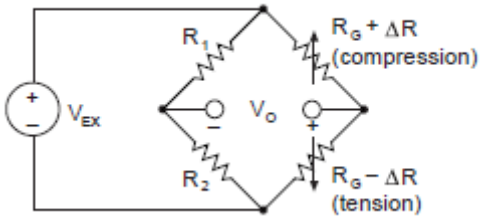

In order to further increase the sensitivity of the device to stress, four strain gauges can be used in full bridge configuration (Fig. 35). In this configuration two strain gauges are mounted to measure compression where as the other two are mounted to measure the tension.

Figure 35: Full Bridge Configuration

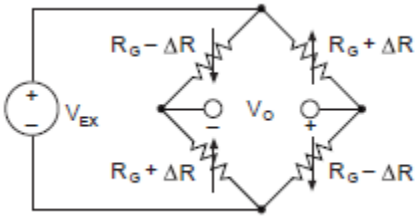

Considering the cost and making the device hand held were important customer requirement, miniature strain gauges were to be integrated. After thorough market research two precision strain gauges manufactured by omega were selected. The SGD-2/350-DY13 strain gauges have dual parallel grids design to measure bending loads. It has an overall length of 5.50mm and width of 5.90 mm. It has a nominal resistance of 350Ω ± 0.5% and a gauge factor of 2.02 ± 5%. It also has a max voltage rating of 6.5 V. The SGT-1/350-TY13 strain gauges have a single grid with length of 4.0 mm and width of 3.0 mm. It has a nominal resistance of 350Ω ± 0.5% and a gauge factor of 2.02 ± 5%. It also has a max voltage rating of 6 V.

11.2.2 Load Cell: Elasticity Measuring Device

To measure the force applied by the moving paddles in the elasticity measuring device, the SGD-2/350-DY13 strain gauges were used in full bridge configuration where one strain gauge is mounted on front surface and the second strain gauge is mounted on the back surface as shown Fig.34. These strain gauges have dual grids where two grids will be connected in the direction of the bending and the other two in the opposite direction of bending.

Figure 36: Moving paddle with strain gauges

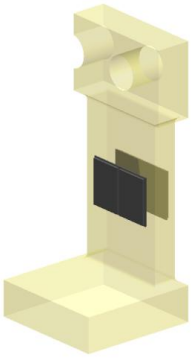

Firstly, this configuration compensates for any temperature effects as all four strain gauges are subjected to the same temperature. Secondly, it rejects the effects of axial force thus measuring only bending force and also increasing sensitivity for bending.

$$Strain = -\frac{V}{GF} \tag{13}$$

$$Force = Strain \times E \times Area \tag{14}$$

The stress can be calculated from the strain equation using hooks law. Where E is the elastic modulus of the material on which the strain gauges are applied. Using the definition stress that is force per unit area, we can calculate force applied.

11.2.3 Load Cell: Hardness Measuring Device

In order to measure the axial force applied by the indenter tip in the hardness measuring device, four SGT-1/350-TY13 strain gauges in full bridge configuration were used. In this configuration two gauges are mounted in the direction of the axial strain with one on the top surface and one on the bottom surface and the other two strain gauges connected in similar fashion but are in transverse direction the axial strain.

Figure 37: Indenter rod with four strain gauges

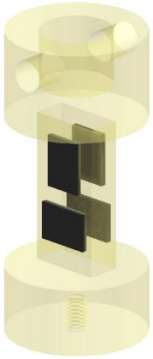

This strain configuration helps compensate for any temperature effects and also helps reject any bending effects, thus increasing the accuracy of measuring the axial force.

$$Strain = -2\frac{V}{GF} \tag{15}$$

$$Force = strain \times E \times Area \tag{16}$$

Similar to the load cell used in elasticity measuring device, the stress can be calculated from the equations (15, 16).

11.2.4 Load Cell: Contact Sensing

It is extremely important to know when the device is making contact. It is also critical to measure the amount of load applied by the user on the surface of skin as it could affect the skin's mechanical properties. A "C" style load cell (Fig. 38) [32] was developed with one strain gauge on the vertical surface of the load cell to sense skin contact and help the user in adjusting the amount force applied on the skin surface.

Figure 38: Contact sensor

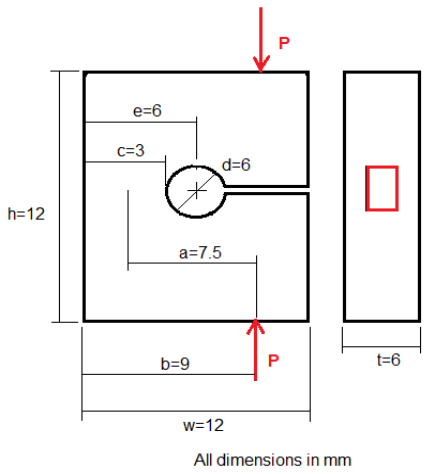

When a force is applied to the load cell, the beam onto which the strain gauge is mounted is subjected to bending and axial stresses. The axial stress is negligible compared to bending, hence is neglected. The strain gauge is mounted in a quarter bridge configuration as geometrical constraints allow us to mount only one strain gauge. A small voltage will be measured as soon as the load cell comes in contact to skin surface hence alerting the user of the contact. As user holds the device on to the surface of the skin the load cell will give the user live reading of force applied. If high load reading is displayed then user can relax their arm to reduce the load thus, decreasing the chance of altering the mechanical properties of the skin.

11.2.5 Load Cell Analysis

In order to develop a load cell, the minimum force that could be measured was calculated for different materials. Using the stress – strain relation the change in length for a known minimum and maximum force applied was used as shown in equation below [30].

$$\Delta L = \frac{L_0 \times F}{E \times A_0} \tag{17}$$

Where E is the elastic modulus of the material of load cell, A_0 is the area of the load cell and L_0 is the initial length of the load cell. The change in the resistance was then calculated using the gauge factor of the strain gauge which is typically 2.0 with an error of 1% [30].

$$GF = \frac{\frac{\Delta R_g}{R_g}}{\frac{\Delta l}{L}} \tag{18}$$

Where $R_{.g}$ is the nominal resistance of the strain gauge. Kirchhoff's voltage law was applied to the wheat stone bridge and the change in output voltage for an excitation voltage was calculated [31].

$$V_O = V_{ex} * \frac{\left((R_g + \Delta R_g) - (R_g - \Delta R_g)\right)}{(R_g + \Delta R_g + R_g - \Delta R_g)} = V_{ex} * \frac{\Delta R_g}{R_g} \tag{19}$$

This output voltage was then compared to the sensitivity of strain gauge, if the output voltage was higher than the sensitivity of a strain gauge thus, validating the optimum function of the strain gauge in the range of force. For aluminum load cells the minimum force that could be measured as calculated is 0.88 N or 90 g (Appendix G). This is higher than the minimum expected force to be measured by the device. Similar calculation as above was performed using a ABS plastic and it was determined a force of 0.05 N or 5 gm load could be measured hence; a possible change in material is advisable (Appendix G).

The contact load cell is a "C" shaped design for compressive loads. A stress analysis was done on this component to determine if it would yield under the applied forces. By determining the maximum stress that would be induced under such loads, a material could then be selected using a safety factor against its yield strength. The following equation shows how to calculate the maximum stress on the load cell, a negative sign indicates compressive loading.

$$\sigma = \frac{-k * P}{c * t}\left(1 + \frac{6a}{c}\right) \tag{20}$$

P is the maximum load that can be applied, and *k* is a constant [32]. The maximum load was determined by summing the masses of all the necessary components and multiplying by the gravitational acceleration. In this case the value for *k* is 1.3, and the maximum load is 1N. The values for *c*, *t*, and *a* are all dimensions that can be read from Figure 38. Calculation of the maximum stress gave a value of 0.712 N/mm^2, and the yield strength for ABS plastic is 53.1 N/mm^2. This results in a safety factor against yielding of 77. This ABS plastic is available via rapid prototyping in the 3D printing lab inside the Duderstadt Center.

11.3 Load Cell Control System

Reading the data the load cells are outputting accurately is very important in creating desirable results within our engineering specifications. To make sure this was accomplished we researched multiple data acquisition systems and circuitry, and selected the best components for our devices application. This section will analyze these two components and state why they were selected.

11.3.1 Data Acquisition

After reviewing multiple data acquisition devices it has been determined that the National Instruments DAQ: NI USB-6210 (Fig. 39) [31]. This selected device is a low cost multifunctional DAQ with a resolution of 16-Bits and a sampling rate of 250kS/s. Also there are a total of sixteen analog pins; a maximum of four pins will be used for our application. One of which will be used for the elasticity device load cell, and another will be used for the hardness device load cell, these pins are the output readings of the load cell. The third analog input will be used for the contact sensor of the elasticity device to read the strain results. The fourth pin is a local ground for all tests. There are also digital pins which will be used to supply a 5V to the load cell circuit described below. This 16 bit resolution allows for a total of 65,536 voltage readings per sample of data. Having a sample rate of 250,000 samples/second also allows for more data throughout the test giving us more useful data allowing for more accurate results. A more detailed analysis of the sampling rate is explained in the section below. From our customer requirements and engineering specifications it is desired to have high accuracy and high sampling rate. These are both satisfied with the selected DAQ.

There are eight digital pins located on this DAQ. These ports are utilized to supply a voltage range from 0-5V allowing for voltage regulation if needed and ground the circuits where necessary. At a maximum supply from the DAQ of 5V each strain gauge would receive 2.5V. This voltage is determined from a voltage analysis of a Wheatstone bridge. When drawing a circuit analysis of this bridge it can be drawn such that there are two parallel wires each with 2 strain gauges. Due to this the voltage has to be split and only 2.5V gets carried to each gauge. This voltage limit is 1V under the maximum each strain gauge can receive. Therefore the gauges will operate as expected and will not be destroyed. It is also important to note that this DAQ connects to the computer and LabVIEW via USB 2.0. It is also powered by this same line eliminating the need of an external power supply, thus saving cost. Overall this DAQ adequately

satisfies our designs needs, and will operate and provide data that satisfies our requirements and specifications.

Figure 39: NI USB-6210

11.3.2 Load Cell Circuitry

Strain gauge measurements typically involve sensing small changes in resistance. Therefore, proper selections of electrical components such as wheat stone bridge configuration, wiring, data acquisition are required. As in previous section load cell for the two devices were to be connected in a full bridge circuit. It is very important that the excitation voltage be very accurate and stable. If the strain is located a distance from the signal conditioner and excitation source, a possible source of error is the voltage drop due to resistance of the wires connecting the excitation voltage source to the bridge [31].

The output voltage of a strain gauge is relatively small. Typically, most strain gauge bridges output less than 10 mV/V. Thus, strain gauge circuits usually integrate amplifiers to boost signal level to increase measurement resolution and improve the signal to noise ratio. A schematic of the load cell circuit is shown below.

Figure 40: Load cell amplifier circuit

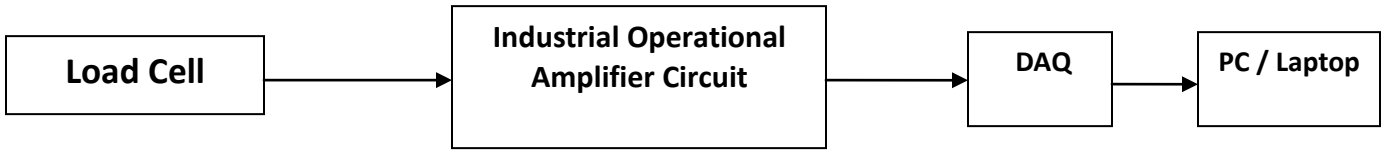

An industrial amplifier (INA 122) will be connecting the Full bridge strain gauge configuration to amplify the signal to be then read by the DAQ which will then be run by LabVIEW on a PC / Laptop. The INA 122 can be operated with single supply from 2.2 V to 36 V. A single extra resistor (R_g) sets gain from 5 V/V to 10000V/V.

Figure 41: Industrial amplifier (INA 122)

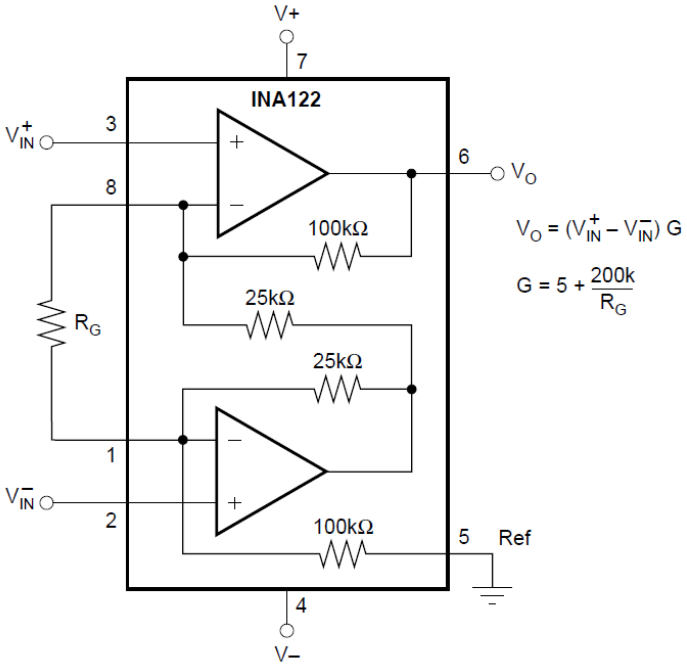

$$Voltage\ Gain = \frac{V_{out}}{V_{in}} = 1 + \frac{R_2}{R_1} \quad (21)$$

This amplified voltage is then fed into a DAQ. When two analog inputs of a 16 bit DAQ are used provides a voltage resolution of 0.15 mV when 0-5 V is measured (Appendix G). The DAQ has a maximum sampling rate of 250,000 Samples/s.

A detailed circuit diagram can be seen in Figure 42. For this circuit multiple parameters have been identified and set. V_{supply} (5 V) is the power supplied to the strain gauge system. As discussed earlier this voltage is then split so that 2.5 V is supplied to each strain gauge. As calculated in the segment above voltage resolution of the selected DAQ is 0.15 mV. Half of this voltage is the V_{res} which is the minimum voltage the DAQ will be able to read from our system. Also calculated from this circuit is the V_{out} which is the voltage output from the strain gauges. This voltage is then ran through the industrial amplifier to match V_{res} with a safety factor of 10. Thus giving us a gain of 500 since gain is equal to V_{res} divided by V_{out}, and multiplied by 10 for the safety factor.

Figure 42: Load cells circuit diagram

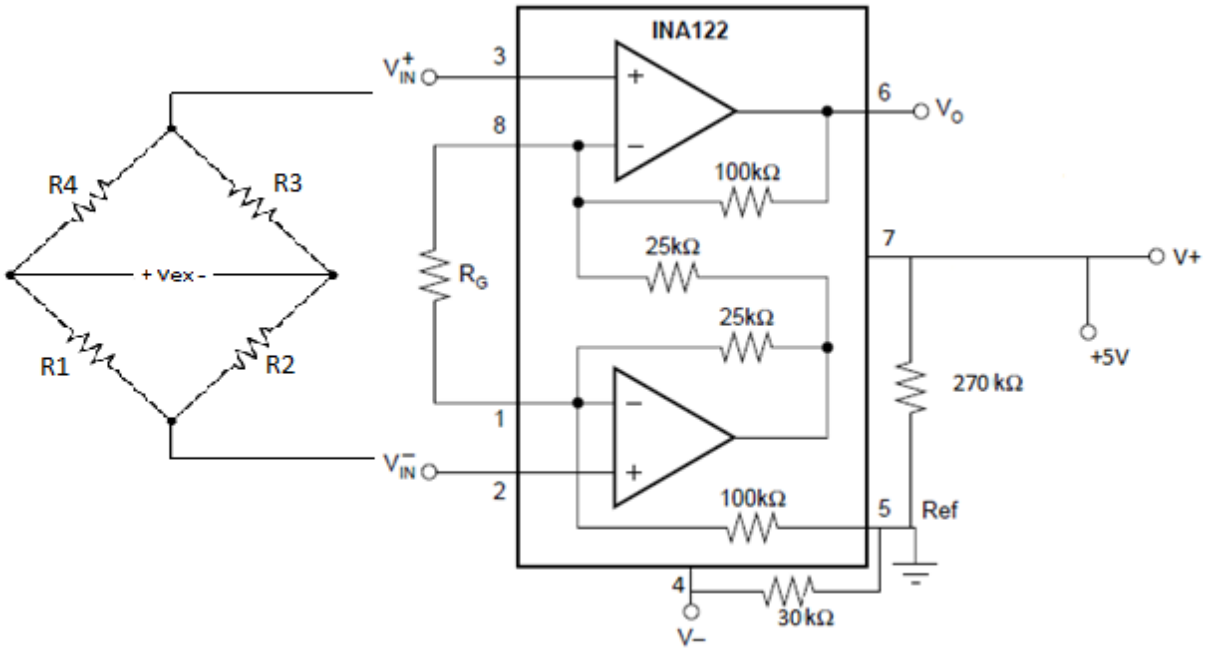

11.4 Overall Device Control

To have effective and efficient control of the device it is important to use a common computer program that communicates with all inputs and outputs. It is also important to install safety measures to ensure that neither the operator nor patient will be in harm. This section will be describing and analyzing our common computer program selected and safety measures devised for our final design and prototype.

11.4.1 Common Computer Program: LabVIEW

LabVIEW is a commonly used program when it comes to laboratory type measurement and automation. Since our motor control and load cell data are both controlled via LabVIEW. Therefore, LabVIEW will be used as our computer program. The benefit of this is that we can command the motor and during that same command can see what data the load cells are producing. This also gives us the option to create feedback loops in LabVIEW allowing us to apply a constant force by having the stepper motor adjust to the measurement the load cells are returning. We will need to program multiple operations inside LabVIEW for each test. Logistics of this program will be unknown until further research is looked into and tests are performed. What we do know is that we need to develop a program for both the elastic device and hardness device.

For the hardness device we must code a program to perform multiple tasks. One is to have the user able to control the stepper motor to set the zero position by using the jog distance (A). This is in order for us to measure properties of skin from the zero or home position. Next would be to

create a program that when the user hits the run button it performs the required operation. This operation is to indent into the skin at a desired rate (C) to a desired length (B). A constant force could also be held after the final length has been achieved however this is unachievable with the allotted time, see section 16. This test reports the load cell data and records a strain or force. This data can then be displayed directly on LabVIEW's GUI (D) and or exported to excel for further data reduction. The elasticity measuring device uses most of the same programming. However, the stepper motor creates linear motion with the paddle at a controllable rate and depth. Using this program we will satisfy our requirement for computer integration.

Figure 43: Sample LabVIEW GUI

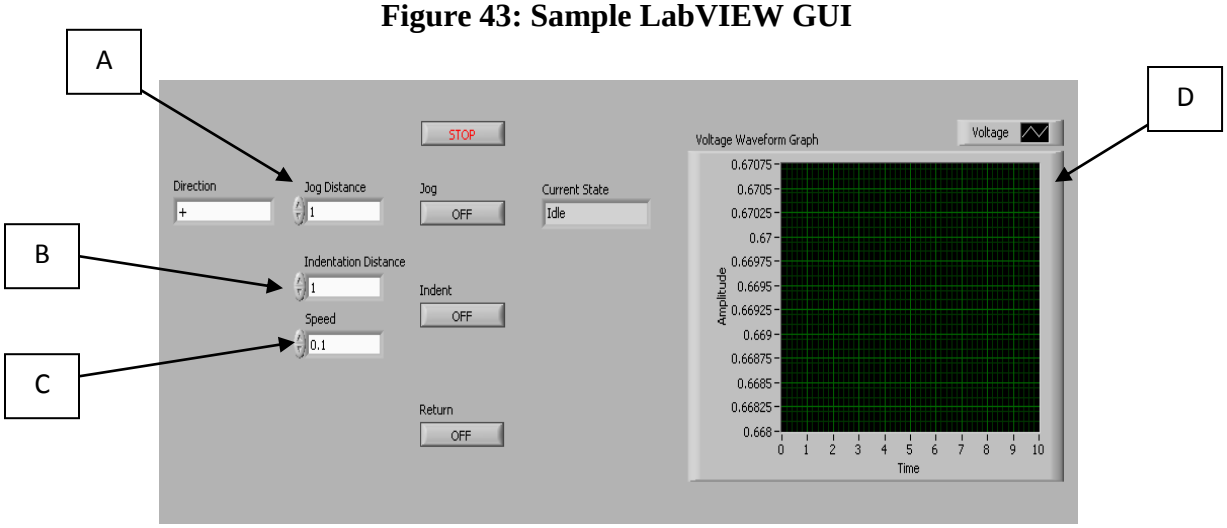

11.4.2 Safety Measures

Safety measures are very important in any mechanical electrical device, especially when it comes to a device to be used in the medical field. This is why we found it necessary to implement multiple safety features into our final design/ prototype. First feature we will be adding is a "kill switch" this switch will be entered in as LabVIEW code, and sets a limit to the stepper motor's toque. This value is currently set at 50 mNm, but could change after further analysis after the device is fabricated. Once this torque is present the program would terminate stopping the motor from moving. Second feature we developed is to have motion limitations built directly into the device by structural guides. For the elastic device this limitation is 26mm, and for the hardness device it is 5 mm. This is to prevent over stretching or an excessive amount of indention into the skin. Lastly, we plan on having an adhesive that does not harm the skin if it has to be quickly removed. This will be completed by testing various types of adhesion materials to select the correct one for our application. There is always room for more safety features in a device, but for our prototype at the current time we believe these three will be sufficient enough.

DesignSafe was used in assessing the possible safety issues with the device. It was important to start by determining what people will come into contact with the device, and then the possible risks that they can encounter. The above described safety measures account for much of the

possible issues, even though none are anticipated to be likely. Most of the components are located inside the device, only the insulated wires and skin contact components are external. The points that touch the skin were designed for certain small loads and smooth edges to prevent patient pain. Care has to be taken when cleaning the device because the water can short circuit any of the electrical parts or corrode the metal inside. The devices were also designed for operator care, in that they are lightweight and fit comfortably into the hand.

12. FABRICATION PLAN

12.1 Mechanical System

12.1.1 Rapid Prototyping

Earlier we discussed how we used CES to choose the material for our housings, and that rapid prototyping with ABS could be used. Tolerances are important in each design where there are two pieces sliding against each other. We designed the inner moving parts to be slightly undersized. In both test modules this occurs where the support wings meet the base housing, and in just the elastic module where the inner and outer housings meet. The estimated time of completion quoted from the design's .STL files was to be 55 hours; however, this work can be completed without supervision. The time that is saved here can be used to fabricate the additional mechanical and electrical components of our design. Once the parts are returned, they are completely finished and require no additional machining.

Each of the load cells were also selected for rapid prototyping for many of the same reasons as the housing. The Young's modulus of ABS allows for 1 gram measurements to be recorded, and it has less creep than most other plastics.

12.1.2 Machining Equations and Reference Values

Our design requires that several mechanical components must be machined with the ME 450 shop. Using these machines it is important to have a plan on how to machine it, and what speeds the machining should be performed. The various machines utilized include the mill, lathe, band saw, drill press, and hand tap and die. The equations and tables used to determine the necessary speeds are as follows:

$$\text{Mill/Lathe/Drill Press: } \frac{12cs}{\pi D} = SS \tag{22}$$

Where CS is the cutting speed in surface feet per minute (SFM), D is the tool/cutting diameter in inches, and SS is the spindle speed in rpm.

Table 4: Values of cutting speeds for various materials [33]

Material type	Meters per min (MPM)	Surface feet per min (SFM)
Steel (tough)	15–18	50–60
Mild steel	30–38	100–125
Cast iron (medium)	18–24	60–80
Alloy steels (1320–9262)	–	65–120[3]
Carbon steels (C1008-C1095)	–	70–130[4]
Free cutting steels (B1111-B1113 & C1108-C1213)	–	115–225[4]
Stainless steels (300 & 400 series)	–	75–130[5]
Bronzes	24–45	80–150
Leaded steel (Leadloy 12L14)	–	300[6]
Aluminium	75–105	250–350
Brass	–	600+ (Use the maximum spindle speed)[7]

Table 5: Values of band saw cutting speeds for various materials [33]

MATERIAL	BANDSAWING SPEED (fpm)	MATERIAL	BANDSAWING SPEED (fpm)
ALUMINUM	200 TO 2,000	RUBBER, HARD	150 TO 250
BAKELITE	200 TO 900	STEEL, ALLOY	50 TO 100
BRASS, SOFT	175 TO 300	STEEL, HIGH CARBON	50 TO 100
BRASS, HARD	75 TO 150	STEEL, HIGH-SPEED	50 TO 90
BRASS, SHEETS	200 TO 900	STEEL, MACHINE	75 TO 175
BRONZE	75 TO 150	STEEL, SHEEET	150 TO 200
CAST IRON	50 TO 100	STEEL, STAINLESS	50 TO 75
COPPER	115 TO 175	STEEL, TOOL	50 TO 150
MONEL METAL	50 TO 100		

12.1.3 Process Plans for Mechanical Components

Process plan sheets were created for each of the parts that need to be machined. The data that can be received from the sheets are what machine, tool, fixture, and cutting speeds are required for each step. The material type and list number are also given and can easily be referenced in the bill of materials. A short description is also given for what types of material attach to the part. A conservative estimate is that it will take 15 work hours to complete this stage of our design fabrication.

The female threaded rod is used as a coupling between the stepper motor shaft and threaded indenting shaft within the hardness test module. It is made from a zinc plated steel, and attaches to a smooth steel shaft and a threaded aluminum rod. Tolerances are important where the motor shaft slides into this part, a reaming is required to ensure the hole diameter is more accurate.

Female Threaded Rod			**Steel**	**#9**		
Machine	**Tool**	**Fixture**	**Cut Speed (SFM)**	**Spindle Speed (RPM)**	**Band Saw Speed (FPM)**	**Description**
Band Saw	N/A	Push Block	N/A	N/A	80	Rough cut to ~30mm length
Mill	3/8" End Mill	Vice	100	1019	N/A	Cut to 30mm length
Mill	Center Drill	Vice	100	1019	N/A	Drill starter hole
Mill	3/16" Drill	Vice	100	2037	N/A	Drill undersized hole 18mm deep
Mill	5mm Ream	Vice	100	1940	N/A	Ream hole to 5mm diameter
Drill Press	#49 Drill	Vice	100	5232	N/A	Drill hole through one wall 7.5mm from end
Hand Tap	#2-56	Vice	N/A	N/A	N/A	Thread previously drilled hole

The male threaded rod connects to the motor coupling and to the indentation load cell. The top threads into the female threaded rod, and allows for vertical height adjustments as the motor turns. The bottom end is made to seat into the load cell and attached using a stabilizing rod that also prevents rotational motion. It is made from the same steel part as previous.

Male Threaded Rod			**Steel**	**#9**		
Machine	**Tool**	**Fixture**	**Cut Speed (SFM)**	**Spindle Speed (RPM)**	**Band Saw Speed (FPM)**	**Description**
Band Saw	N/A	Push Block	N/A	N/A	80	Rough cut thread length to ~14mm
Mill	3/8" End Mill	Vice	100	1019	N/A	Cut thread length to 14mm
Band Saw	N/A	Push Block	N/A	N/A	80	Rough cut to ~19mm length
Mill	3/8" End Mill	Vice	100	1019	N/A	Cut to 19mm length
Mill	Center Drill	Vice	100	7463	N/A	Drill starter hole
Mill	1.30mm Drill	Vice	100	7463	N/A	Drill hole through ends
Hand Tap	M1.7*0.35	Vice	N/A	N/A	N/A	Thread previously drilled hole

The gear rack converts the rotary motion from our stepper motor into linear motion, resulting in stretching of the skin surface. The rack is made of carbon steel, and interlocks with a steel spur gear and slides on two steel rods. The contact between the rack and slides is important to allow for tolerances, so the holes will be machined slightly oversized to allow for a close fit. The edge will also be epoxy to the moving aluminum paddle.

Gear Rack			**Carbon Steel**	**#1**		
Machine	**Tool**	**Fixture**	**Cut Speed (SFM)**	**Spindle Speed (RPM)**	**Band Saw Speed (FPM)**	**Description**
Band Saw	N/A	Push Block	N/A	N/A	80	Rough cut to ~34.6mm length
Mill	3/8" End Mill	Vice	100	1019	N/A	Cut rack to length of 34.6mm
Mill	Center Drill	Vice	100	1019	N/A	Drill starter holes
Mill	7/64" Drill	Vice	100	3492	N/A	Drill through hole lengthwise
Mill	7/64" Ball Mill	Vice	100	3492	N/A	Drill rounded channel lengthwise across backside
Mill	7/64” Ream	Vice	100	3492	N/A	Ream last two holes

There are two 7/64” steel rods that are used as slides for the rack. The ends are attached through the ABS housing. One rod stays fixed in the housing and only requires cutting to length. Epoxy is used to permanently fix this rod into place. A second rod goes through both ends of the housing and is threaded on both ends.

7/64" Rod			**Steel**	**#3**		
Machine	**Tool**	**Fixture**	**Cut Speed (SFM)**	**Spindle Speed (RPM)**	**Band Saw Speed (FPM)**	**Description**
Band Saw	N/A	Push Block	N/A	N/A	80	Rough cut to ~69mm length
Lathe	Facing Bit	3 Jaw Chuck	100	3492	N/A	Square up ends and cute to 69mm length

7/64" Threaded Rod			**Steel**	**#3**		
Machine	**Tool**	**Fixture**	**Cut Speed (SFM)**	**Spindle Speed (RPM)**	**Band Saw Speed (FPM)**	**Description**
Band Saw	N/A	Push Block	N/A	N/A	80	Rough cut to ~95mm length
Lathe	Facing Bit	3 Jaw Chuck	100	3492	N/A	Square up ends and cute to 95mm length
Hand Die	#4-40	Vice	N/A	N/A	N/A	Thread 10mm on each end

The stationary aluminum paddle is attached to the bottom of the ABS housing using a steel screw and epoxy. The bottom face of the paddle will have an adhesive that must be applied to it prior to any testing.

Stationary Paddle			**Aluminum**	**#13**		
Machine	**Tool**	**Fixture**	**Cut Speed (SFM)**	**Spindle Speed (RPM)**	**Band Saw Speed (FPM)**	**Description**
Band Saw	N/A	Push Block	N/A	N/A	1000	Cut to rough dimensions
Mill	3/16" End Mill	Vice	250	5093	N/A	Square all edges and mill to size
Mill	Center Drill	Vice	250	5093	N/A	Drill starter hole
Mill	2.05mm Drill	Vice	250	11833	N/A	Drill hole 1mm deep
Hand Tap	M2.5*.45	Vice	N/A	N/A	N/A	Tap previously drilled hole

13. PROTOTYPE ASSEMBLY

The assembly process is broken into mechanical and electrical sections to allow for easier referencing. Some mechanical and electrical assembly steps must be completed before one another and will referenced properly to the correct steps.

13.1 Mechanical Assembly

The mechanical assembly includes all of the manufactured parts, as well as other purchased parts (screws, nuts, hand knobs, etc.).

13.1.1 Hardness Measuring Device Assembly

The hardness test device consists of the module that performs linear indentations on the patient's skin. Figure 44 shows a CAD model of the complete assembly of this device.

Figure 44: CAD model of assembled hardness test device

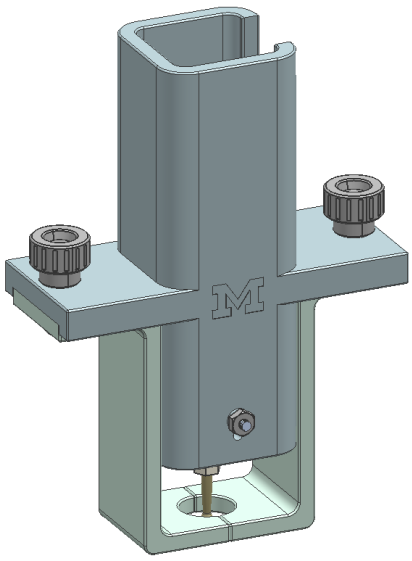

1. Attach the female threaded rod to the stepper motor shaft using a #2-56 set screw. Be cautious that over tightening can cause damage to the motor shaft.

2. Thread the male threaded rod to the female threaded rod from step 1. This step requires attaching aluminum and steel rods, take caution not to over tighten and damage the threads.

Figure 45: Strain gauge configuration on male threaded rod

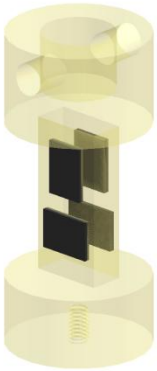

3. Attach four strain gauges with epoxy to the ABS plastic load cell mount in a configuration (Fig. 45). Refer to Section 13.2 to see how to attach the wires to the strain gauges, this step must be completed before moving on.

4. Epoxy the load cell mount to the bottom of the male threaded rod. Be sure to keep the holes aligned and keep any epoxy from seeping in them.

5. Place the stepper motor assembly into the top of the housing. Screw four M2.5*0.45 machine screws through the housing and into the motor. Wiring of the stepper motor is shown in Section13.2, and can be completed at a later stage.

6. Align the holes on the side of the housing to the hole in the load cell which is now adhered to the male threaded rod (step 4). Thread #4-40 rod through the load cell until equal amounts of threads are visible on each side of the housing. On each side place a washer and corresponding nut, and tighten until snug.

7. Thread in whichever indenter tip is desired into the bottom of the load cell, once again taking caution with threading to dissimilar materials together.

8. Attach two M4*0.7 nuts to the underside of the support wings using an epoxy. Ensure that nuts are aligned with the holes on the support wings. The epoxy must be allowed to properly cure before moving onto the next step.

9. Align the two support wings into the channels provided on each side of the housing. Place the hand knobs through the holes and tighten into the corresponding nuts until snug. The assembly for steps 1- 7 is shown in Figure 46.

Figure 46: Assembly of support wings and indenter tip

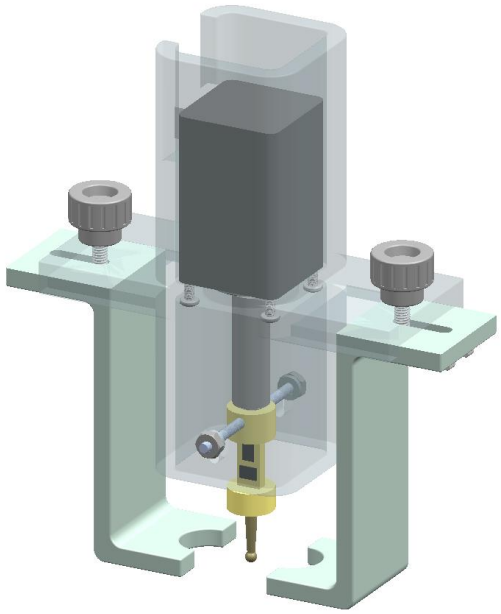

13.1.2 Elasticity Measuring Device Assembly

The elasticity test device consists of the module that performs stretching on the patient's skin. Figure 47 shows a CAD model of the complete assembly of this device.

Figure 47: CAD model of assembled elasticity test device

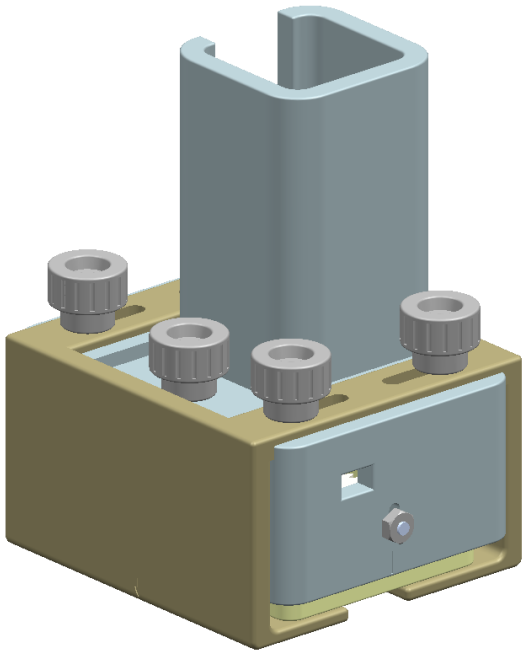

1. Place the stepper motor through the hole in the top of the housing. Screw four M2.5*0.45 machine screws through the housing and into the motor. Wiring of the stepper motor is shown in Section 13.2, and can be completed at a later stage.

2. Attach the spur gear to the motor shaft using a #2-56 set screw, once again taking care not to over tighten and possibly causing damages to the shaft. Assembly of steps 1 and 2 are shown in Figure 48.

Figure 48: Assembly of motor and spur gear

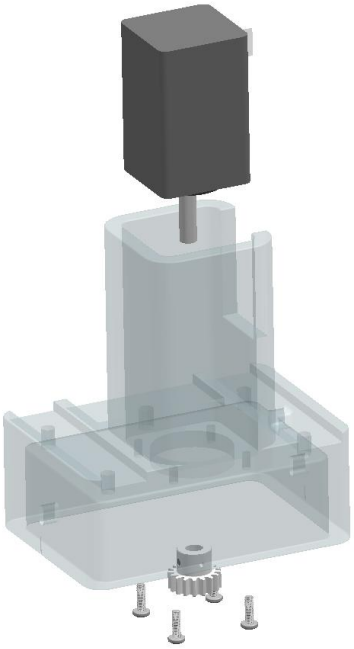

3. Epoxy four M4*0.7 nuts onto the underside of the housing, while also ensuring proper alignment with the holes.

4. Attach a strain gauge to the contact load cell piece with epoxy. Allow the epoxy to dry before moving on. Refer to Figure 49 for the configuration of the strain gauge. The connection of wires should be done after this step and is shown in Section 13.2.

Figure 49: Contact sensing load cell assembly

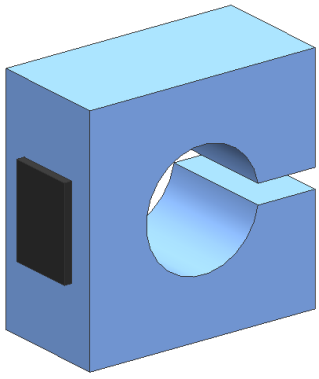

5. Using epoxy, attach the contact load cell and stationary paddle to the bottom of the inner housing (Fig. 50). To aide in alignment, a M2.5*0.45 machine screw is tighten through

the top of the housing and into the paddle. Allow the epoxy to dry before moving on. Refer to Figure 50 for proper alignment of these components.

Figure 50: Alignment of components on base of device

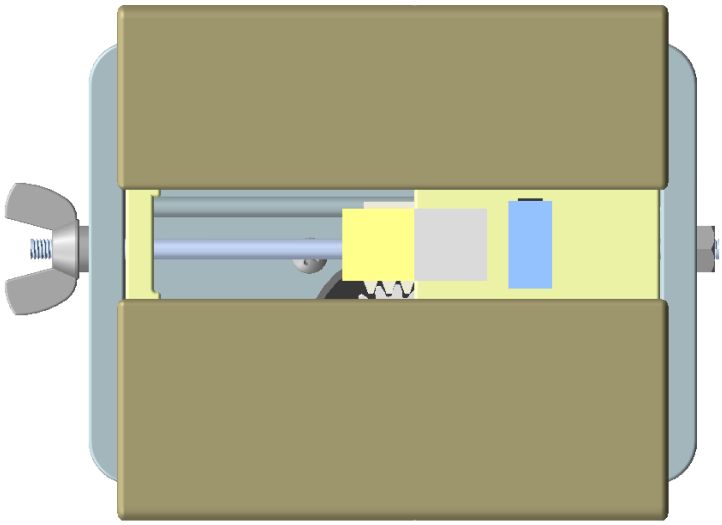

6. Attach duel strain gauges to the moving paddle (Fig. 51). The strain gauges are mounted using epoxy on the underside. The connection of wires should be done after this step and is shown in Section 13.2. Secure the moving paddle to the rack with epoxy by aligning the holes through each side. Allow the epoxy time to cure before going to the next step.

Figure 51: Stretching load cell assembly

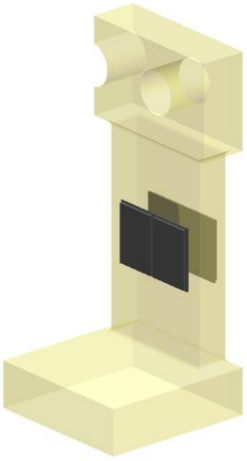

7. Attach the shorter sliding rod by pushing into guide holes on the side walls of the inner housing piece.

8. Epoxy a M4*0.7 nut above the hole on the inner housing, ensuring proper alignment for a threaded rod to go through.

9. Slide the outer housing over the inner one, aligning the holes on each side. Push one end of the longer sliding rod through a side of the housing, through the rack assembly, and out through the other side of the housing. The grove in the back side of the rack should also seat on the shorter sliding rod. Make sure the rack and gear are properly aligned and engaged, and then tighten a nut on each side of the housing to fully secure the rod. Figure 52 shows the inner mechanical assembly from steps 6-9.

Figure 52: Assembly of inner mechanical components

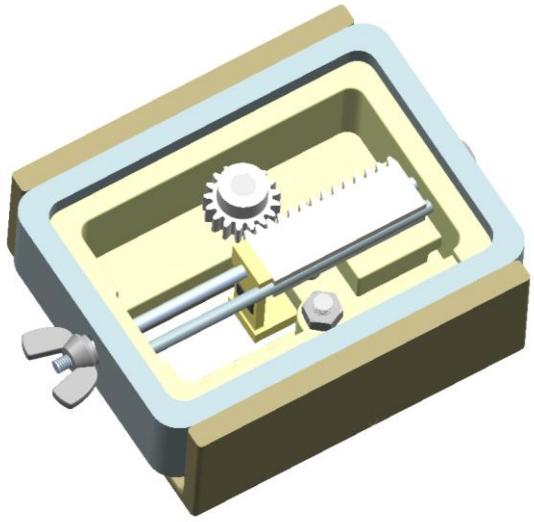

10. Align the support wings with the guides on the housing. Thread the four hand knobs through these parts and into the nuts from step 3. Thread an additional hand knob into the remaining hole and into the nut from step 8. The resulting assembly is the CAD model in Figure 47.

13.2 Electrical Assembly

Figure 53: Complete system circuit diagram

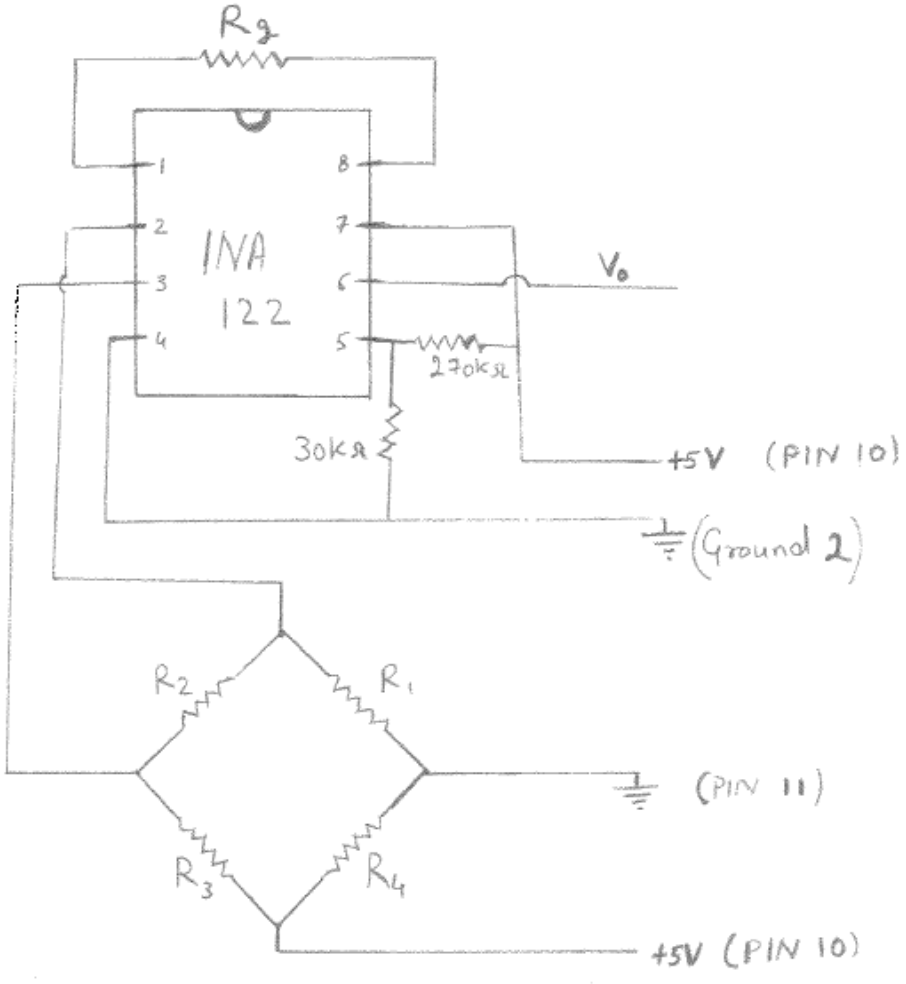

13.2.1 Elastic Device Electrical Assembly

Prior to completing the mechanical system, specifically prior to mounting the paddle on the rack wires must be soldered to each strain gauge; also the load cell should not be mounted yet. For the wiring system it has been decided that a double shielded 9 pin DB cable will be used (Bill of Materials # 25).

1. The DB cable is cut to a length of 2 feet 5in (size subject to change as manufacturing takes place) the other end of this cut wire should be a male DB connector. Both of these cut pieces will be utilized during this assembly.
2. This wire is then stripped down 5 inches to expose the 9 single wires, all with dedicated color patterns.
3. Use a voltage meter to determine which pins correspond to which color wire, this data will be recorded. It is vital that the colors and pins match up or the circuit will not work.

4. On a project board (item # 26) solder the connections as shown in the circuit (Fig. 53) using R_g as 400Ω to set the gain to 500 V/V.
5. The four strain gauges on the moving paddle are to be connected in full bridge connections as shown in the circuit represented as resistors (R1, R2, R3 and R4).
6. Connect the wires that are marked 5 V to the 5 V power output (Pin 10) of the DAQ.
7. Connect the ground wire from the strain gauges to ground (Pin 11) of the DAQ.
8. Connect the V_0 to an analog input pin on the DAQ (Pin 17) and Connect the ground 2 to pin 18 and connect pin 18 to analog ground (pin 28) of the DAQ.
9. The strain gauge on the contact load cell should be connected in quarter bridge connection represented as R1, 1 MΩ resistors for R3 and R4 and a 350Ω resistor as R2 in the circuit.
10. Connect the wires that are marked 5 V to the 5 V power output (Pin 10) of the DAQ.
11. Connect the ground wire from the strain gauges to ground (Pin 11) of the DAQ.
12. Connect the V_0 to an analog input pin on the DAQ (Pin 20) and Connect the ground 2 to pin 21 and connect pin 21 to analog ground (pin 28) of the DAQ.
13. After the soldering is complete the wires of the paddle should be adhered to the rack and left enough slack in order to allow the rack to move without strain and/or breaking cables.
14. With enough slack left lose in the system the remaining wire is then constrained to the housing wall.
15. The contact load cell wires should also be constrained within the casing to make sure they do not interfere with moving parts.

CHECK: After this point the assembly of the mechanical system can be completed.

At this point we should have the entire mechanical system of the elastic device assembled with a DB cable coming out of the device with a male end remaining. The other part of this DB cable can now be utilized.

16. The DAQ can then be plugged in via USB cable provided by national instruments.

13.2.2 Hardness Device Electrical Assembly

Before completion of the mechanical assembly of the indenter test, wires must be soldered to the strain gauge system.

17. The DB cable is cut to a length of 2 feet 5in (size subject to change as manufacturing takes place) the other end of this cut wire should be a male DB connector. Both of these cut pieces will be utilized during this assembly.
18. This wire is then stripped down 5 inches to expose the 9 single wires, all with dedicated color patterns.

19. Use a voltage meter to determine which pins correspond to which color wire, this data will be recorded. It is vital that the colors and pins match up or the circuit will not work.
20. On a project board (item # 26) solder the connections as shown in the circuit (Fig. 53) using R_g as 400Ω to set the gain to 500 V/V.
21. The four strain gauges on the hardness device load cell are to be connected in full bridge connections as shown in the circuit represented as resistors (R1, R2, R3 and R4).
22. Connect the wires that are marked 5 V to the 5 V power output (Pin 10) of the DAQ.
23. Connect the ground wire from the strain gauges to ground (Pin 11) of the DAQ.
24. Connect the V_0 to an analog input pin on the DAQ (Pin 17) and Connect the ground 2 to pin 18 and connect pin 18 to analog ground (pin 28) of the DAQ.
25. These wires will be fed through the hole in the side of the hardness device and then pulled out of the bottom.
26. Having some wire outside of the device the manufacturer can now solder one wire to both input and output of all 8 strain gauges, recording which color went to which strain gauge and its connection (input or output).
27. With enough slack left loose in the system the remaining wire is then constrained to the housing wall.

CHECK: After this point the assembly of the mechanical system can be completed.

13.2.3 Stepper Motor Assembly

Each Stepper motor is a 4 wire configuration. Each wire is roughly 300mm long and will possibly need to be extended to reach the driver/control system.

Figure 54: Motor Connections

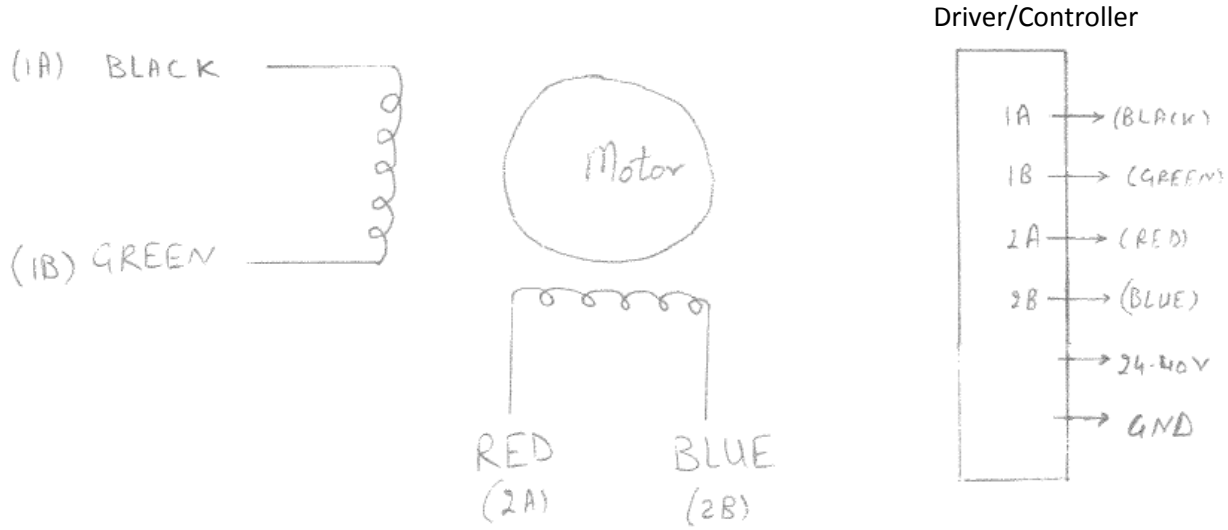

28. The process of connecting these wires requires reading the manual of the driver/control system and stepper motor.
29. The corresponding wires would be connected onto the driver/control's board (Fig. 54).
30. The driver/control system connects to the computer via sin 11 intelligent converter. Most common computers have these connections available to them.

14. VALIDATION

14.1 Calibration and Component Verification

Proper calibration and verification of correctly functioning components will be key to the successful development of our prototype. Therefore, we have produced various tests to be conducted on each of the critical components once the devices are completed.

14.1.1 Mechanical Calibration

The actuation provided by the stepper motor is the most important parameter for both the elasticity and hardness measurement devices. The resulting linear or vertical displacements must have a predictable resolution and be repeatable among all test cases. We have previously calculated the expected displacement increments for both configurations to be 31.4 microns for the elastic testing and 4.5 microns for the indentation testing, as described in Section 11.1. Because these calculations were made with perfect condition assumptions, we anticipate the actual displacements to differ slightly from theory. Thus, it is important to physically measure this result and confirm that our motion range specifications will be met. This was accomplished by controlling the motor through a specific number of steps. The final displacement of both the moving paddle on the elastic device and the indenter tip of the hardness device were then measured using a micrometer. These tests were repeated five times each to get precise results.

Figure 55: Indenter Tip Displacement with Full Steps

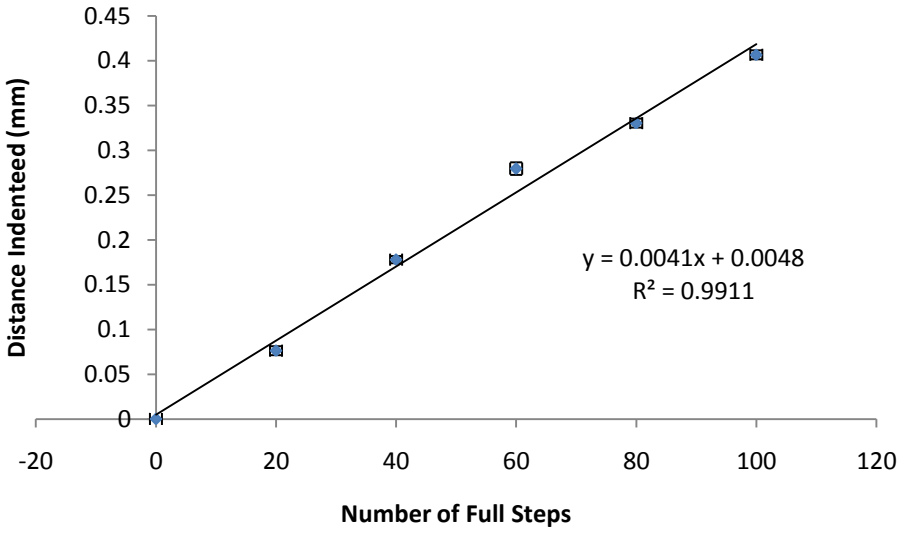

The indenter tip was displaced by providing full steps from the motor and the displacement was then measured in millimeters. It was determined the indenter tip follows the equation

$$y = 0.0041x + 0.0048 \quad (23)$$

Where *y* is the indenter tip displacement and *x* is number of full steps the motor provides (Eq. 23).

.

Figure 56: Elastic Device Moving Paddle Displacement with Micro Steps

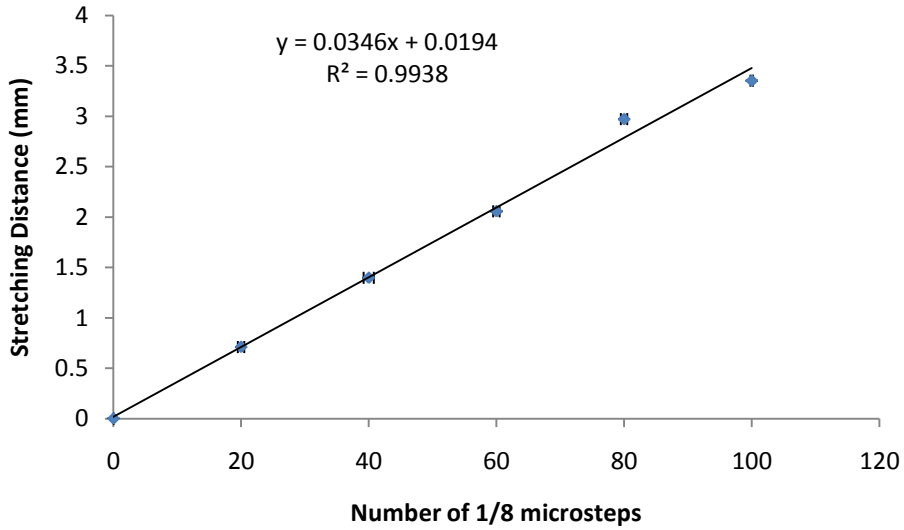

The elastic device moving paddle was displaced by providing 1/8 micro steps from the motor and the displacement was then measured in millimeters. It was determined the moving paddle follows the equation

$$y = 0.0346x + 0.0194 \quad (24)$$

Where *y* is the moving paddle displacement and *x* is number of 1/8 micro steps the motor provides (Eq. 24).

The major concern associated with the use of a rack and pinion system is the backlash associated with tolerances in the manufacturing of the gear teeth. This is the specific amount of free rotation of the gear that does not produce a linear motion of the rack. Therefore it is important for us to characterize the specific amount of backlash in our system for calibration of the controls system. With the available measurement instruments, we could not quantify the backlash associated as the instruments did not provide the resolution needed.

Even with this backlash accounted for, it will also be important to develop a zero point for on demand calibration. This will be accomplished by first moving the paddle an arbitrary distance out from the stationary paddle. Then, as the moving paddle is returned, the motor must slowly

increment until the two paddles are touching. Contact between the paddles will be confirmed by obtaining a very small strain response. Once this point is set is reached, the distance will be zeroed. We can confirm our calibration of the zero by again measuring with a either calipers or a micrometer.

14.1.2 Load Cell Calibration

In order to record proper strain and force data it is required that we calibrate the load cells. To do this we applied known loads to the load cell in the direction it would be receiving a force when used in the device. These loads were 0, 10, 20, 50, 100, 200 grams. With each load applied change in voltage with respect to no load was measured. This was completed multiple times to determine repeatability of the load cell. A linear relationship was then formed showing the change in voltage vs. the known loads applied. However, it was examined that this relationship was dominated by the noise and an accurate calibration curve could not be obtained. This is due to multiple aspects such as a faulty amplifier circuit due to malfunctioning instrumentation amplifiers, along with other noise issues which can be read in Section 16, along with recommended solutions. The figure below shows the calibration curve of the indentation load cell. Note the error bars dominated by the noise as described.

Figure 57: Indenter load cell calibration curve

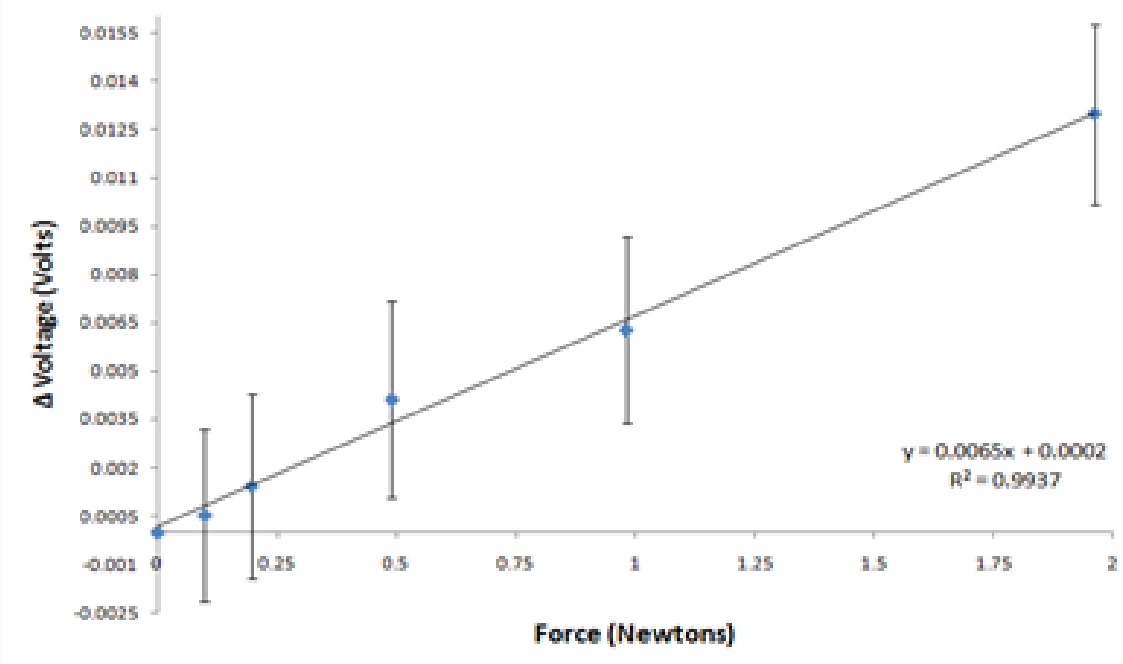

14.2 Device Validation

It will be important to carry out these initial tests on known materials, to confirm that properties are measured properly. Various size ranges and test rates will be analyzed for these materials to further verify the full capabilities desired. As different size ranges are examined the forces applied must be scaled to maintain a constant stress applied between tests. We have determined that the stress applied during an extension test should be approximately 65 kPa [3] and an indention test should be 900 kPa [22]. Further testing and analysis will need to be done to develop a correlation between various sized indenter tips. This will allow us to confirm that consistent hardness ratings are recorded by each.

Due to the issues we encountered with calibration of the load cells and our amplifiers, we were unable to fully validate that accurate elasticity and hardness measurements are achievable on test material. However, we do believe that with the improvements and using recommendations (Section 16), this device will be able to follow the proposed validation process. It should also be noted that our mechanical system is fully operational as specified in Section 14.

15. DESIGN CRITIQUE

Our team believes that we have developed a design that has the capability to meet all customer requirements and engineering specifications. Mechanical components of the design critical to precise positioning have been manufactured with tight tolerances. The stepper motor and control system implemented utilizes micro-stepping, allowing for actuation with a resolution on the micron level as desired. With our current LabVIEW configuration, the user has full control over the resulting displacement and motion velocity. The device also conforms such that the user can test at most locations on the body with the freedom to position at any orientations. This was one of the major customer requirements as specified in Section 3. Regarding the electrical system, our current amplifier circuit does not achieve the level of amplification expected in theory calculations and most of the data is noise dominated. Our design will maintain the ability to measure force once the load cell system is improved. Recommendations for this improvement are further described in Section 16. The true responses of the load cells we developed are difficult to accurately gauge with the inadequate amplifier, but from data we were able to acquire, we believe they would be sensitive to at least a 10 gram (0.1 N) load, meeting requirements specified by the customer. It is also important to note that this 10 gram sensitivity is comparable to other load cells on the market costing around $300 each, where ours costed $175 for all three load cells. However, the production of our own load cells has exposed certain issues that can hinder their functionality such as pre-straining or imperfect mounting of the strain gauges. In addition, a concern encountered when using ABS plastic was the noticeable expansion and contraction of material as a result of thermal effects. This may have further attributed to force reading errors and also caused minor issues with hole alignments and tolerances.

16. FUTURE DESIGN CONSIDERATIONS

With the completion of the device it is recommended that some aspects of the design are redesigned and further developed as this project continues into the future. These considerations cover both mechanical and electrical aspects of the device.

The first consideration is to produce a finalized controls system used to control the displacement of the motor and the overall LabVIEW programming code. To best develop a functional system, an individual with extensive LabVIEW and programming knowledge is desirable. The main controlled test to be programmed, which we were unable to accomplish within the time constraints, is the ability to maintain a constant force while applying an indentation or stretch to the skin sample, allowing the acquisition of time dependent property results. An intricate LabVIEW code will be required with multiple loops including feedback to both the motor controller and user. In addition, it is also important to consider the efficiency of the program itself to ensure smooth execution and minimize delays between sub-functions. If this is done correctly, graphs representing the elasticity and hardness will be able to be produced in rapid succession to further reduce testing and analysis time.

Another recommendation for change to the design is the redevelopment of the amplifier circuits used in conjunction with all implemented load cells. We propose that the power supply into this circuit and into load cell should be transmitted from a precision analog voltage supply rather than using the digital supply from the DAQ. With the current configuration, there is an abundance of noise in the strain data recorded determined to be partially caused by this. For further reduction in signal noise, it is also recommended to create a precision voltage-to-current converter. This would be added to the existing circuit arrangement and allows for a smoother signal input to the instrumentation amplifier. With these improvements in place, the device would be capable of achieving the requested level of precision.

The next item to be considered is the improvement of load cell development. Though much time has been put into researching the best way to mount the strain gauges, it is recommended that alternate methods be researched. This is due to the execution of placing these strain gauges being quite tedious and requiring experience to make sure there are no pre-strains applied to the gauges. Another issue encountered during the fabrication of the load cells was the process of soldering wires to the strain gauges. Currently, in the lab available to ME450 students, we do not have the equipment capability for micro-soldering. For reduction of signal noise and to ensure that wire connections are solid, it is recommended that in future design iterations these gauges be micro-soldered to the wires. Lastly our current design uses rapid prototyped ABS plastic for load cell material. This type of material has a greater thermal effect and weaker stiffness than initially calculated. Therefore it is recommended that various materials be analyzed for use as load cells and an optimal one be selected. Since this is a sensitive device, a type of plastic will still be

preferred over metal. The current load cell design, from a mechanical standpoint, should be applicable to almost any plastic material.

Within the constraints of ME450, teams are initially given a limited budget to work with during the semester with further funding up to the discretion of the sponsor. For a device which requires high accuracy and precision at a micron level, it is important that adequate equipment and materials are purchased. These generally tend to cost more then what is allotted in an ME 450 project. However, if this project is to be carried further as an independent research project or a project outside the classroom, an increased budget may be more acceptable. With a budget increase, we would first recommend replacing the stepper motors with linear actuators. This would simplify both devices by eliminating the screw-driven indention and rack and pinion systems resulting in direct linear motion rather than translation from rotation. Another expense would be the employment of a higher quality rapid prototyping process which allows for higher quality plastics with tighter tolerances. For improvement of displacement tracking, position sensor may be implemented with the exact selection dependent upon the desired resolution. However, position sensors with sensitivity to the micron level cost about $700 dollars each, leading our design to track motion through the stepper motor. In addition, it may be decided that pre-made load cells could be purchased, thus eliminating errors associated with developing components in-lab. Even though this may seem more desirable, load cells at the resolution required of this device cost approximately $300 each, compared to that of the total $175 quote for the three load cells we designed.

There are many design considerations involved with a design that is still in its early development stages. It is suggested that these considerations are taken and implemented before the second prototype is made. As further design iterations are developed, more design considerations should be expected to become apparent.

17. CONCLUSION

We believe that we have developed a device with the capability of meeting all customer requirements and engineering specifications. Through validation and calibration it has been concluded that the mechanical portion of our design meets these. However, the electrical system does not due to an excise amount of noise and circuitry issues. Therefore, it is recommended that this project be continued as an independent research project or student project to further develop the device using the proposed design considerations.

18. ACKNOWLEDGEMENTS

Our team would like to thank our sponsors (Professors Gordon Krauss and Gary Fisher) for giving us the opportunity to work on their project this semester, professor Grant Kruger and Dan

Johnson for continued input and guidance throughout the term, Bob Coury and John Mears for aiding in manufacturing, Toby Donajkowski for aiding in electrical system manufacturing, and all others who have provided us with input and support all semester.

19. REFERENCES

[1] Dobrev H.P., 1998, "*In vivo study of skin mechanical properties in patients with systemic sclerosis*" Journal of the American Academy of Dermatology, Vol. 40, No. 3, pp. 436-442

[2] Diridollou S, Berson M, Vabre V, Black D, Karlsson B, Auriol F, Gregoire J.M., Yvon C, Vaillant L, Gall Y, Pata F, 1998 "*An In Vivo method for measuring the mechanical properties of the skin using Ultrasound,*" Ultrasound in Med. & Biol., Vol. 24, No. 2, pp. 215–224

[3] "*Mechanical properties of normal skin and hypertrophic scars*," 1996, Burns, Vol. 22, No. 6, pp. 443-446

[4] "*Age-Related Mechanical Properties of Human Skin: An In Vivo Study*," 1989, Vol. 93, No. 3, pp. 353-357

[5] "*Mechanical property and the effects of pressure therapy*," 1980, PhD Thesis, Bioengineering Unit, University of Strathclyde, Glasgow

[6] Agache P.G., Monneur C, Leveque JL, De Rigal J, 1980, "*Mechanical properties and Young's modulus of human skin in vivo*," Arch Dermatol Res, Vol. 3, pp. 269, 221–232.

[7] Courage + Khazaka Electronic GmbH. Scientific Measurements of Skin and Hair. Koln, Germany: Courage + Khazaka Electronic GmbH. CK Electronics. Web. 18 Sept. 2010. <http://www.courage-khazaka.de/start.htm>

[8] Seehra G.P, Silver F.H, 2006, "*Viscoelastic properties of acid- and alkaline-treated human dermis: a correlation between total surface charge and elastic modulus*," Skin Res Technol, pp. 190-198

[9] Mohatta C.D, "Why does the skin age?" http://ezinearticles.com/?Why-Does-The-Skin-Age?&id=208085

[10] R. Sanders, 1973 "*Torsional Elasticity of Human Skin in Vivo*," Vol. 342, No. 3, pp. 255-260

[11] Findley, W. N., Lai, J. S., and Onaran, K., 1976, *Creep and Relaxation of Nonlinear Viscoelastic Materials*, General Publishing Co., Toronto, Ontario, Chap. 1, pp. 1-5

[12] Agache, P. G., Monneur, C., Leveque, J. L., and Rigal, J. D., 1980, "*Mechanical Properties and Young's Modulus of Human Skin in Vivo*," Archives of Dermatological Research, pp. 221-232

[13] Katz, S.M., Frankm,D.H., Leopold, G.R., Wachtel, T.L., 1985, "*Objective measurement of hypertrophic burn scar: a preliminary study of tonometry and ultrasonography,*" Annals of plastic surgery [0148-7043], Vol.14, No. 2, pp. 121-125

[14] Berardesca, E., Borroni, G., Gabba, P., Borlone, R., Rabbiosi, G., 1986, "*Evidence for elastic changes in aged skin revealed in an in vivo extensometric study at low loads*," Bioeng Skin, Vol. 2, pp. 261–270

[15] Berson, M., Vaillant, L., Patat, F., Pourcelot, L., 1992, "*High-resolution real time ultrasonic scanner*," Ultrasound Med Biol., Vol. 18, pp. 471– 478

[16] Wickman, M., Olenius, M., Malm, M., Jurell, G., Serup, J., 1992, "*Alterations in skin properties during rapid and slow tissue expansion for breast reconstruction*," Plastic

Reconstruction Surgery, pp. 945–950
[17] Sugihara, T., Ohura, T., Homman, K., Igawa, H. H., 1991, "*The extensibility in human skin: variation according to age and site*," British Journal Plastic Surgery, pp. 418–422
[18] Boyer, G., Laquieze, L., Bot, A. L., Laquieze, S., Zahouani, H., 2009, "*Dynamic Indentation on Human Skin in vivo: Ageing Effects*," Skin Research and Technology, pp. 55-67
[19] Nielsen, L. F., 1995, "*Viscoelastic Material Properties Determined from Experimental Vibration Analysis of Systems*," pp. 1-25
[20] Dowling, N. E., 2007, *Mechanical Behavior of Materials: Engineering Methods for Deformation, Fracture, and Fatigue*, Prentice Hall, Upper Saddle River, pp. 772-836
[21] ASTM, 1983, *Annual Book of ASTM Standards: Rubber, Natural and Synthetic – General Test Methods; Carbon Black*, Easton, pp. 602-605
[22] Warner, M.K., 2006, "CCSi DuroMatters: Durometer Types and Specifications," http://www.ccsi-inc.com/html-instruments.htm
[23] *The Luxurious Hair Boutique*. 5 Oct. 2010 <http://www.lhboutique.com/krylon-mega-hold-kit-p/ krymedkit2.htm>.
[24] *Metro Medical Online*. 5 Oct. 2010 <http://www.metromedicalonline.com/7730.html>.
[25] *Kryolan Professional Make-up*. 5 Oct. 2010 <http://www.kryolan.com/en/ index.php?cid=117&mnu=32&id=171&pageid=1>.
[26] *3M Polyurethane Medical Tape*. 5 Oct. 2010 <http://www.3m.com/product/information/ polyurethane-medical-tape.html>.
[27] Oberg, E., Jones, F. D., Horton, H. L., Ryffel, H. H., 2000, Machinery's Handbook (26th Edition), Industrial Press, New York, pp. 621-667
[28] Pololu Robotics and Electronics. 25 Oct. 2010 <http://www.pololu.com/catalog>
[29] Advanced Micro Systems. 27 Oct. 2010 <http://www.ams2000.com/productPages/dc_DCB261.html>
[30] Omegadyne, 1996, The Pressure, Strain and Force, Handbook, Omega Press LLC
[31] National Instruments, 1998, Strain Gauge Measurement Tutorial, <http://zone.ni.com/devzone/cda/tut/p/id/3642>
[32] Richard Nakka, 2007, Strain Gauge Load cell for thrust measurement, <http://www.nakka-rocketry.net/strainlc.html>
[33] "How To Use A Band Saw from American Machine Tools Corp." American Machine Tools Company -US Metalworking Machinery Distributor. Web. 31 Oct. 2010. <http://www.americanmachinetools.com/how_to_use_bandsaw.htm>.

20. TEAM BIOS

Brandon Kerins - Team Contact

I am originally from New Jersey and a transfer student from Penn State University in 2008. I have been interested in mechanical engineering for many years now. Having the ability to help shape the future is something that keeps me driving to get the best education I can receive through The University of Michigan. As for future plans I have accepted a job offer at The General Electric Company-Energy, in the Edison Engineering Development Program, which will lead to my master degree in mechanical engineering.

Joseph Kirby - Treasurer

My hometown is Warren, Michigan; a northern suburb of Detroit. My interests in mechanical engineering started several years ago while rebuilding a 1965 Corvette Stingray. The University of Michigan gave me the opportunity to delve deeper into my interests, and a chance to make a positive impact on the future. Right now I am undecided between receiving a master's degree and searching for a job upon graduation. If I didn't become an engineer I would most likely be a builder. Currently, I have more experience building homes than I do engineering.

Divyarajsinh Raol - Facilitator

I am a transfer student from Indiana University Purdue University Indianapolis but originally from Ahmadabad, Gujarat, India. My interest in mechanical engineering began in my early childhood. I had always been good in math and science, so engineering was a suitable match for me. My forte is in areas of Controls, manufacturing and structure mechanics. In future I plan to pursue master degree in mechanical engineering in the field of control systems.

Matthew Valvano – Facilitator

I'm originally from Saginaw, Michigan, a city about 90 miles north of Ann Arbor. I came to the University of Michigan with the plan to major in Computer Engineering, but found Mechanical Engineering to be a stronger interest after the first year. I enjoy working through the conceptual design process for mechanical components and applying engineering tools such as Finite Element Analysis. I have spent two summers working in automotive engineering and am currently working part-time as a designer and FEA analyst for my company. After I graduate this December, I plan to work with this company full-time. Further down the road I plan to continue my education and earn my masters degree in mechanical engineering.

APPENDIX A: BILL OF MATERIALS

In order to successfully fabricate a prototype a bill of materials is required. This allows for easy price reference and vender/part number. It also provides part number references allowing for a simplified fabrication and assembly process. The total cost for our device is $1,349.18 without shipping and $1,489.13 with shipping.

A.1 Mechanical

#	Item	Manufacture	Part No.	Quantity	Cost	Total Cost	Shipping Cost
1	Rack	SDP/SI	A 1C12MY08A075	1	$11.50	$11.50	18
2	Spur Gear		S10T08M018S0505	1	$10.62	$10.62	
3	7/64 * 36 in Rod	wttool.com	0700-0020	1	$1.88	$1.88	-
4	Indenter Tips		1233-1440	3	$5.50	$16.50	
5	Knobs	McMaster-Carr	62935K15	7	$1.52	$10.64	20
6	30 mm Threaded Rod M4x0.7		93805A266	1	$0.73	$0.73	
7	20 mm Threaded Rods M4x0.7		93805A259	6	$0.61	$3.66	
8	Threaded 1/4-28 Rod		6516K13	1	$6.70	$6.70	
9	Female Bolt Rod End		6516k55	1	$12.29	$12.29	
10	2in 4-40 Threaded Rods		95412A870	1	$6.91	$6.91	
11	Set Screws		92695A005	1	$6.54	$6.54	
12	Epoxy	Stadium Hardware	-	1	$6.00	$6.00	-
13	Statonary Paddle Scrap Aluminum Stock	N/A	-	1	$0.00	$0.00	-
14	Manufacturing + Material	UM 3D Printing	-	1	$160.00	$160.00	-
15	Fasteners	Local	-	1	$7.09	$7.09	-
15a	M4-Keep nut	Local	-	1	-	-	-
15b	M4-Hex nut	Local	-	5	-	-	-
15c	M2.5 Pan head Screw	Local	-	9	-	-	-
15d	4-40 Hex nut	Local	-	3	-	-	-
15e	1/8 Washer	Local	-	3	-	-	-
15f	4-40 Nylon Wing nut	local	-	1			
	Total	-	-	-	-	$261.06	38

A.2 Electrical

#	Item	Manufacture	Part No.	Quantity	Cost	Total Cost	Shipping Cost
16	Stepper Motor	Iolu Robotics and Electron	1206	2	$16.95	$33.90	16
17	Strain Gauges single (5 Pack)	Omega	SGT-1/350-TY13	2	$27.60	$55.20	14
18	Stain Gauges Double (5 Pack)		SGD-2/350-DY13	1	$65.00	$65.00	
19	Bondable terminal pads (70 Pack)		BTP-1	1	$18.50	$18.50	
20	Bondable terminal pads (60 Pack)		BTP-2	1	$18.50	$20.50	
21	DAQ	National Instruments	USB-6210	1	$566.00	$566.00	25
22	Motor Controller/Driver	Advanced Micro Systems	DCB 261	1	$179.00	$179.00	30
23	Power Supply		MPS 25W-40V	1	$49.00	$49.00	
24	Adapter (Labview)		SIN 11-USB	1	$69.00	$65.00	
25	DB M/F cable	MonoPrice.com	444	2	$2.04	$2.04	5.55
26	Electronic Project Board	Radio Sack	276-148	1	$1.99	$1.99	-
27	Non inverting amplifier	Digikey.com	INA122	3	$8.00	$24.00	11.4
28	Wires (20 AWG)	Radio Shack	278-1222	1	$7.99	$7.99	-
	Total					$1,088.12	101.95

APPENDIX B: DESIGN CHANGES

B.1 Elasticity Device Load Cell – Moving Paddle

WAS:

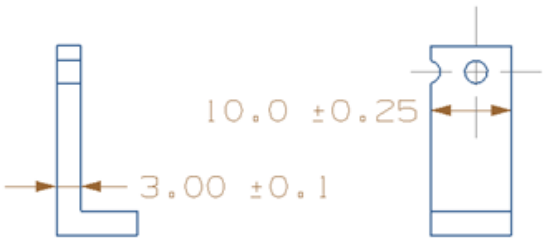

IS:

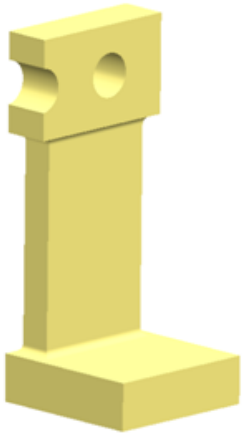

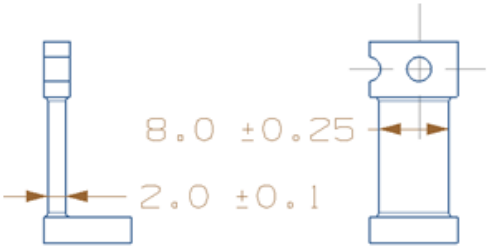

Needed to improve sensitivity of load cell to obtain lower force resolution. Decreased thickness by 1 mm and width by 2 mm. Material to be used changed from Aluminum to ABS plastic.

Team Derma (17)	
Elasticity Measurement Device	
Engineer: M. Valvano	11/4/2010
Proj. Mgr.: G. Kruger	11/4/2010
Sponsors: G. Krauss G. Fisher	11/4/2010

B.2 Hardness Device Support Wings

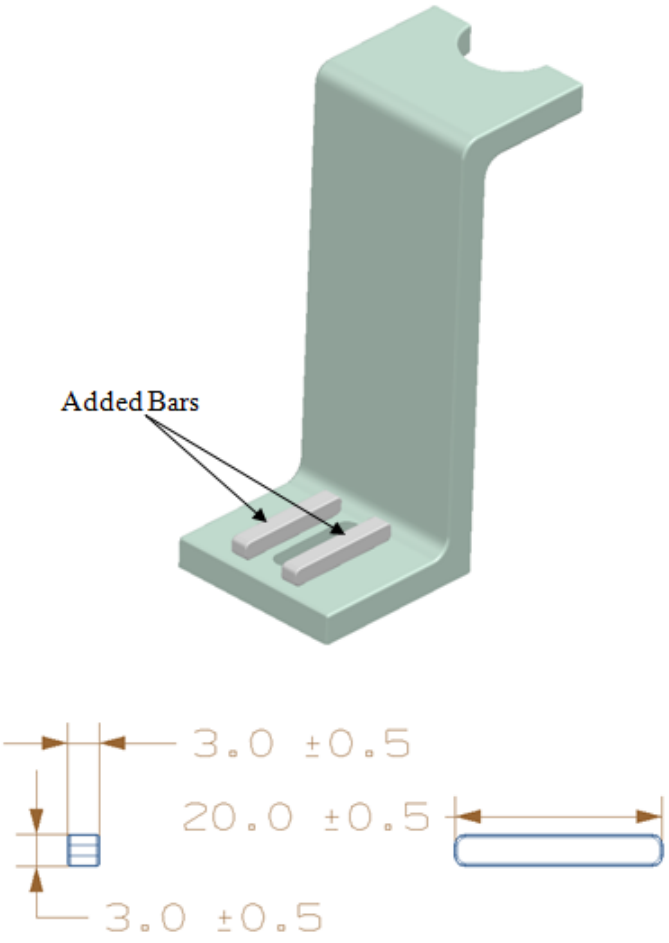

Needed to allow user to tighten/loosen the adjustable supports using only one hand and no mechanical assists. Added two parallel plastic bars to act as a guide and prevent rotation of the hex nut. Bars were attached with plastic epoxy.

Team Derma (17)	
Hardness Measurement Device	
Engineer: M. Valvano	11/4/2010
Proj. Mgr.: G. Kruger	11/4/2010
Sponsors: G. Krauss G. Fisher	11/4/2010

B.3 Hardness Device Load Cell

WAS:

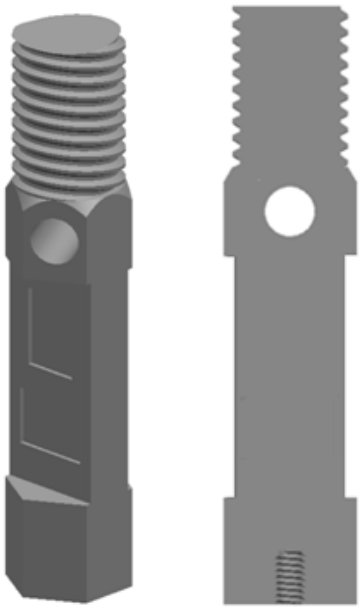

IS:

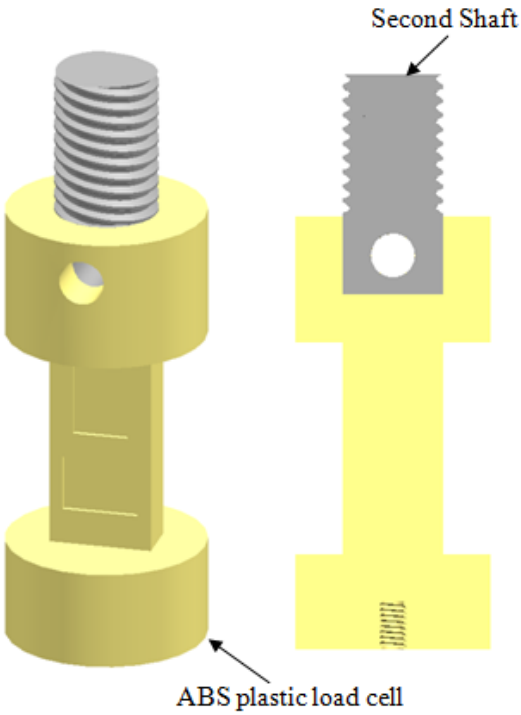

Needed to increase sensitivity of indentation load call to allow for finer force reading resolution. The load cell material was changed from Aluminum to ABS plastic. To maintain a rigid interface between the male and female threads, a second shaft, made of carbon steel, was implemented. The two components are held fixed to one another through the common shaft.

Team Derma (17)	
Hardness Measurement Device	
Engineer: M. Valvano	11/4/2010
Proj. Mgr.: G. Kruger	11/4/2010
Sponsors: G. Krauss G. Fisher	11/4/2010

APPENDIX C: DESIGN ANALYSIS

C.1 Material Selection Assignment (Functional Performance)

C.1.1 Bending Load Cell

1. Function: To support bending loads
   Objective: Inexpensive
   Loading Constraints: Stand up to 1N bending loads, with up to 0.1mm deflection
   Dimensional Constraints: 20mm length, 16mm2 area
   Cost Constraints: Maximum cost of $5.

2. Material Indices:
   $M_1 = 1250\ \text{MPa} \leq E \leq 3016\ \text{MPa}$
   $M_2 = \sigma_y \geq 0.94\ \text{MPa}$
   $M_3 = c_m\rho \leq 1.56\times10^{7}\ \$/m^3$
   $M_4 = \frac{E^{0.5}}{c_m\rho} \geq 2.26\times10^{-3}\ Pa^{1/2}m^3/\$$
   $M_5 = \frac{\sigma_y^{2/3}}{c_m\rho} \geq 6.13\times10^{-4}\ Pa^{2/3}m^3/\$$

Figure C.1: CES results for bending load cell

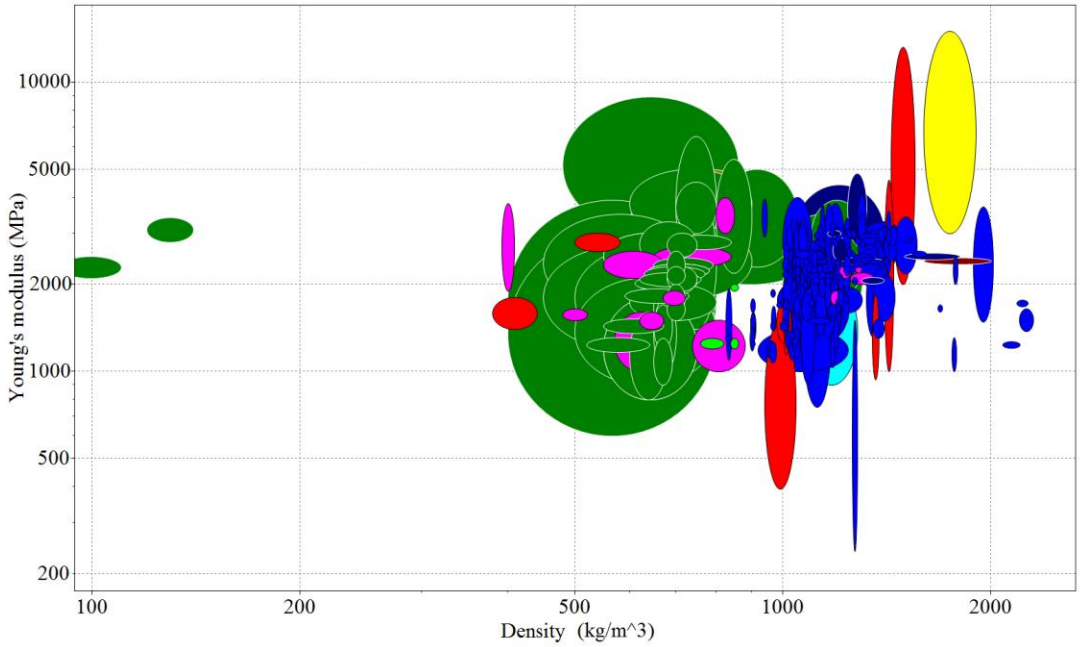

3. Top five material choices from CES:
   1. ABS/PC
   2. PVC
   3. PC
   4. POM
   5. PP

4. The range for the Young's modulus was chosen due to two reasons: to minimize deflections below 0.1 mm (Eq. C.1); and to be able to read 0.1 gram loads (Eq. C.2) once the strain gauges are applied. One side of the load cell will experience tension in bending and at the maximum force it is important to withstand yielding. The total cost of the complete component was set to not exceed $5 (Eq. C.3), but even smaller prices are more favorable. The last material indices are derived from the above constraints.

$$\delta = \frac{4F \times L^3}{E \times A^2} \tag{C.1}$$

$$F_{min} = \frac{\Delta L \times E \times A}{L} \tag{C.2}$$

$$C_m \times \rho = \frac{C}{A \times L} \tag{C.3}$$

Where δ is the deflection, F is the maximum applied load, F_{min} is the minimum readable load, L is the length, A is the area, E is the Young's modulus, C_m is the cost per kg weight, and C is the total cost.

The constraint on the Young's modulus narrowed the material choices down to only a handful. It was dominated by plastics, woods, and paper products. Obviously, for our function wood or paper would not suffice, and therefore a list of the top choices contains all plastics. Each of the above listed materials have similar material properties and densities, however there is a variation in the prices. ABS is the most expensive of the top five choices, but only by a couple of dollars. The ABS also meets all constraints with some form of safety factor. The reason why ABS was selected over all other plastics is because it is available on campus, saving us time and shipping costs.

C.1.2 Indenter Load Cell

1. Function: To support compressive axial loads
   Objective: Inexpensive
   Loading Constraints: Stand up to 8N axial loads without buckling.
   Dimensional Constraints: 13.5mm length, 12mm^2 area
   Cost Constraints: Maximum cost of $5.

2. Material Indices:
   $M_1 = 51.57\ \text{MPa} \leq E \leq 6033\ \text{MPa}$
   $M_2 = \sigma_{cs} \geq 0.67\ \text{MPa}$
   $M_3 = c_m\rho \leq 3.09\times10^7\ \$/m^3$
   $M_4 = \frac{E^{0.5}}{c_m\rho} \geq 2.33\times10^{-4}\ Pa^{1/2}m^3/\$$

Figure C.2: CES results for indentation load cell

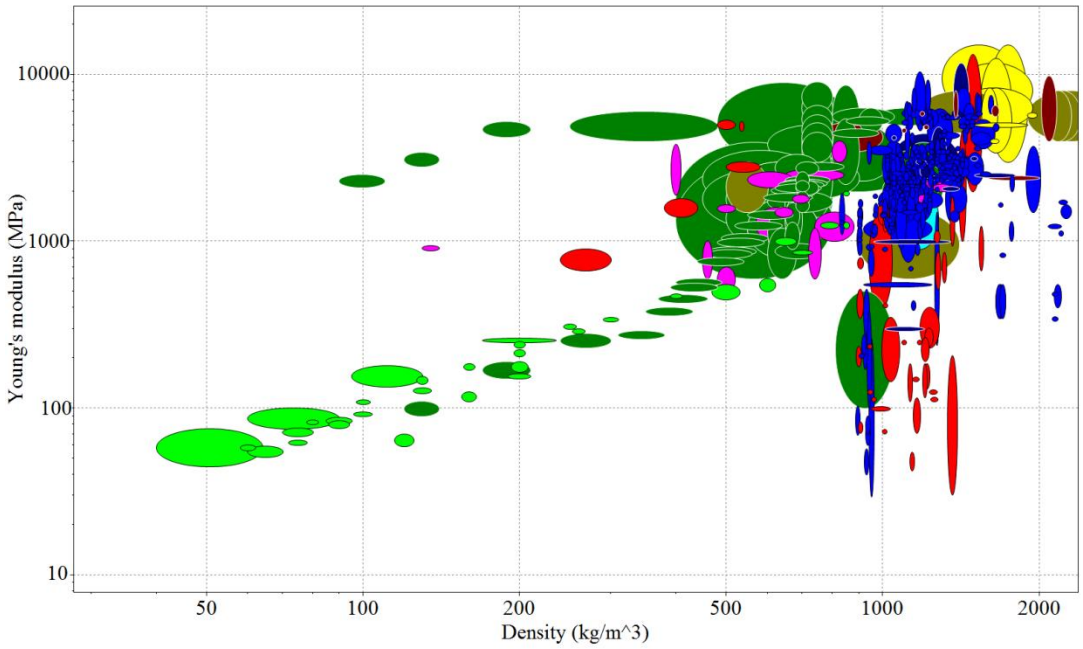

3. Top five material choices from CES:
   1. ABS/PC
   2. PVC
   3. PC
   4. POM
   5. PP

4. The range for the Young's modulus was chosen due to two reasons: to withstand buckling at 8 N loads (Eq. C.4); and to be able to read 0.1 gram loads (see Eq. C.2) once the strain gauges are applied. It is also important to keep the materials compressive strength (Eq. C.5) larger than the maximum stress to prevent fracturing failure. The total cost of the complete component was set to not exceed $5 (see Eq. C.3), but even smaller prices are more favorable. The last material indices are derived from the above constraints.

$$F = \frac{\pi \times E \times A^2}{4(K \times L)^2} \quad \text{(C.4)}$$

$$\sigma_{cs} = \frac{F}{A} \quad \text{(C.5)}$$

Where $K = 2$ is a constant, F is the maximum applied load, L is the length, A is the area, E is the Young's modulus, and σ_{cs} is the compressive strength.

The constraint on the Young's modulus narrowed the material choices down to only a handful. It was dominated by plastics, woods, resins, and paper products. Obviously, for our function wood, resin or paper would not suffice, and therefore a list of the top choices contains all plastics. Each of the above listed materials have similar material properties and densities, however there is a variation in the prices. ABS is the most expensive of the top five choices, but only by a couple of dollars. The ABS also meets all constraints with some form of safety factor. The reason why ABS was selected over all other plastics is because it is available on campus, saving us time and shipping costs.

C.2 Material Selection Assignment (Environmental Performance)

The masses of the bending and indentation load cells are 0.80g and 2.01g, respectively. Using SimaPro 7.2, we were able to input both the materials and their masses to determine the environmental impact of each. Figure C.3 shows the total mass (in grams) of raw material usage, air emissions, water emissions, and soil pollution. Raw material usage is 1.234g and 3.085g for the bending load cell and indentation load cell, respectively. Air emissions were by far the highest value at 2.977g and 7.442g. Water emissions are much lower at 0.105g and 0.262g. Soil pollution has the smallest emissions and is a factor 1000 less at 0.142mg and 0.356mg. This plot shows that the indentation load cell has over twice the environmental impact (per the EcoIndicator 99 damage classifications) in every category.

Figure C.3: Total mass of various emissions and material usage

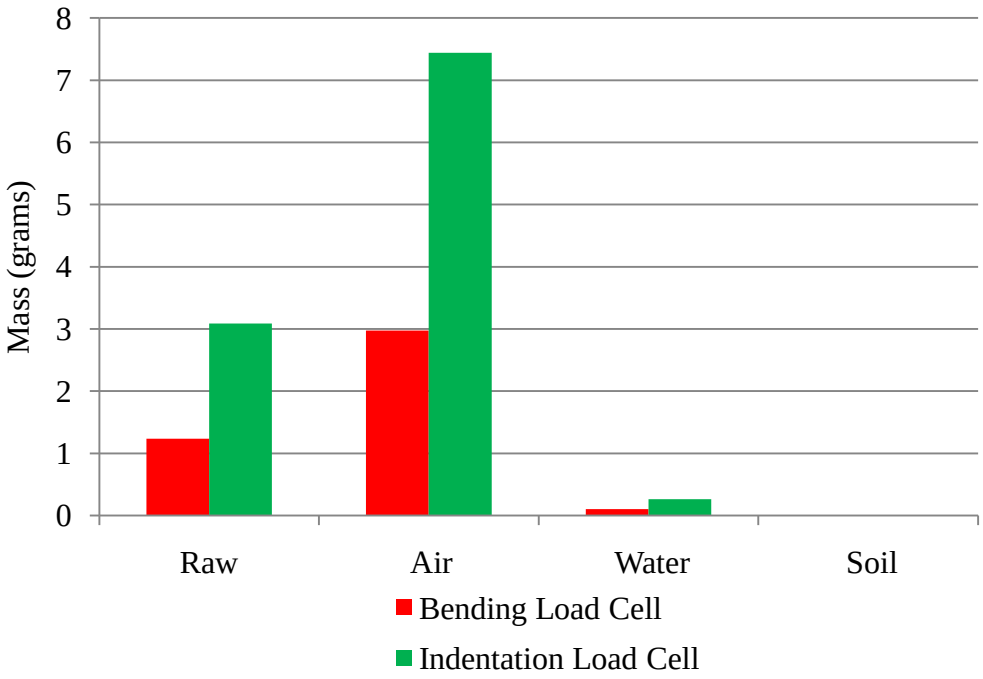

Figure C.4 shows the relative impact of each component on different damage categories. Several of the categories are carcinogens, climate change, radiation, ozone layer, land use, etc. The graph shows that relative to each other, the bending load cell would only have 40% of the impact as the indentation load cell.

Figure C.4: Relative impacts in disaggregated damage categories

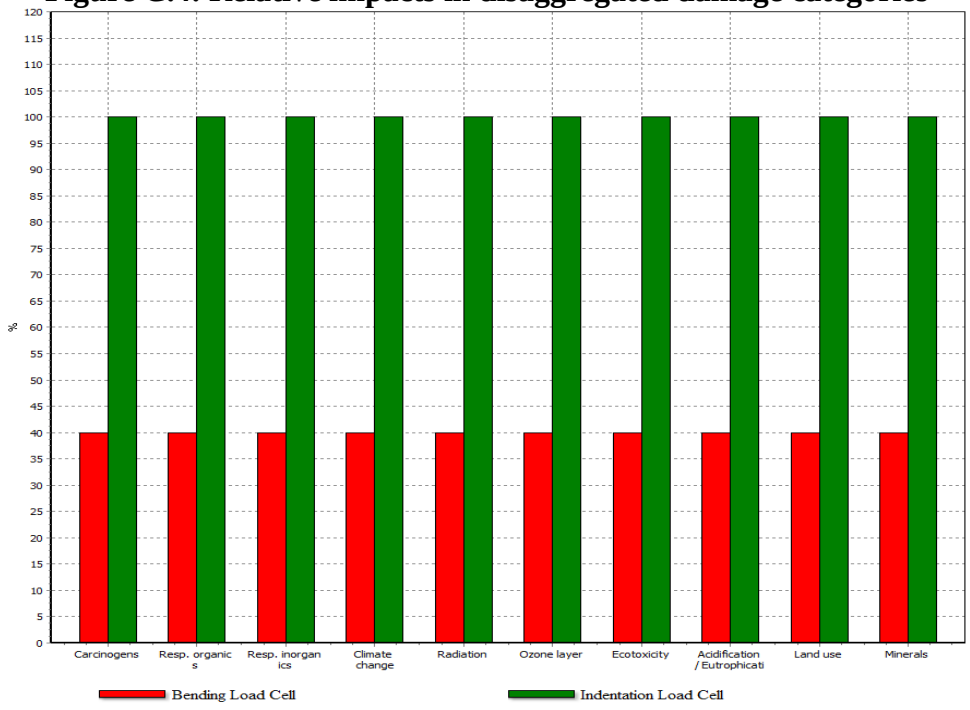

Based on the EcoIndicator 99 point values, human health is likely to be the most affected by processing of these parts, followed by resources, and then eco-toxicity (Fig. C.5). The scale shows that the magnitude of these values are small, however. In every case, the Indentation load cell had over twice the impact as the bending load cell.

Figure C.5: The normalized score in human health, eco-toxicity, and resource categories

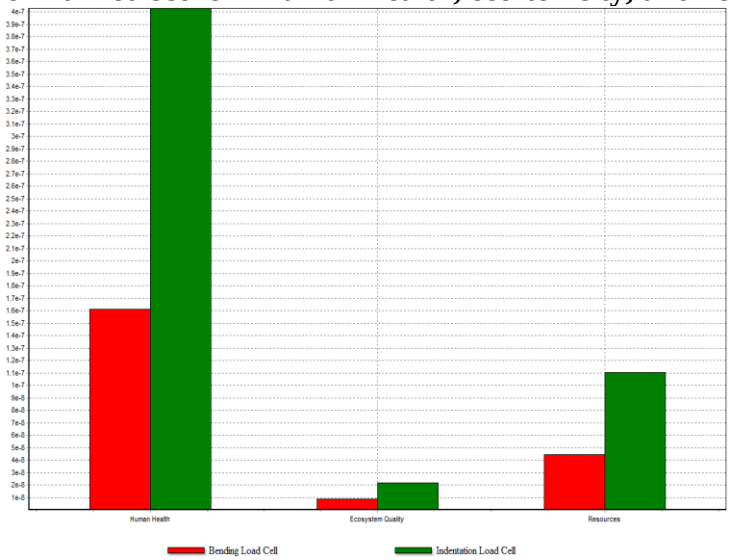

As confirmation to the above statement that in every case the indentation load cell has a higher EcoIndicator 99 point value, Figure C.6 shows the summation of the three damage meta-categories for each component. The plot shows that summed up, the indentation load cell has over twice the impact. This can be attributed to being the same material, but with different weights. The indentation load cell is most likely to have a bigger impact when the life cycle of the whole product is considered.

Figure C.6: Single score comparison of each load cell in points

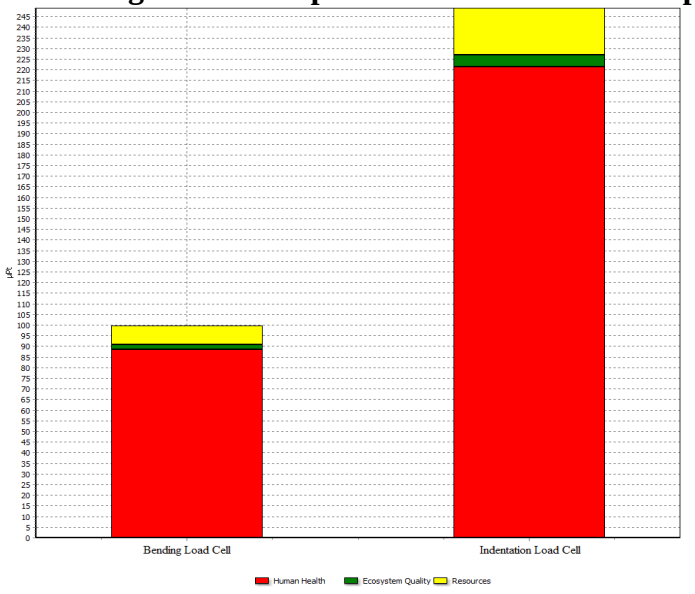

The consideration of the full life cycles does not make either component more important than the other. The only difference in environmental impact is due to the different masses of each component. This analysis shows that the total raw materials and emissions are small, but not insignificant. Selecting a different material would be out of the question because the ABS plastic was needed to achieve the desired force readings. The overall design was rather simple for each device, but there was little choice in material selection. Most of the purchased parts came with only one material option. The only options left were the load cells and device housings.

C.3 Manufacturing Process Selection

The skin measurement device has many commercial applications within the skin care industry. Since there is a possible large demand from dozens of companies, a production volume of 1 million units was chosen.

Each load cell as previously discussed is to be manufactured using ABS/PC plastic, and the current method used is rapid prototyping. However, this is not suitable if the device were to become commercialized because rapid prototyping is only suitable for low volume production. Injection molding is the preferred method if 1 million units are to be produced. The CES software shows that the chosen ABS plastic can be both injection molded or extruded. Advantages to injection molding: low labor cost, repeatable high tolerances, minimal material waste, ability to make complex shapes, and no finishing after molding. The same process can be used for both parts because they are made from the same material and only have differing geometries for their specific functions.

APPENDIX D: CONCEPT PRODUCTION

Appendix D.1: Measure Elasticity

The Pugh Chart for the sub function Elasticity testing was derived using customer requirements and engineering specifications. The design should be less sensitive to noise and should be robust.

Elasticity Testing	Weight	Horizontal Rack & Pinion	Pressure induced Stretching	Torsion
Variable Testing Rates	7	4	4	5
Maintain Const. Force	9	4	4	4
Sensitivity to positioning (min)	8	5	5	4
Sample Variable Skin Size	8	4	5	2
Minimize Complexity	6	3	2	4
Robustness	10	4	2	3
Data Readability	6	5	5	5
Cost	7	3	3	3
Total Rating		245	227	224

1. Horizontal Rack and Pinion (245)

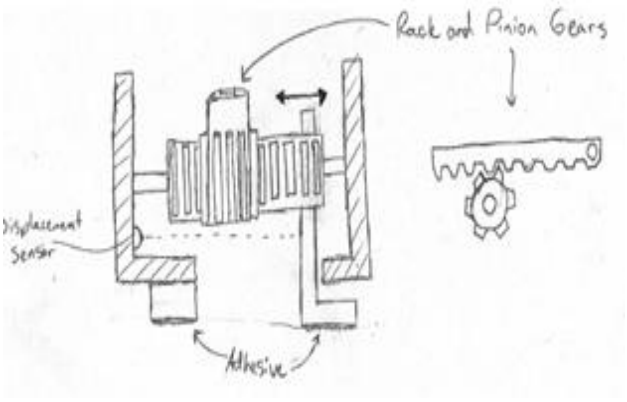

The rotational motion from the DC motor is converted to linear motion using horizontal rack and pinion. Pin stretches the skin and the displacement and force is measured by sensors and recorded using a DAQ.
An advantage of this design is that it allows to test at variable test rates and skin sizes. Disadvantage is that it increases complexity in the design.

2. Torsion (227)

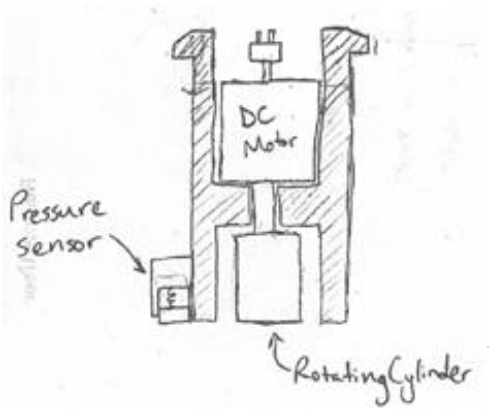

Torque from the DC motor is directly applied to skin by the rotating cylinder. Pressure sensor and optical sensors record the torque and displacement which is relayed to a computer software through DAQ. This design is less sensitive to positioning but limits the test sample sizes.

3. Pressure induced Stretching (224)

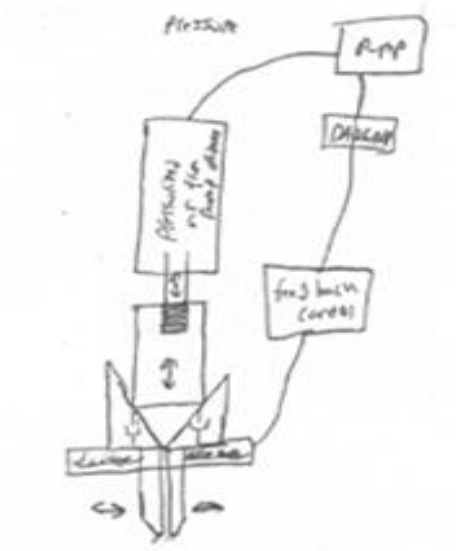

The pressure from the pressure pump pushes a plunger on to the paddles and the two pins are stretched apart. This device setting helps to test at variable test rates and test sizes but the force applied on the both paddles may not be constant and equal adding to the complexity of the design.

Elasticity Testing	Weight	oscillation translation	oscillation linear act	Linear Actuator Stretching
Variable Testing Rates	7	4	4	5
Maintain Const. Force	9	4	4	4
Sensitivity to positioning (min)	8	4	4	4
Sample Variable Skin Size	8	2	2	5
Minimize Complexity	6	3	3	1
Robustness	10	4	4	2
Data Readability	6	4	4	5
Cost	7	3	2	1
Total Rating		215	208	206

4. Oscillation translation (215)

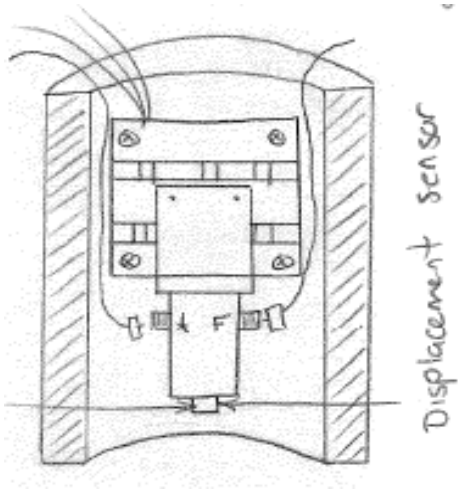

This method uses a translation stage to apply a sinusoidal force onto the skin. The translation stage is equipped with a servo motor to provide accurate positioning; however, the components are costly.

5. Oscillation Linear actuator (208)

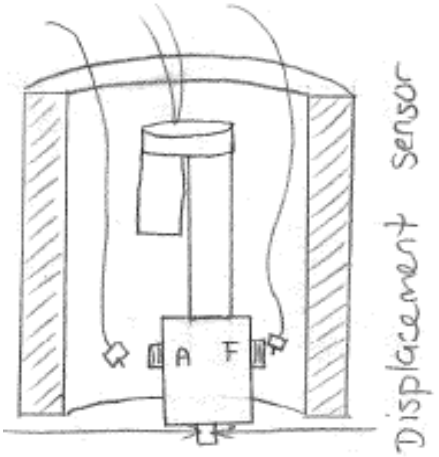

For this design a linear actuator applies a sinusoidal force onto the skin. Although linear actuators provide accurate results, they are high in costs.

\

6. Linear Actuator Stretching (206)

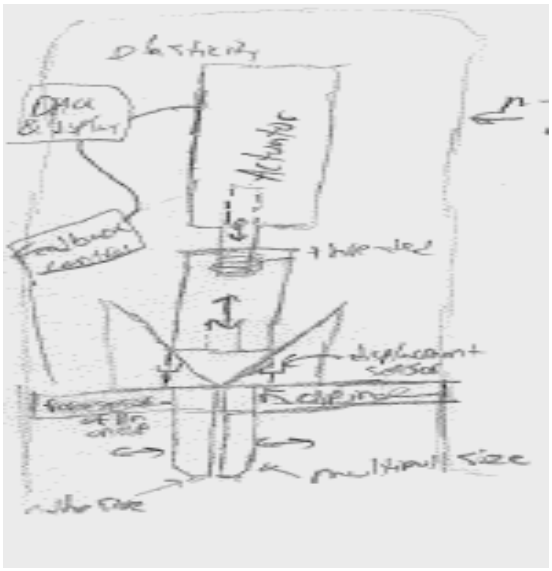

Same concept as pressure induced stretching. However, instead of pressure a linear actuator is used. This method is more costly than using pressure, but is better in measuring variable testing rates.

Elasticity Testing	Weight	Pressure Pump	Vertical Rack & Pinion Stretching	oscillation rack and pinion	oscillation crank shaft
Variable Testing Rates	7	4	4	3	3
Maintain Const. Force	9	4	3	3	2
Sensitivity to positioning (min)	8	4	4	2	3
Sample Variable Skin Size	8	2	5	2	2
Minimize Complexity	6	3	1	3	3
Robustness	10	3	1	3	3
Data Readability	6	2	5	4	4
Cost	7	3	2	3	3
Total Rating		193	187	173	172

7. Pressure pump (193)

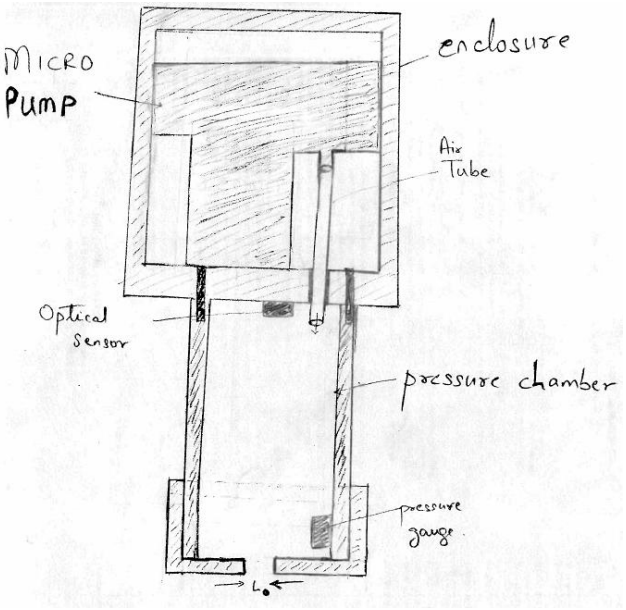

Using a pump, this device creates a negative pressure chamber. When skin is places to seal this container it is suctioned, causing a deformation in the skin which can be measured to find the elasticity. This leads to a complex and costly design. Also using pressure it would be hard to maintain a constant force on the applied skin, thus affecting the data we are collecting.

8. Vertical Rack & Pinion Stretching (187)

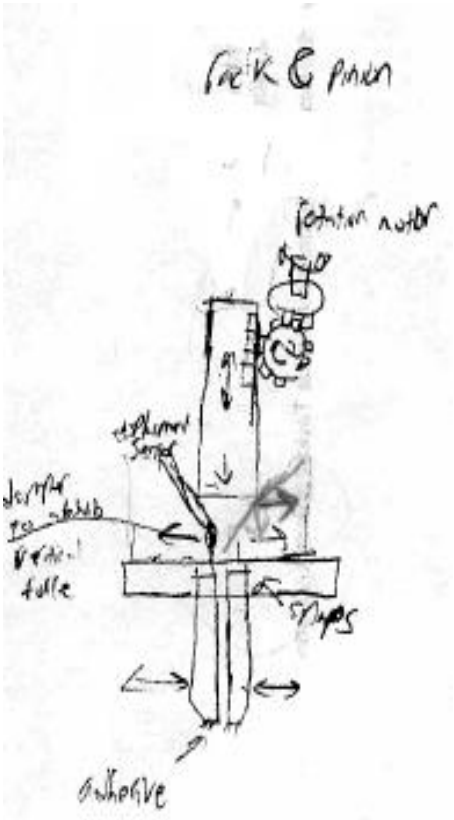

Same concept as pressure induced and linear actuator stretching. This design adds complication though due to the use of a DC motor to translate the rotational motion to vertical linear motion. This requires a multiple gear configuration. The advantage of DC motors is that they can be very small, allowing us to use them in smaller devices which improve mobility of the device. Cost of this device varies from moderately expensive to reasonable pricing depending on size.

9. Oscillation Rack and Pinion (173)

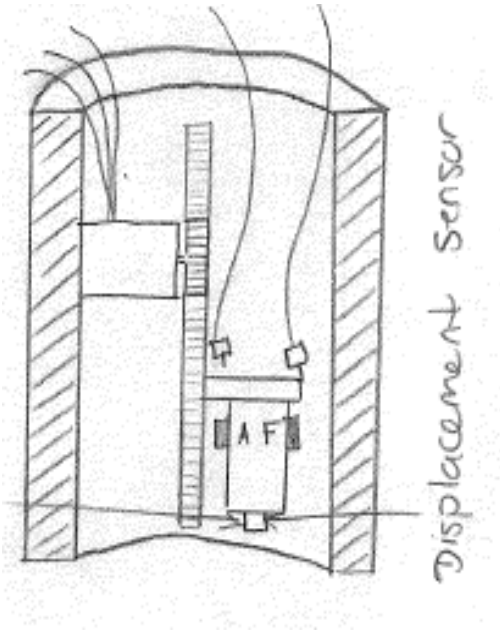

A DC motor turns a pinion, which moves a rack up and down. The cost for this method is low, but a rack and pinion is not exceptional for micron scale measurements.

10. Oscillation Crank shaft (172)

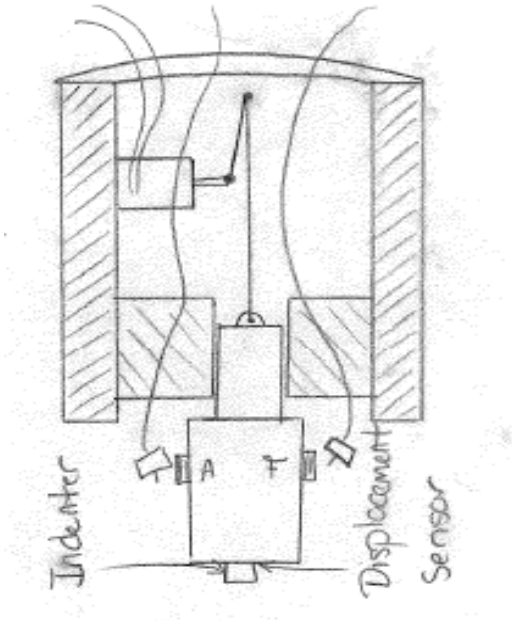

A DC motor operates a crank that converts into a linear oscillating motion, similar to the pistons in an IC engine. The cost for purchasing the components would be low, but the design is very complex.

Elasticity Testing	Weight	Gravity Induced Stretching	Hand Applied Stretching	Piston/Pressure
Variable Testing Rates	7	2	3	3
Maintain Const. Force	9	4	1	3
Sensitivity to positioning (min)	8	1	3	3
Sample Variable Skin Size	8	4	4	2
Minimize Complexity	6	2	4	2
Robustness	10	2	1	2
Data Readability	6	4	3	2
Cost	7	3	4	2
Total Rating		167	166	146

11. Gravity Induced Stretching (167)

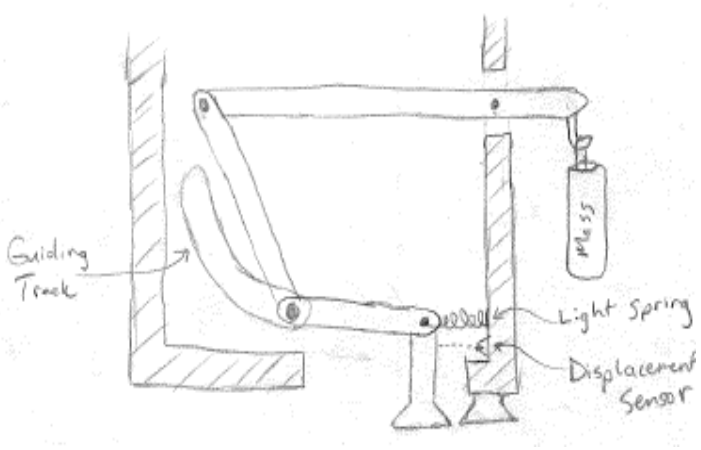

This concept operates by using a link system and a mass. The object of this concept is to create a manual device that can measure the elasticity. An advantage to this test is that the force is always constant due to gravity. However, unless this device is vertical to the ground the system will not work properly. This does not meet the requirement to measure on any skin location and therefore is infeasible. The data collected is recorded using sensors.

12. Hand Applied Stretching (166)

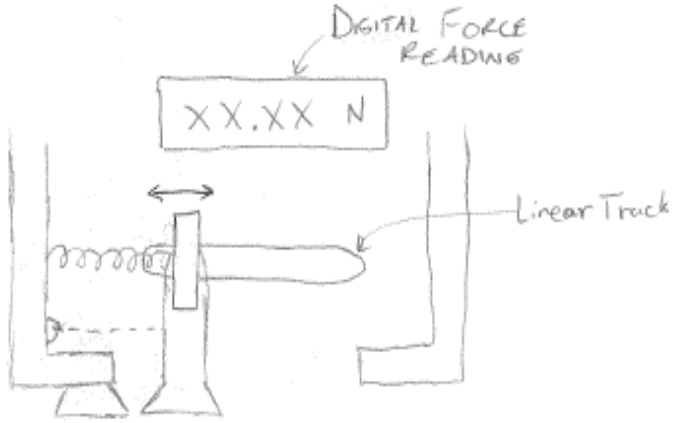

This device takes use of the operators hand to stretch the skin. Though this device is cheap, it does not meet many of the design requirements. It cannot be held at a constant force, it cannot test variable size ranges, and it cannot measure any skin location

13. Piston/Pressure (146)

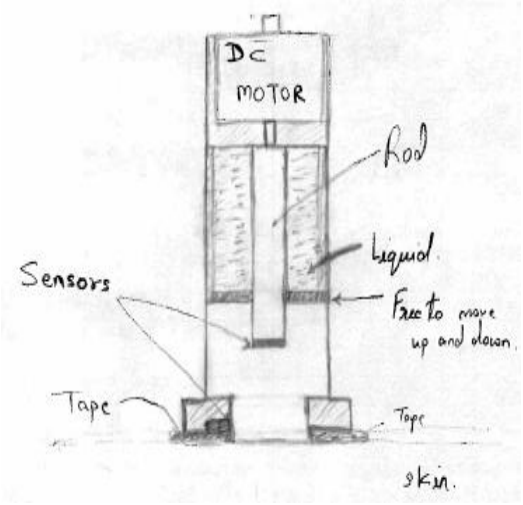

This concept works like the pressure pump concept. Except instead of using a pump this concept uses a piston cylinder set up using displaced liquid to create the suction to the skin. This uses a DC motor as the actuation device.

Appendix D.2: Measure Hardness

The criteria for hardness measuring device are the same as elasticity measuring device shown appendix D.1.

Hardness Testing	Weight	Screw Driven Indentation	Pressure Induced Indentation	Linear Actuator Indentation
Variable Testing Rates	7	4	4	4
Maintain Const. Force	9	4	4	5
Sensitivity to positioning	8	5	5	4
Sample Variable Skin Size	8	5	5	5
Minimize Complexity	6	4	4	4
Robustness	10	4	3	3
Data Readability	6	5	5	4
Cost	7	3	4	2
Total Rating		259	256	237

1. Screw Driven indentation (259)

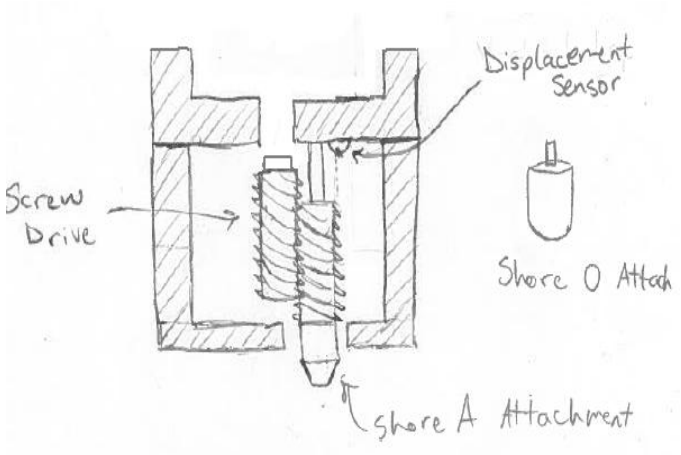

For this design a indenter tip is pressed on to the surface of skin by a screw and the displacement is measured by a LVDT displacement sensor. The attachments are adhered to skin by Hollister medical spray. This concept is moderately priced and not as complex as other designs. Being able to be less sensitive to positioning and can measure variable skin sizes.

2. Pressure induced Indentation (256)

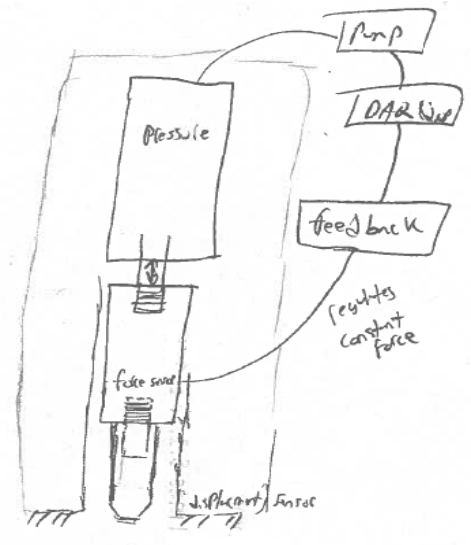

Using pressure created by a pump connected to the device, this device uses a pressure actuator to create linear movement. This movement is attached to an indenter, which is pressed into the skin. This device is low cost and can sample various skin sizes. However, due to the actuation being pressure it is hard to maintain a constant force at all times during the test. This could lead to some discrepancies in the data.

3. Linear actuator Indentation (237)

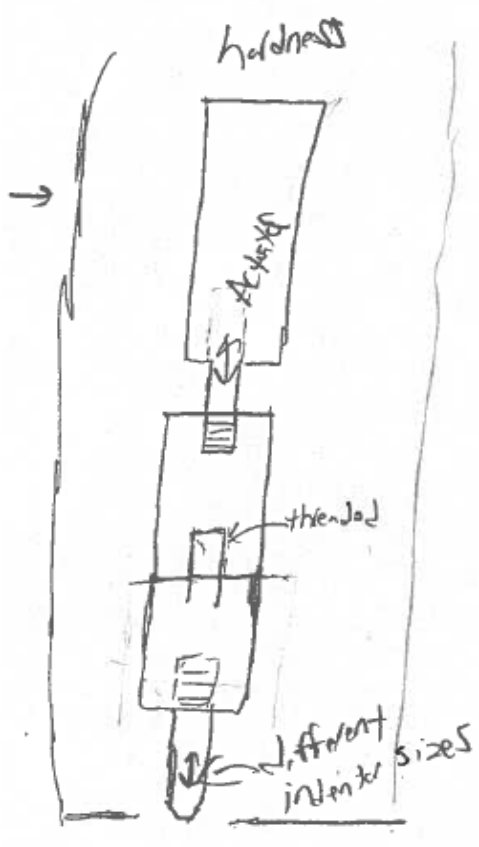

This concept is the same as the Pressure induced indentation. Except the actuation method is by linear actuator. This concept eliminates the issue of not being able to hold a constant force. However it is quite costly compared to the pressure induced indentation.

Hardness Testing	Weight	Vertical Rack & Pinion Indentation	Gravity Induced Indentation	Hand Applied Indentation
Variable Testing Rates	7	4	1	3
Maintain Const. Force	9	3	4	1
Sensitivity to positioning	8	4	1	3
Sample Variable Skin Size	8	5	5	4
Minimize Complexity	6	4	4	5
Robustness	10	2	3	1
Data Readability	6	5	5	3
Cost	7	3	3	5
Total Rating		222	196	179

4. Vertical Rack & Pinion Indentation (222)

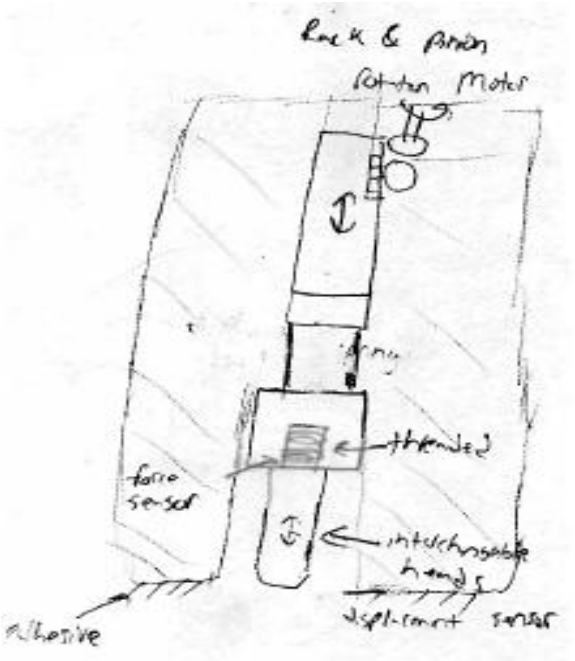

This concept is the same as the pressure induced indentation and linear actuator indentation. However, the actuation device is now changed to a DC motor. This leads to a lower cost than the linear actuator. This design is also more complex due to the DC motor's translation from rotation to vertical linear displacement.

5. Gravity Induced Indentation (196)

a 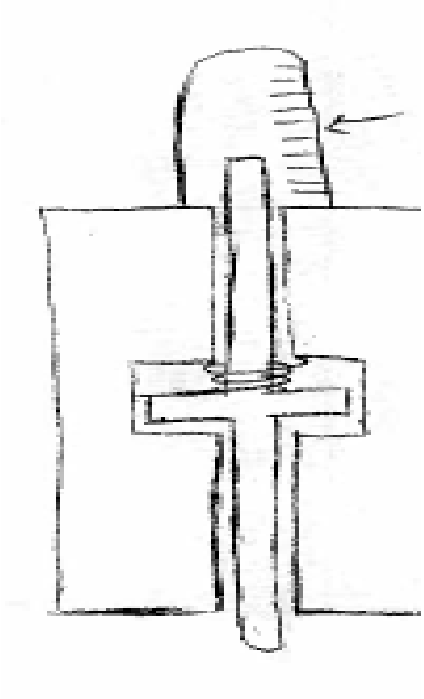

Using a simple mass indentation system an indenter would be pushed into the skin using a constant force of the mass times gravity. This is a cheap costing design and will always remain at a constant force. However this device cannot be tested on any location where this device is not vertical to the ground. Thus this design does not satisfying major customer requirement, to measure any skin location. The measurements are read by a gauge.

6. Hand Applied Indentation (179)

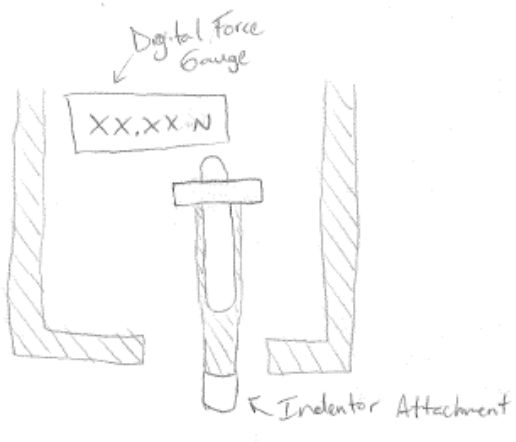

Attached to the hand applied stretching, this device is operated by a handle and pressed onto the skin to perform indentation. This concept is infeasible due to the fact that it does not meet some of the important customer requirements such as; testing variable skin locations, maintain a constant force, and have variable testing times.

Hardness Testing	Weight	Pressure Pump indenter	Manual Spring Indenter	Piston/Pressure
Variable Testing Rates	7	4	2	3
Maintain Const. Force	9	3	1	3
Sensitivity to positioning	8	3	4	3
Sample Variable Skin Size	8	2	3	2
Minimize Complexity	6	3	3	2
Robustness	10	2	2	1
Data Readability	6	2	3	2
Cost	7	3	4	2
Total Rating		166	163	136

7. Pressure Pump Indenter (166)

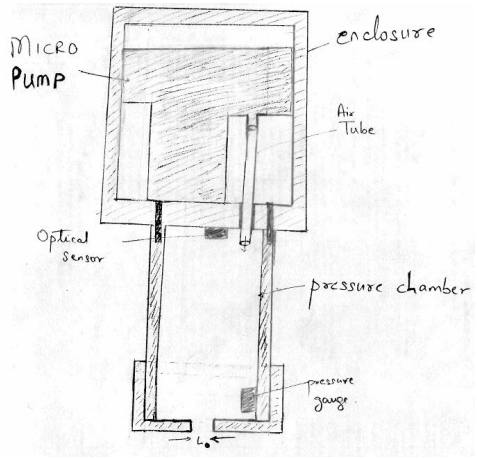

As pressure is increased by the pressure pump, indentation of skin occurs. Displacement is then relayed to DAQ by optical sensors and pressure is measured by a pressure gauge. A disadvantage of the concept is that it will not apply the intended constant force for the indentation test.

8. Manual Spring Indenter Test (163)

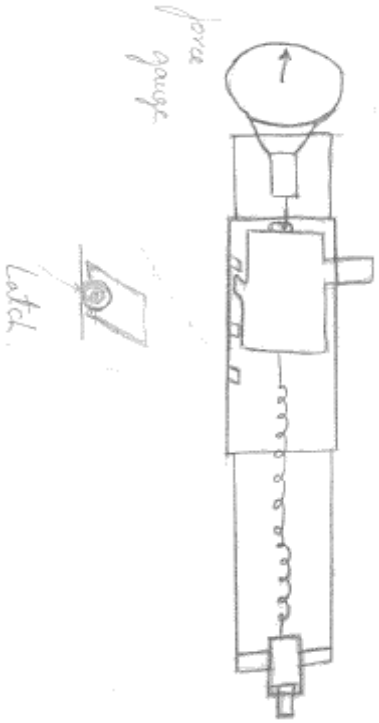

Working like a mechanical pencil, this design has a push top where the operator manually applies the indenter onto the skin until it locks in place. This device is not feasible due to the fact that we cannot test at variable testing rates since the indenter is manually applied.

9. Piston/Pressure Indenter (136)

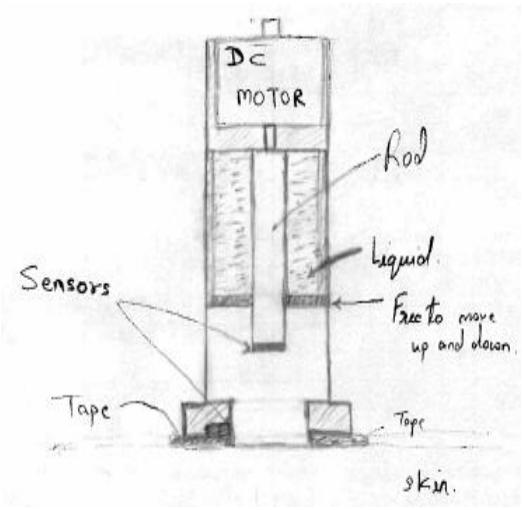

DC motor causes pressure increase, due to this indentation of skin occurs. Displacement is then relayed to DAQ by optical sensors. A disadvantage of the concept is that it will not apply the intended constant force for the indentation test.

.

Appendix D.3: Actuation Methods

The actuation should serve the purpose of achieving desired motion and different actuators were rated against our engineering specifications.

Actuation	Weight	Miniature DC motor	Linear Actuator	manual	Stepper motor	pressure pump
Cost (Min)	5	3	2	5	3	4
Size (Min)	6	5	2	2	1	2
Achieves desired function	10	3	5	4	3	3
controllability	8	4	4	2	5	3
Sensitivity/Response	7	3	3	1	4	3
Power Consumption(min)	5	4	3	5	1	2
Total Rating		148	140	125	124	117

1. Miniature DC motor (148)

This DC motor is designed small enough to fit in our device. This helps reduce the weight and size to create our device more ergonomic and mobile. The DC motor comes at a moderate cost. A DC motor has controllability to stop and go when told to, and also achieves the desired functions that we need it to.

2. Linear Actuator (140)

The linear actuator is a solid method of actuation for our device. It achieves the desired functions at a higher rate than other actuation devices researched, and is controllable. The disadvantage to a linear actuator is the steep cost it has compared to other devices.

3. Manual Actuation (125)

Being able to control our device test with only manual power is the most cost effective method of actuation. However, manual movement is not as controllable as an electrical actuator since the reaction time is slower. Also sensitivity and response time are solely dependent on the operator, which can always vary.

4. Stepper motor (124)

This actuation device is the most controllable device we can use in our design. However this device consumes a power amount above the desired rate, and it is too large for us to put inside our design. Having this actuation method would render our desired mobile device to set locations and create too much force to affect the skin being tested.

5. Pressure pump (117)

This actuation method is composed of a small pressure chamber and pump. The pump then creates either a vacuum or pressure into the chamber which can be used to translate linear motion. The main difficulty with this device is that it is hard to maintain a constant force, even with a feedback control. Also it is on the larger scale making it difficult to implement into the design.

Appendix D.4: Adhesion Methods

The Pugh chart for the adhesion methods was developed by weighing them against customer requirements and customer specifications. The adhesive has to have good bond strength and should have minimized effects on skin properties.

Adhere to Skin	Weight	Kryolan Extra Strength	Hollister Medical Spray	Velcro Strap	Kryolan Spirit Gum	Double sided Tape
Sensitivity to skin	8	5	4	5	5	4
Bond/ Attach Strength	10	4	3	2	2	3
Precise Application	9	2	5	2	2	2
Removability	6	4	5	5	4	4
Minimize Affect on Skin Properties	10	3	1	3	3	1
Cost	3	1	2	4	5	4
Total Rating		155	153	150	147	126

1. Kryolan Extra-Strength Medical Adhesive (155)

Kryolan adhesive is commonly used in holding wigs and other various facial features in costumes. It uses a brush on application and easily removable by purchasing the special remover. It works well even for sensitive skin and is strong, but the cost is high compared to other options. [23]

2. Hollister Medical Spray (153)

The spray is commonly used in the application of medical appliances. The spray allows for easy application, even on sensitive skin. It has strong bonding that remains flexible, but still comes at a high price. [24]

3. Velcro Straps (150)

Velcro straps would be attached to the housing and easily and inexpensively secured around the patient in some way. This limits the mobility requirement because it would be hard to strap around certain regions of the body.

4. Kryolan Spirit Gum (147)

Like the extra strength adhesive in its applications and uses, but it comes at a much lower cost and strength. [25]

5. Double Sided Tape (126)

The double sided tape can be attached to the device and then adhered to the skin. It is easily removable, and does not require a special remover. Difficulties arise when trying to precisely apply the tape on the small surfaces of the paddles. [26]

APPENDIX E: QFD

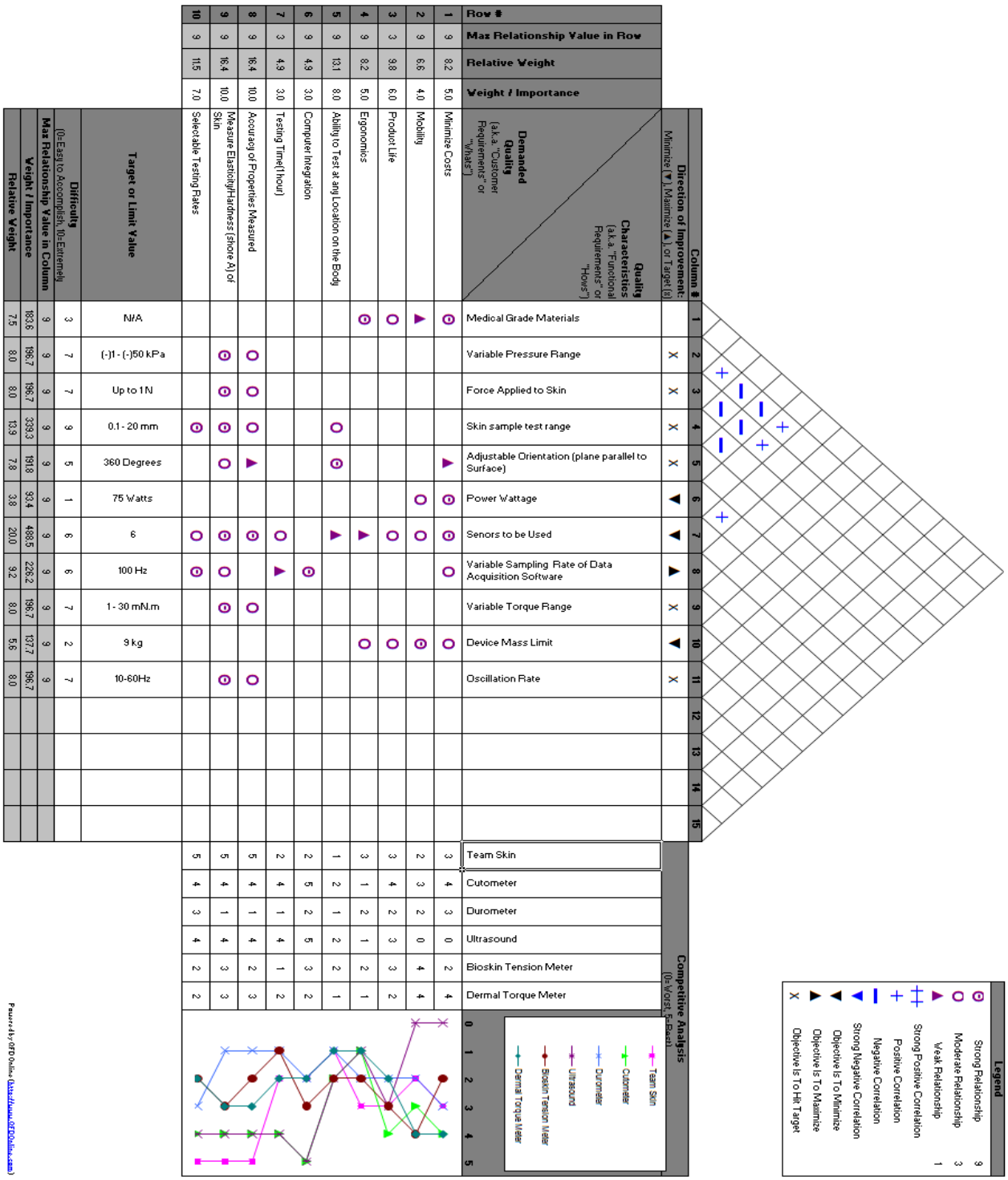

APPENDIX F: GANTT CHART

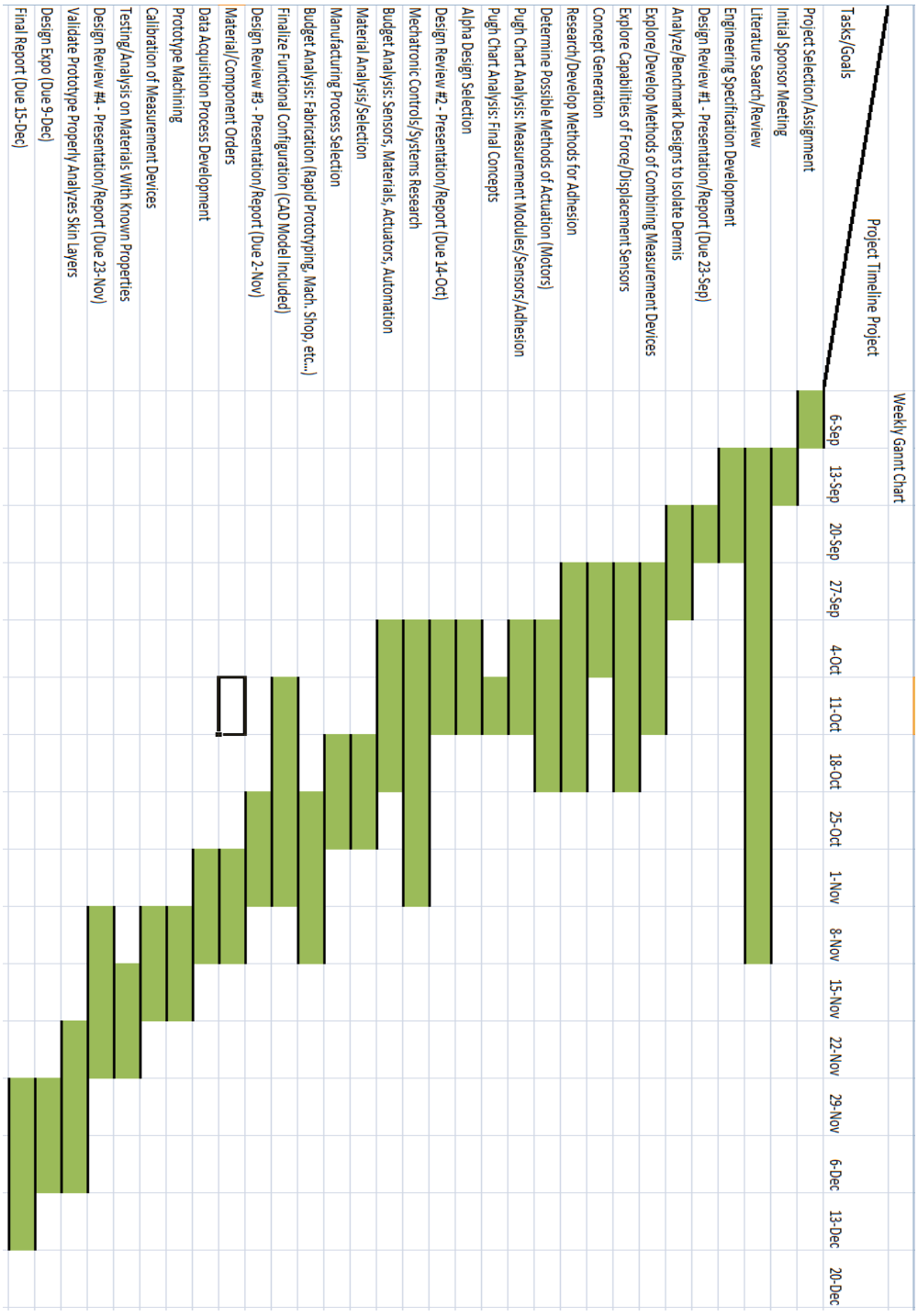

Appendix G: ENGINEERING ANALYSIS

Load Cell Analysis

Evaluating the minimum measured by the load cells developed. The output voltage is calculated that need amplification to be read by the DAQ.

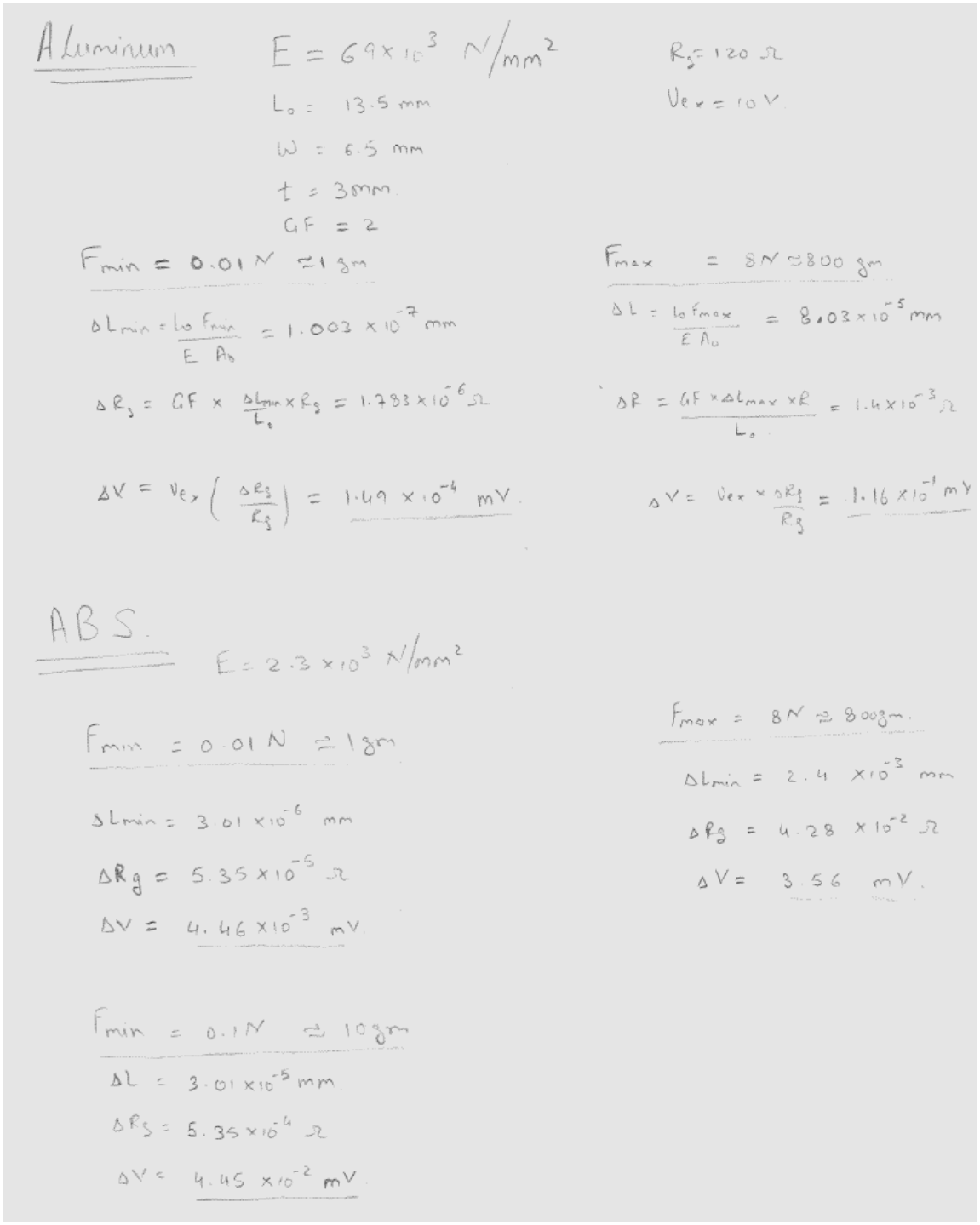

Calculations for the friction force on the steel rods passing through the rack in the elasticity measuring device.

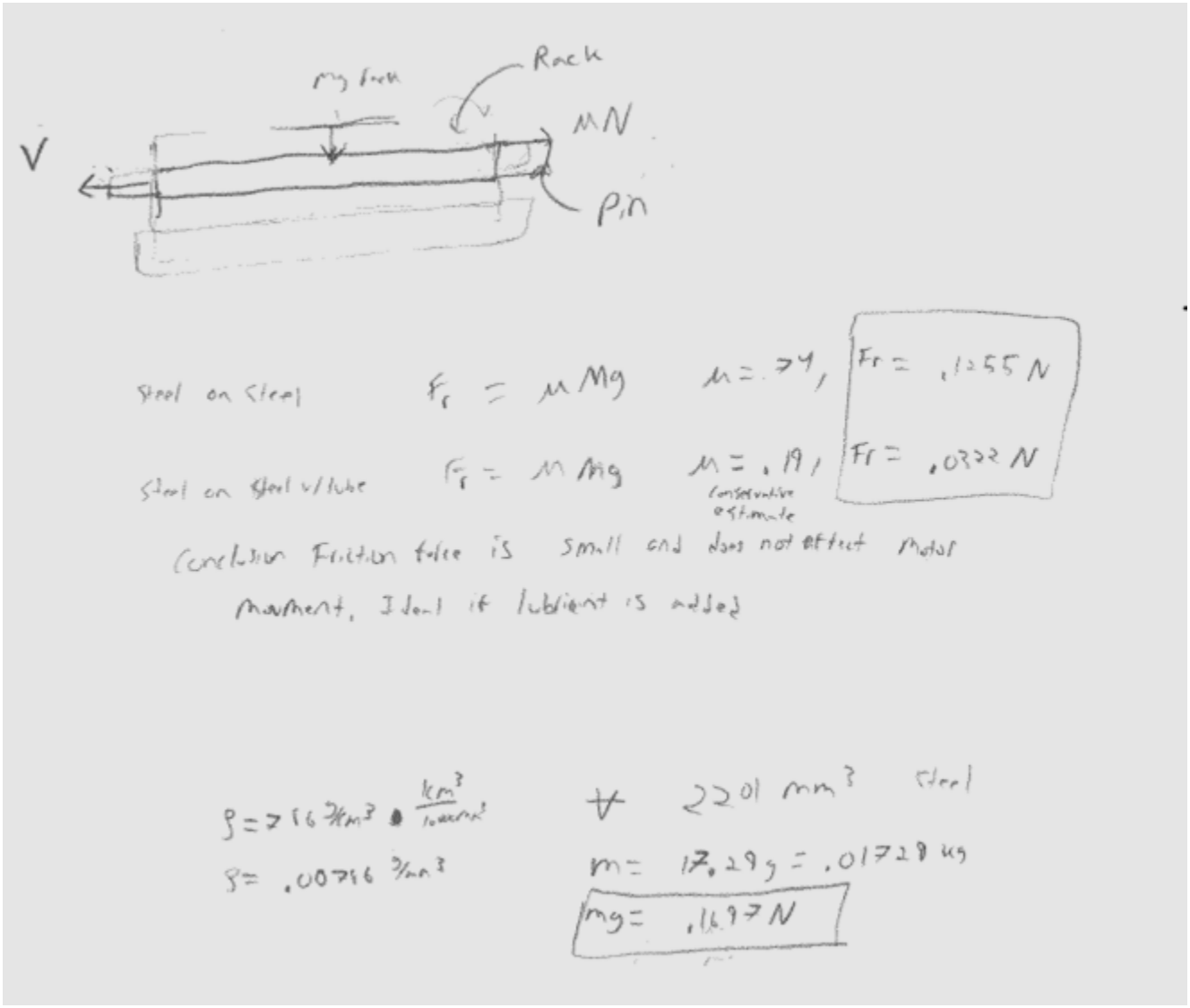

APPENDIX F: ENGINEERING DRAWINGS

All Units in mm
(Unless otherwise stated)

*Machined Part must be free of burrs

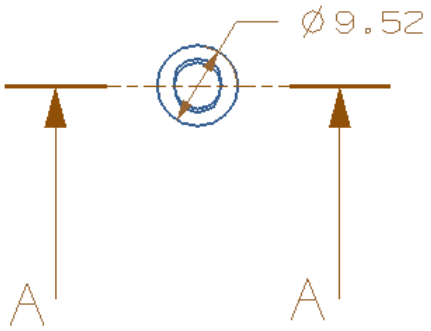

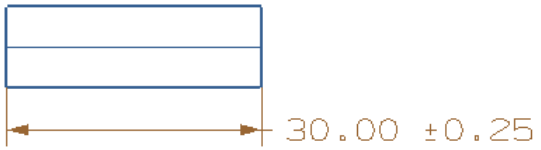

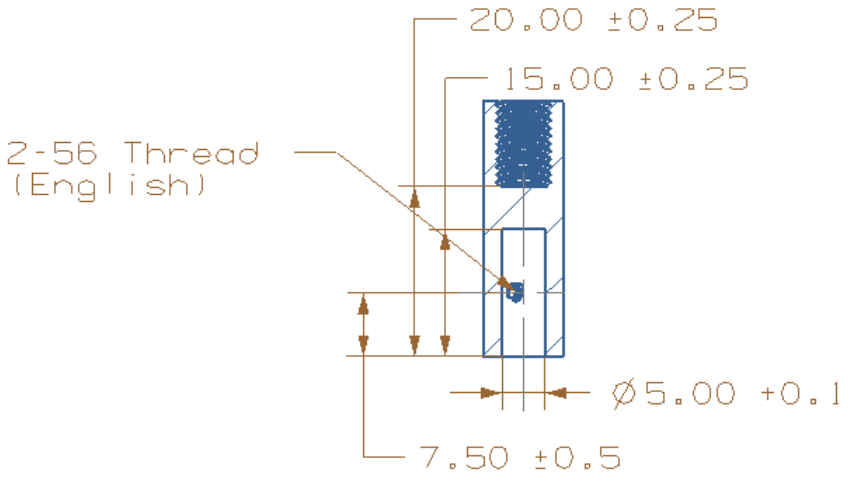

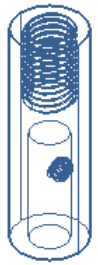

SECTION A-A

All Units in mm
(Unless otherwise stated)

*Machined Part must be free of burrs

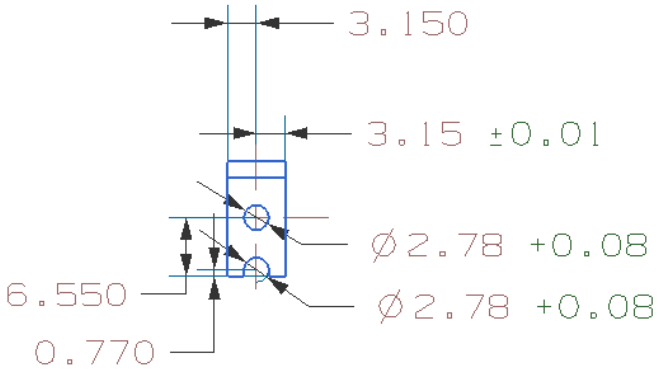

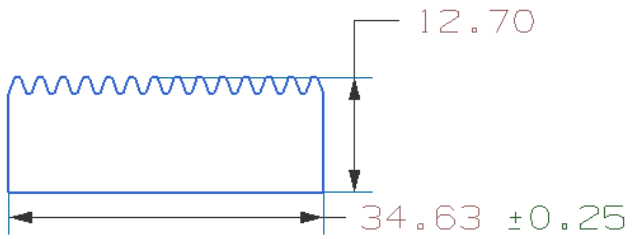

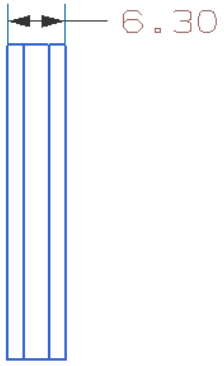

All Units in mm
(Unless otherwise stated)

*Machined Part must be free of burrs

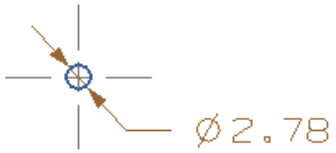

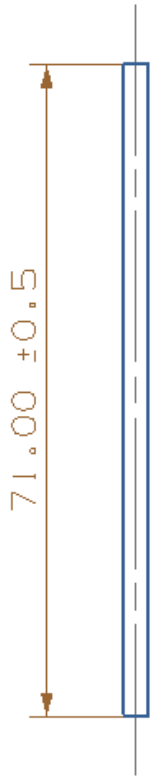

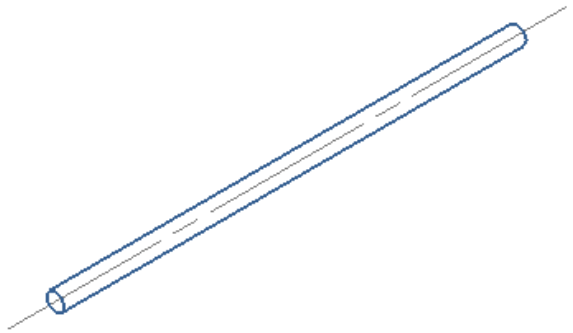

All Units in mm
(Unless otherwise stated)

*Machined Part must be free of burrs

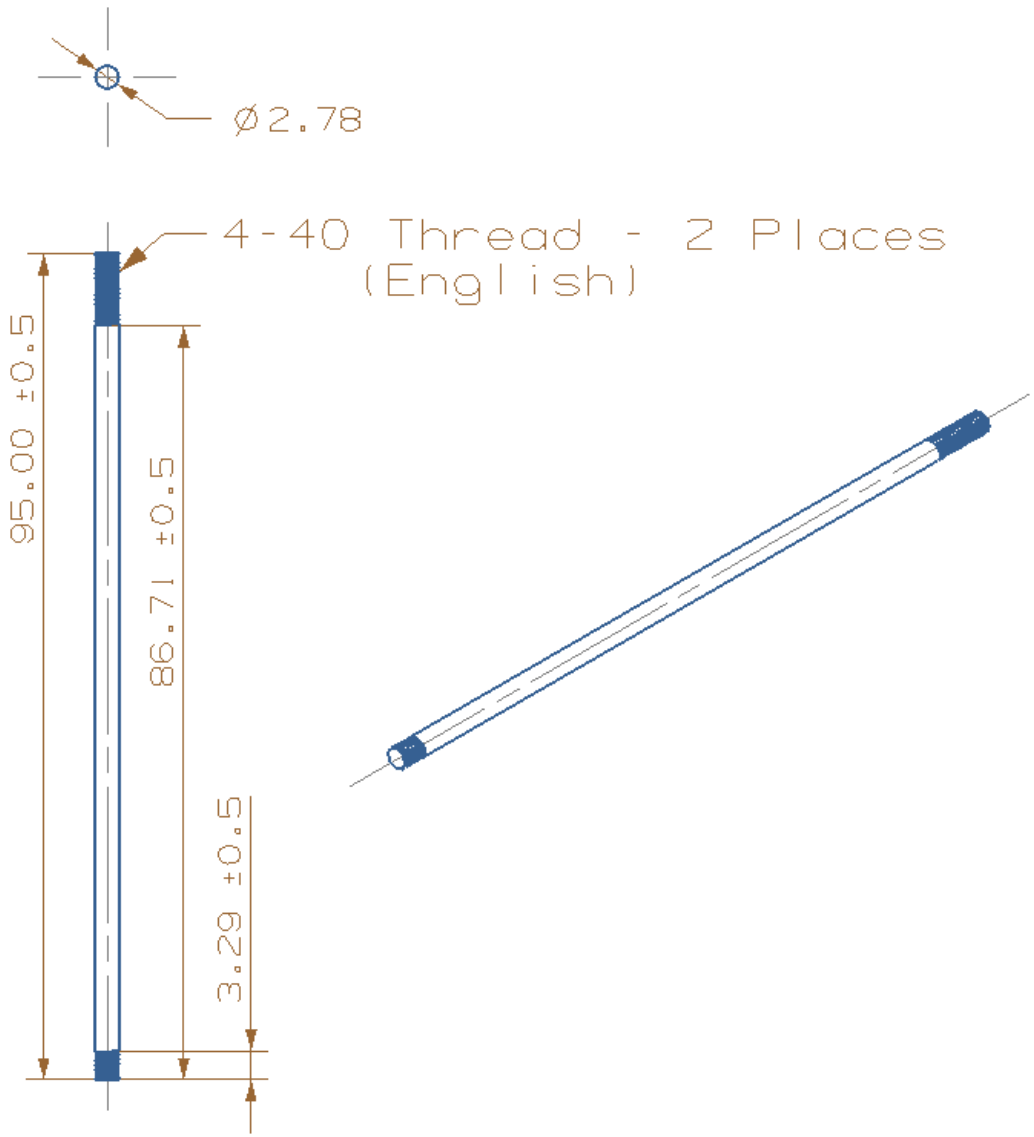

All Units in mm
(Unless otherwise stated)

*Machined Part must be free of burrs

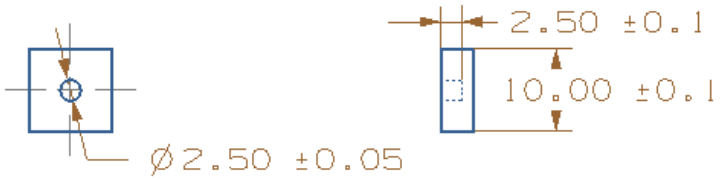

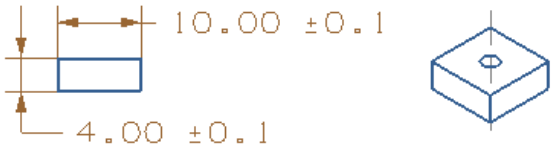

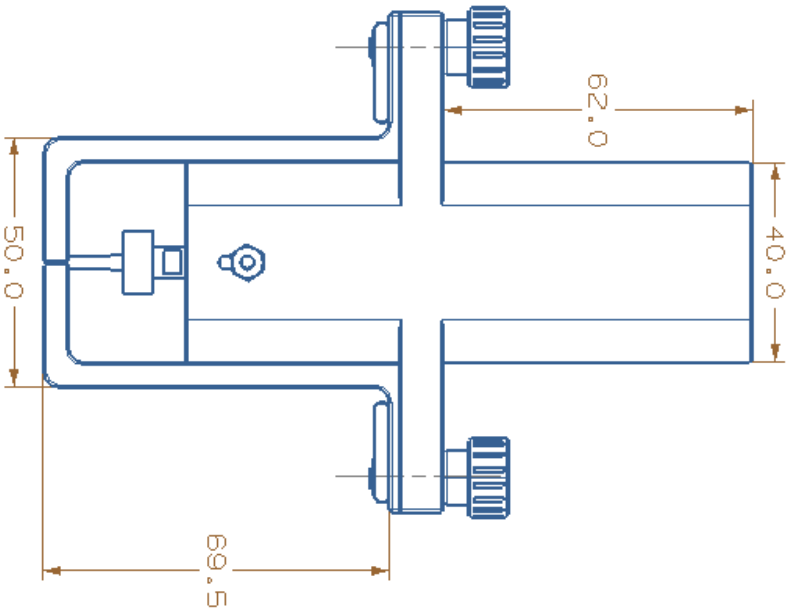

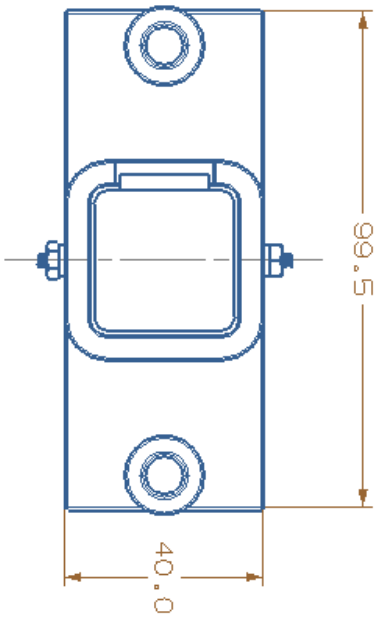

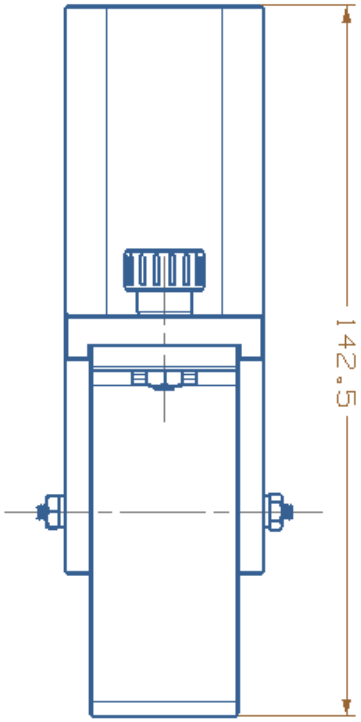

ALL DIMENSIONS IN MM

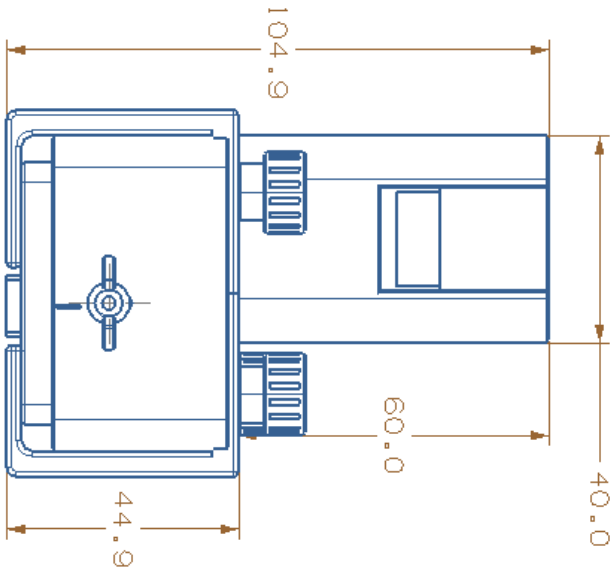

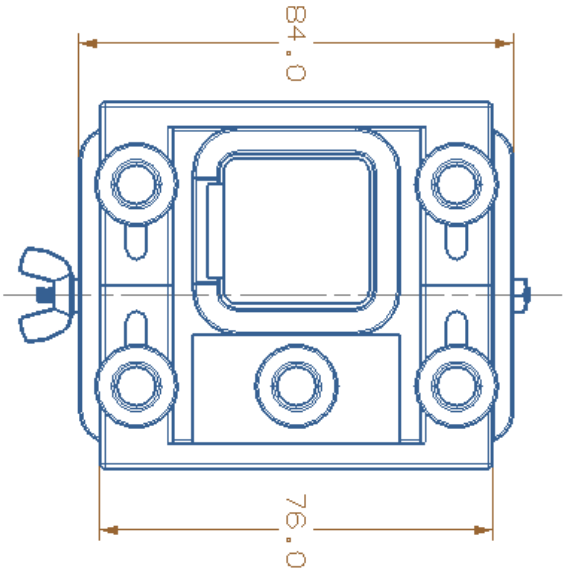

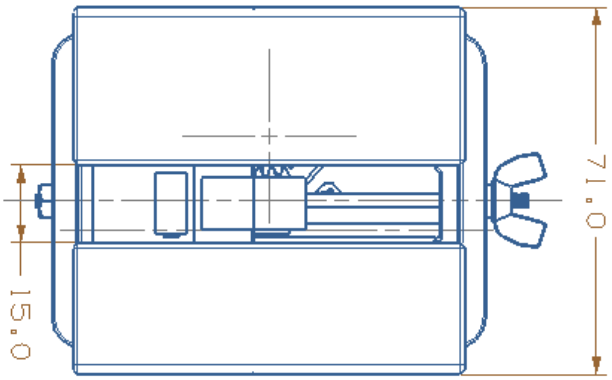

ALL DIMENSIONS IN MM